

**SOME TOPICS IN THE THEORY OF
MIXED SPIN ISING MODELS**

Thesis submitted in accordance with the
requirements of the University of
Liverpool for the degree of
Doctor in Philosophy

by

MOHAMAD MEHRAFARIN
Department of Applied Mathematics
and Theoretical Physics

SEPTEMBER 1986

ACKNOWLEDGEMENTS

I am very grateful to Dr. R.G.Bowers for his constant supervision and advice throughout the research period and the writing of this thesis.

I am indebted to my parents for their encouragement and financial support throughout my years of study. I would like to take this opportunity to also thank the rest of my family for their interest.

I wish to thank the O.R.S for a partial financial assistance during the period in which this work was carried out.

ABSTRACT

In this thesis critical phenomena in mixed spin Ising models are investigated. Such models are relevant to a study of ferrimagnetism as well as ferro- and antiferromagnetism. Specific applications are confined to a two sublattice assembly of spin-1/2 and spin-1 objects, where each spin 1/2 has spin 1's as nearest neighbours and vice versa. Some use is made of an exact correspondence between ferromagnetism in a uniform (staggered) field and ferrimagnetism in a staggered (uniform) field.

The model is considered on various loose packed lattices and several theoretical approaches, based on the appropriate statistical mechanics, are employed.

Low-temperature series expansions are derived for the free energy density of the system on the honeycomb, diamond and hydrogen peroxide lattices, using the method of partial generating functions and its generalizations. Series expansions are then obtained for various thermodynamic quantities of interest; these expansions are subsequently analysed via Pade'-approximant techniques. The honeycomb series considerably extends previous results. The diamond and hydrogen peroxide results are entirely new. The 'correspondence principle' mentioned in the first paragraph is employed in the interpretation of the results. Various exponents are estimated, some for the first time. The results support the view that our mixed spin model belongs to the same universality class as the standard Ising model. They also shed some light on the question of the equality or otherwise of related staggered and uniform field exponents.

The simple quadratic lattice is treated approximately through the application of the real space renormalisation group technique of Niemeijer and van Leeuwen. Two distinct analyses are employed, the cluster method being applied in this context for the first time. In one of these analyses a direct study of ferrimagnetism without the use of the above correspondence is made possible. The results are mainly of qualitative relevance.

A novel generalization which allows to formally include an arbitrary real value for the spin, of any Ising Hamiltonian, in particular the mixed spin Hamiltonian under consideration, is derived. This extends the domain in which such questions as the spin independence of the critical indices can be considered. This is relevant to universality.

CONTENTS

1.	General Introduction	
1.1	Introduction	1
1.2	Magnetic orderings: Ferro-, antiferro- and ferrimagnetism	2
1.3	Mixed spin Ising Hamiltonian: Model of ferrimagnetism	8
1.4	Theoretical approaches	10
2.	Derivation of Low-Temperature Series Expansions	
2.1	Introduction	17
2.2	Direct method of evaluation of free energy	20
2.3	PGF's and their use in determining $\ln \Delta$	22
2.4	Some results: Free energy polynomials	32
2.5	Thermodynamic functions and their series expansions	73
2.6	γ - Δ transformation and the hydrogen peroxide lattice	80
3.	Low-Temperature Critical Behaviour	
3.1	Introduction	82
3.2	Series analysis: Ratio and Pade'-approximant methods	83
3.3	Pade' analysis of critical points	88
3.4	Analysis of zero field thermodynamic series functions	91
3.5	Uniform field critical isotherm	100
3.6	Discussion	106

4.	Real-Space Renormalisation: Preliminaries	
4.1	Introduction	107
4.2	Theory of RSRG: An outline	110
4.3	The cumulant method and its application to our mixed system	118
5.	RSRG: Calculations Using Cluster Approximation Method	
5.1	Introduction	130
5.2	Cluster approximation theory	131
5.3	Calculations on blocks of four spins	135
5.4	Calculations on blocks of five spins	150
5.5	Numerical analysis of results	154
5.6	Discussion	164
6.	Ising Model With Real Spin	
6.1	Introduction	165
6.2	Definition of the model	171
6.3	Some consequences	177
	Appendix	184
	References	186

CHAPTER 1

GENERAL INTRODUCTION

1.1 Introduction

The aim of statistical physics is to predict the observable macroscopic properties of a physical system from the more fundamental ones occurring at a microscopic level. In actual theoretical investigations 'model systems' are considered which appropriately approximate the physical situation of interest. One of the most fascinating aspects of statistical physics is the study of the equilibrium theory of phase transitions and critical phenomena. Within this context, there has been a lot of work with models designed to simulate the critical properties associated with magnetic ordering of systems consisting of interacting spins on a lattice. In particular attention has been given to single spin Ising models (Ising, 1925) appropriate to the critical behaviour of ferro- and antiferromagnets. For a general review of the field of critical phenomena, the reader is referred to the extensive literature available, for instance Hahne(1983) and numerous references therein.

Quite recently, a study of mixed spin Ising systems relevant to a particular form of ferrimagnetism has been undertaken (see for e.g Schofield and Bowers, 1980;1981 , Yousif and Bowers, 1983;1984). Initially the investigations centred around Ising models consisting of both spin-1/2 and spin-1 objects (Schofield, 1980) and certain aspects were later generalized to include lattices composed of spin-1/2 and arbitrary spin-S constituents (Yousif, 1983), where nearest neighbour

spins are, of course, of different magnitudes. This thesis is concerned with the theory of phase transitions and critical phenomena associated with magnetic orderings in such mixed spin systems. Attention is given to phenomena appropriate to critical behaviour in ferro-, antiferro- and ferrimagnets.

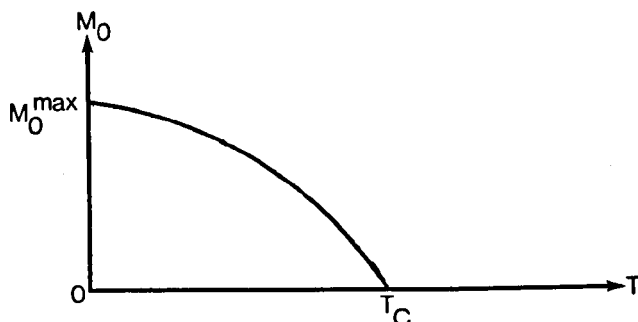
In succeeding sections of this chapter the general background of the theory of critical phenomena is outlined in a manner suited to the context of the thesis. The final section briefly reviews several approaches to the theoretical treatment of critical phenomena with regards to the previous and present work on our particular mixed Ising model.

1.2 Magnetic orderings: Ferro-, antiferro- and ferrimagnetism

There exist materials which become spontaneously magnetised at sufficiently low temperatures in the absence of an applied magnetic field. This macroscopic magnetic moment is a consequence of interactions between magnetic atoms inside the material, as it undergoes a phase transition at sufficiently low temperature. Such a phase transition consists of an order-disorder transition of the electron spins (i.e atomic magnetic moments as far as we are concerned): above the transition temperature the electronic spins are disordered in direction, but below it; the spin directions have order in some way. The material is then termed ferro-, antiferro- or ferrimagnetic, depending on the specific pattern of spin order (there is also a fourth type of ordering, namely helimagnetism, with which we are not concerned).

In ferromagnets, the interaction between atoms favours a parallel alignment of the atomic magnetic moments. In the ground state (absolute zero), the alignment is complete and the spontaneous

magnetisation M_0 has its maximum value. Above the transition temperature T_C (called the Curie temperature) there is no order in the 'spin' alignment and so M_0 vanishes.

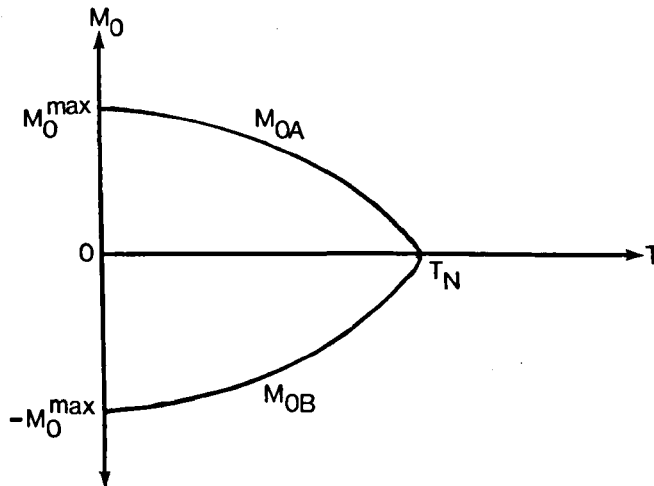


Fig(1.1): Schematic behaviour of the spontaneous (zero field) magnetisation as a function of temperature T in ferromagnets.

In the simplest form of an antiferromagnetic material, the interactions favour antiparallel spin alignment with respect to the nearest neighbour coupling. (The atomic magnetic moments are situated at the sites of a lattice decomposable into two equivalent interpenetrating sublattices A and B having spins of the same magnitudes.) Again at $T=0$ each sublattice has its maximum saturation magnetisation which is reduced steadily, in the same way as for ferromagnets, by the effect of thermal agitation as the temperature increases, until it vanishes at the transition temperature T_N (called the Ne'el temperature). Since within each sublattice magnetic moments have the same average magnitude and direction, the net magnetic moment $M_0 = M_{0A} + M_{0B}$ of the whole lattice vanishes at all temperatures (see Fig(1.2)) .

As understood from above, the study of simple ferro- and antiferromagnetism is confined to the case of identical atoms on essentially equivalent sites. If these restrictions are removed, discussion can be extended to materials having non-equivalent magnetic sublattices and/or atoms. These materials generally possess different

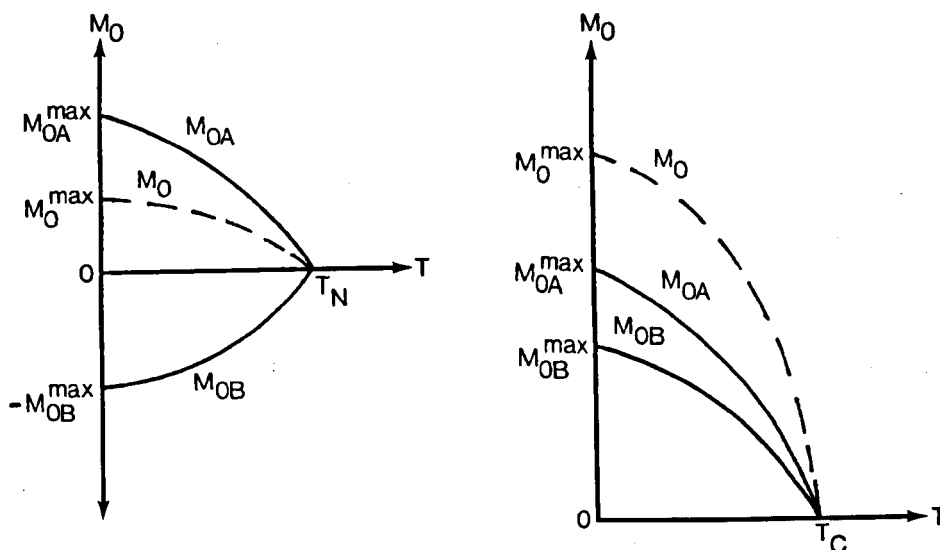
magnetic properties from those of ferro- and antiferromagnets, and are termed ferrimagnets. One might say that the possibility of simple ferrimagnetism arises when the lattice consists of two interpenetrating sublattices A and B, which contain distinct atoms. The nearest neighbour interactions may now prefer parallel or antiparallel alignment of spins, exactly as before.



Fig(1.2): Schematic picture of the temperature variation of sublattice spontaneous magnetisations M_{0A} , M_{0B} in antiferromagnets.

Considering the latter option first, the resulting behaviour of the sublattice magnetisation is then analogous to that of an antiferromagnet, except that the net magnetisation does not vanish below T_N , as the neighbouring atoms are not identical and their moments will not cancel (see Fig(1.3a)). This is genuine ferrimagnetism. For the case where parallel alignment is favoured, the two sublattice magnetisations are aligned in the same direction and so the net magnetisation for the whole lattice will be greater than that of the former situation, for all temperatures below T_N . Thus a parallel aligning 'ferrimagnet' is essentially a ferromagnet in that the interactions favour alignment of atomic moments; making it convenient to

classify the two cases above according to whether the nearest neighbour couplings prefer antialignment or alignment, respectively. In this classification we restrict the term ferrimagnetism to describe the former situation only (i.e Fig(1.3a)) while ferromagnetism is employed to cover the latter case of Fig(1.3b). This terminology is adopted throughout the thesis.



Fig(1.3): Schematic behaviour as a function of T of M_{OA} , M_{OB} and M_0 in (a) ferrimagnets and (b) ferromagnets.

The critical behaviour of a system is determined by the singularities of the thermodynamic functions manifested mathematically through a set of 'critical exponents'. Since emphasis is placed on a model of ferrimagnetism in this thesis, it is appropriate to discuss the critical behaviour of ferrimagnets, from which the relevant critical exponents naturally arise. Let H_A and H_B denote the magnitudes of applied external fields experienced by a ferrimagnet at sublattices A and B, respectively. We will be considering the behaviour of ferrimagnets in both uniform and staggered fields denoted respectively by H ($=H_A=H_B$) and H^\dagger ($=H_A=-H_B$). It is useful to introduce the

uniform and staggered magnetisations which are conjugate to H and H^\dagger , via the relations

$$M = M_A + M_B, \quad M^\dagger = M_A - M_B \quad (1.2.1)$$

respectively. We shall only give the definition of a few selected critical indices which will be of interest in this thesis. These are $\alpha, \alpha', \beta, \gamma, \gamma'$ and δ . The critical exponents α, α' associated with the singularities of the zero-field specific heat capacity C_0 are defined via

$$C_0(T) \sim (T - T_N^+)^{-\alpha} \quad \text{as } T \rightarrow T_N^+, H=0 \quad (1.2.2a)$$

$$C_0(T) \sim (T_N^- - T)^{-\alpha'} \quad \text{as } T \rightarrow T_N^-, H=0 \quad (1.2.2b)$$

where the relation $X \sim Y$ means that X/Y tends to a non-zero limit. The primed and unprimed exponents in (1.2.2a,b) obviously relate to the low and high temperature side of the critical point T_N respectively. The behaviour of the spontaneous (uniform) magnetisation $M_0(T)$ is given by

$$M_0(T) \sim (T_N^- - T)^\beta \quad \text{as } T \rightarrow T_N^-, H=0. \quad (1.2.3)$$

The divergence of the (uniform) zero-field susceptibility is defined by the two exponents γ and γ' in the following manner.

$$\chi(T) \sim (T - T_N^+)^{-\gamma} \quad \text{as } T \rightarrow T_N^+, H=0 \quad (1.2.4a)$$

$$\chi(T) \sim (T_N^- - T)^{-\gamma'} \quad \text{as } T \rightarrow T_N^-, H=0. \quad (1.2.4b)$$

Finally, the exponent δ determines the behaviour of the (uniform) magnetisation on the critical isotherm ($T=T_N$) through

$$M_C(H) \sim H^{1/\delta} \quad \text{as } H \rightarrow 0, T=T_N. \quad (1.2.5)$$

The staggered field critical exponents of the same system can be defined in an identical fashion to those of the uniform field above through replacing H, M_0, χ, M_C by $H^\dagger, M_0^\dagger, \chi^\dagger$ and M_C^\dagger respectively; which yield exponents $\alpha, \alpha', \beta^\dagger$, etc. (note that for the zero-field specific ^{heat} there is no distinction between the uniform and staggered cases). It is generally believed that the two groups of indices are identical (Bowers, 1981). This will be studied within the context of mixed spin models in the following chapters.

Having discussed the critical exponents, this is a suitable place to talk about their 'universality'. Thermodynamic properties such as $M(T, H)$ are of course expected to depend on the microscopic forces in the system. However it is believed (Fisher, 1966; Griffiths, 1970) that the critical exponents are 'universal', i.e independent of the small scale details of the model characterised by Hamiltonian \mathcal{H} . They will only depend on the dimensionality of the system and on certain symmetries in \mathcal{H} . One could thus take a realistic and complicated situation and appropriately approximate it by a highly idealised Hamiltonian and still obtain exactly the same critical indices. On these grounds all phase transitions belonging to the same 'symmetry' class, have identical behaviour in the critical region, only the name of the variable being changed (Barber, 1977). There is experimental (Heller, 1967) as well as theoretical (Fisher, 1967) evidence that a given exponent appears to possess the same value for all spin systems having identical spin dimensionality n ($n=1$ for Ising models, see section 1.3) and spatial dimensionality d . This naturally brings about the idea of 'universality classes' for the classification of various critical behaviours. For Ising models the following well known values for critical exponents have been conjectured: $\alpha=\alpha'=0$, $\beta=1/8$, $\gamma=\gamma'=7/4$, $\delta=15$ for two-dimensional and $\alpha=\alpha'=1/8$, $\beta=5/16$, $\gamma=\gamma'=5/4$, $\delta=5$ for

three-dimensional systems. (Recently there has been some doubts on whether the exponents are indeed fractions as these conjectures represent. Nevertheless they provide reliable estimates at least.) The existing evidence strongly suggests the validity of the universality hypotheses, although there are exceptions which occur only for a very special class of Hamiltonians (an example is the zero-field eight vertex model of Baxter (1971;1972)). This hypotheses is also examined in the following chapters within the context of mixed spin models, which have less translational symmetry than their traditional single spin counterparts.

1.3 Mixed spin Ising Hamiltonian: Model of ferrimagnetism

In this section we consider a model system designed to reflect the essential features of a particular form of ferrimagnetism. The model basically consists of a d -dimensional lattice of objects simulating the atomic magnetic moments which occur in reality. These objects, in general, consist of n -dimensional spins interacting with their neighbours through any desired order. We here restrict ourselves to the special case where the spins are one-dimensional and the interactions are confined to nearest neighbours, i.e the (pure) Ising model. (However in chapters 4 and 5, the inclusion of farther neighbour interactions becomes necessary. This is a more general case of the Hamiltonian (1.3.1).) The loose-packed lattice of a ferrimagnetic problem is assumed decomposable into two non-equivalent sublattices A and B as in section 1.2 . We designate the spins situated on A by $S_{A,i}^z$ and on B by $S_{B,j}^z$, where i and j represent the appropriate lattice site in A and B , respectively. In Ising models the quantum mechanical spin operators are reduced to classical (one-dimensional) quantities by considering only their z -components $S_{A,i}^z$ and $S_{B,j}^z$

which take the values $S_A, -S_A+1, \dots, S_A-1, S_A$ and $S_B, -S_B+1, \dots, S_B-1, S_B$; respectively. Then A and B are said to contain Ising spins of magnitudes S_A and S_B , respectively. The Hamiltonian corresponding to this mixed spin model takes the form

$$\mathcal{H} = -(J/S_A S_B) \sum_{\langle ij \rangle} S_{A,i}^z S_{B,j}^z - (m_A H_A / S_A) \sum_{i \in A} S_{A,i}^z - (m_B H_B / S_B) \sum_{j \in B} S_{B,j}^z \quad (1.3.1)$$

with J representing the coupling between spins from different sublattices. Here m_A and m_B are magnetic moments per spin at sublattices A and B respectively; and the summation on $\langle ij \rangle$ is over all pairs of nearest neighbour sites. A particular case of (1.3.1) is when S_A and S_B are identical, reducing the Hamiltonian to that describing ferro- or antiferromagnetism. The sign convention is such that $J > 0$ favours alignment whilst $J < 0$ is favourable to antialignment of atomic moments. Thus (1.3.1) with $J < 0$ is representative of a certain kind of uniaxial ferrimagnetism (when S_A and S_B are different of course).

Now, employing the canonical ensemble, the total partition function corresponding to the Hamiltonian (1.3.1) is

$$Z_N = \sum_{\text{all states}} \exp(-\beta \mathcal{H}) \quad (1.3.2)$$

where N is the number of spins and the sum is over all allowed microscopic states of the system. In (1.3.2) $\beta = 1/\kappa T$; κ being the Boltzmann constant. Also for the Gibbsian free energy G_N , we have

$$-\beta G_N = \ln Z_N \quad (1.3.3)$$

Equation (1.3.1-3) determine all the thermodynamic properties via standard thermodynamic formulae (after taking the thermodynamic limit

of course, see section 1.4) or equivalently through the use of the average (or expectation) values

$$\langle F \rangle = Z_N^{-1} \sum_{\text{all states}} F \exp(-\beta \mathcal{H}) \quad (1.3.4)$$

where F is some appropriate (observable) function of state whose average is its observed thermodynamic value.

With this preliminary, we note the following which is easily obtained through consideration of spin reversal symmetry (e.g. $S_{B,j}^z \rightarrow -S_{B,j}^z$) associated with Hamiltonian (1.3.1) [see Schofield, 1980 and Yousif, 1983]:

$$Z_N(J, H_A, H_B) = Z_N(-J, H_A, -H_B) . \quad (1.3.5)$$

This essentially states that the total partition function (and consequently the thermodynamic behaviour) of a ferromagnetic in a uniformly (staggeredly) oriented field (H_A, H_B) is identical to that of a ferrimagnetic in a staggeredly (uniformly) oriented field $(H_A, -H_B)$ [or $(-H_A, H_B)$]. We shall make use of this fact where appropriate throughout the succeeding chapters, which (except chapter 6) deal with the study of the particular case $S_A=1/2, S_B=1$, in application.

1.4 Theoretical approaches

To obtain singular behaviour as occurs in critical phenomena, one must in fact take the thermodynamic limit as the size of the system tends to infinity, since such singularities are not generally expected to occur within finite sized systems for which the summation in (1.3.2) is bounded. In this limit the sum becomes unbounded and the statistical mechanical formulae must be used in a manner which allows the calculation of thermodynamic functions per particle (per unit volume) [see for example Huang, 1963].

With this remark in mind, the basic problem is therefore to calculate the sum-over-states in (1.3.2). Although the model Hamiltonian (1.3.1) is a simple idealisation compared with the real ferrimagnet; the evaluation of Z_N is far from straightforward. Indeed an exact solution via analytical considerations for the partition function has only been obtained for a very limited number of models, to date. These include the (linear) spin-1/2 Ising chain in one dimension (Ising, 1925). Schofield (1980) applied the transfer matrix technique (Onsager, 1944) to the case of (one-dimensional) mixed spin ($S_A=1/2$, $S_B=1$) linear Ising chain, modelled by Hamiltonian (1.3.1), which enabled an exact form for the corresponding partition function to be obtained. This was later generalized by Yousif (1983) to the case of $S_A=1/2$, $S_B=S$ (S arbitrary).

Another way to proceed to evaluate Z_N for a given system, is to ignore certain particular aspects of the statistical ~~problem~~, thereby reducing the problem to an 'exactly solvable' one. These are referred to as 'closed form approximations', the best known example of which is the mean (or molecular) field theory (MFT). In MFT interactions between the constituent particles are approximated by means of the assumption that each particle is acted upon by a 'mean field' due to all the other particles of the system. It was first adapted to the phenomena of ferromagnetism by Weiss in 1907 and to antiferromagnetism by Ne'el in 1930's (see Smart, 1966). A generalization to include ferrimagnetic ordering was later introduced by Ne'el (1948). In both Ne'el's developments, the Hamiltonian in question was based on the quantum mechanical Heisenberg model (Heisenberg, 1928). The application of MFT to the case of ferrimagnetism based on the Ising Hamiltonian (1.3.1) was considered

by Schofield (1980) and later generalized by Yousif (1983) which yielded a closed form for Z_N .

Below we present an outline of two well established methods of analysis of critical phenomena, namely the low- temperature series expansions and the real space renormalisation group (RSRG) technique, with view to applying these ^{to} derive properties of the ferrimagnet modelled by (1.3.1).

(i) Low- temperature series expansions: Series expansion methods consist essentially of obtaining an approximation to Z_N through the truncation of an exact series. In general, exact series expansions are derived at high and low temperatures (above and below T_C , respectively) in some appropriate variable. Here we only consider the low-temperature expansions. For the applications of high-temperature expansions to our mixed spin problem see ^hSchofield (1980) and Yousif (1983) who used the method of Brout (1959;1960) for a number of loose-packed lattices.

In ground state $T=0$, for the ferromagnetic case, all the spins on the lattice align with any sufficiently high unidirectional applied field. The partition function (1.3.2) and the free energy (1.3.3) of the system may then be expanded in terms of increasing number of overturned spins from this ground state. It is then necessary to determine the counts of configurations which describe the different perturbations (see section 2.1). A relatively early method of investigation is the direct method (Domb, 1960) in which Z_N (or G_N) is expanded in terms of a 'field variable' and an 'interaction variable', in as many terms as computationally possible. One then derives from this expansion, series expansions for the physical quantities of interest. The asymptotic behaviour of these functions is found by ex-

trapolation procedures. Low-temperature series expansions are, however, difficult to obtain, due to the extremely rapid increase in the number of possible classes of configurations as the number of overturned spins increases; together with the difficulty of finding lattice constants (see the next chapter). A more efficient technique of evaluating the series of interest is that of partial generating functions (PGF's), which was introduced for the spin-1/2 Ising ferromagnet by Sykes et al (1965) and generalized for higher spins by Sykes and Gaunt (1973).

The technique of low-temperature expansions and in particular the method of PGF's was adapted to the low-temperature study of ferrimagnetism (defined via (1.3.1)) by Bowers and Yousif (1984) for a number of loose-packed lattices including the honeycomb. Here, using (1.3.1) of course, we have been able to obtain longer series expansions for the thermodynamic quantities of interest, through full and proper use of the symmetry principle of PGF's (see section 2.3) on the mixed spin honeycomb lattice. In particular, the mixed spin lattices of diamond and hydrogen peroxide are also studied. These are of theoretical interest as they are expected to yield low-temperature expansions for thermodynamic properties along the coexistence curve, all of whose coefficients are of one sign (this is certainly the case for their spin-1/2 counterparts; see Sykes et al, 1973, Betts et al, 1974 and the references therein). Low-temperature expansions are the subject study in chapters 2 and 3.

(ii) RSRG: In equilibrium (away from the critical point), a system has statistically independent parameters in the sense that the average value of the product of these parameters is zero and so their variation will have no effect on each other. In other words the fluctuations

are not correlated. This is, however, not the case in the critical region where fluctuations become long-ranged (infinite at the critical point; $T=T_C, H=0$ in a magnetic system) as a certain kind of cooperative phenomena is enhanced. The effect of these correlations is to increase the domain of microscopic interactions within the system, so that they are no longer restricted to the domain of a non-critical situation. As a consequence the 'effective length scale' of our problem is hugely enlarged. For example it is no longer the lattice spacings in the case of a lattice model. Then all interactions with a characteristic length between that of lattice spacings and this 'new' length are important. The new length is called the correlation length ξ and tends to infinity as the critical point is approached.

The ideas of renormalisation group (RG) method were first applied to the critical phenomena by Wilson (1971a;b). The RG is a set of symmetry transformations which act in space of parameters characteristic of the model of interest. Each transformation is defined by means of two operations: a Kadanoff transformation and a spatial re-scaling (Kadanoff, 1966). The motivation behind the first operation is based upon the idea that the predominant feature of all critical phenomena is the collective behaviour of the particles, in accordance with the presence of very long-range fluctuations. This leads to the absence of fine details of the constituent particles associated with short-range fluctuations. Then the second operation simply introduces 'bigger scales' in order to shrink down the size of the correlation length ξ , so that the system appears somewhat farther from criticality. The technique then proceeds to evaluate the sum over states in Z_N via successive stages; a 'renormalised' Hamiltonian being defined at each stage. This defines a mapping in Hamiltonian space. At critical point, after many applications of the RG, we can suppose that the

Hamiltonian tends to a certain 'invariant' Hamiltonian which does not change anymore by a further application of the RG. The way this invariant Hamiltonian is approached will reveal all the properties inherent and universal to the critical point, because the renormalisation procedure is to magnify the phenomena near the critical point by eliminating the microscopic details. This mapping is assumed to exhibit a fixed point corresponding to the (critical point) invariant hamiltonian where the rescaling also has no effect on ξ (which is now infinite). Furthermore, if one makes some fairly mild assumptions about this RG mapping, notably that it is analytic, then it follows that the thermodynamic functions do have branch-point singularities such as (1.2.2a) at the critical point, that the scaling laws (such as (4.2.15)) are satisfied and that the exponents of the singularities should normally be universal (Fisher, 1974).

In this thesis we deal with a particular realisation of the RG method, namely that of RSRG, which is specifically designed to treat systems of discrete spins in particular lattice models (see section 4.2). The cumulant form of RSRG (Niemeijer and van Leeuwen, 1974) has been employed by Schofield (1980) for a number of cell choices, in particular that of Fig(4.2), on the mixed spin square lattice. We shall employ the cluster technique (Niemeijer and van Leeuwen, 1974) to study this situation. This seems to be the first such application as far as mixed models are concerned. The methods of cumulant and cluster theory are also applied to investigate the same lattice with a different choice of cells which is of more physical significance. RSRG is the subject of study in chapters 4 and 5.

Lastly, for the sake of completeness, we ought to say something about chapter 6. This chapter proceeds to define a new model by

generalizing the Ising Hamiltonian (1.3.1) [the generalization is in fact made for any Ising model] to formally include any real value for S_A and S_B , instead of the usual 'quantum' values. Through this generalization the domain of that particular aspect of the universality principle referred to as spin-independence of critical exponents can be investigated for real spins. Various approaches may then be employed to analyse the resulting generalized Ising model within a specific context.

CHAPTER 2

DERIVATION OF LOW-TEMPERATURE SERIES EXPANSIONS

2.1 Introduction

As discussed in the introductory chapter, Hamiltonian (1.3.1) [with $J < 0$] represents certain kinds of ferrimagnets, whose low temperature thermodynamic properties we wish to study. With $J > 0$, this Hamiltonian corresponds to ferromagnets which, owing to some symmetry properties (see section 1.3), possess the same thermodynamic behavior^u in a uniform (staggered) field as do the ferrimagnets in a staggered (uniform) field. We shall, therefore, study this Hamiltonian with $J > 0$ in both uniform and staggered fields near the Curie temperature. This can then be immediately interpreted ferrimagnetically.

Our particular model has $S_A = 1/2$ and $S_B = 1$, however the theory and methods of this chapter can be extended to suit any mixed spin model. In order to study the low temperature critical behavior^u, we must first obtain the low temperature series expansions for the desired thermodynamic functions, which is the purpose of this chapter.

At temperature $T=0$, all spins of each sublattice point up parallel to any unidirectional applied field, forming the ordered ground state. As the temperature is raised, disorder increases due to thermal agitation and spins tend to change state. This flipping increases the total energy by $2J$ (a 'pair' energy) as the interacting spin pairs change from parallel position to the antiparallel position. Let us call $S_A^z = S_A$ and $S_B^z = S_B$, the ground state (parallel alignment) of the

system, and represent the values accessible to $S_{A,i}^z$, $S_{B,j}^z$ by $(S_A - x)$ and $(S_B - y)$, where $x=0,1,\dots,2S_A$ and $y=0,1,\dots,2S_B$; respectively. Then $x=y=0$ corresponds to the ground state and x,y can be used to label states. Also we define N_x^A to be the number of spins in the x th state on sublattice A and N_y^B to be that in the y th state on sublattice B. Denote by $N_{x,y}^{AB}$, the number of bonds between nearest neighbour spins in the x th and y th states, on the sublattices A and B, respectively.

Employing the canonical distribution, it can be shown (Bowers and Yousif, 1984) that Hamiltonian (1.3.1) implies for the Gibbsian free energy $G_N(T,H)$, assuming $N/2$ spins on each sublattice,

$$G_N(T,H) = -\frac{1}{2} qJN - \frac{1}{2} N(m_A H_A + m_B H_B) - \kappa T \ln \Lambda_N(\mu, \nu, u) \quad (2.1.1)$$

where q is the lattice coordination number and $\ln \Lambda_N(\mu, \nu, u)$ is the perturbed (reduced) free energy, and

$$\begin{aligned} \mu &= \exp(-\beta m_A H_A / S_A) \quad , \quad \nu = \exp(-\beta m_B H_B / S_B) \\ u &= \exp(-\beta J / S_A S_B) \quad . \end{aligned} \quad (2.1.2)$$

The first term in (2.1.1) represents the ground state energy. Contributions to the total energy, as explained above, come from anti-parallel pairs that are formed after flipping. Thus, in order to calculate these contributions, we must work out all the possible configurations with given number of bonds, up to a certain order. These embedding constants (number of ways a given configuration can occur) are clearly polynomials in N . As seen from (2.1.1), $\ln \Lambda_N(\mu, \nu, u)$ is thus related to these embedding constants. By generalizing the method given by Domb (1960), one finds (Yousif, 1983), for the Gibbsian free energy per spin $G(T,H)$, that

$$G(T,H) = -\frac{1}{2} qJ - \frac{1}{2} (m_A H_A + m_B H_B) - \kappa T \ln \Lambda(\mu, \nu, u) \quad (2.1.3)$$

where $\ln \Lambda(\mu, \nu, u)$ is the coefficient of N in the expansion of $\Lambda_N(\mu, \nu, u)$. The relationship between $\Lambda_N(\mu, \nu, u)$ of equation (2.1.1) and the embedding constants is given by (Yousif, 1983),

$$\Lambda_N(\mu, \nu, u) = \sum_{r,t,d} \Omega_N(r,t,d) u^{q(S_B r + S_A t) - d} \mu^r \nu^t \quad (2.1.4a)$$

with

$$r = \sum_{x>0} x N_x^A, \quad t = \sum_{y>0} y N_y^B \quad (2.1.4b)$$

$$d = \sum_{x,y \neq 0,0} xy N_{x,y}^{AB}$$

where $\Omega_N(r,t,d)$ is the embedding constant with given r,t and d . Now $\ln \Lambda(\mu, \nu, u)$ is the coefficient of N in the expansion of $\Lambda_N(\mu, \nu, u)$. So if $g_{r,t}(u)$ is to represent the sum, over d , of the coefficients of N in the embedding constant Ω_N multiplied by $u^{q(S_B r + S_A t) - d}$, we will have

$$\ln \Lambda(\mu, \nu, u) = \sum_{r,t} g_{r,t}(u) \mu^r \nu^t. \quad (2.1.5)$$

It is also desirable to let $a[r,t,d]$ denote the sum of the coefficients of N in Ω_N , so that

$$g_{r,t}(u) = \sum_d a[r,t,d] u^{q(S_B r + S_A t) - d} = \sum_n a_n[r,t,d] u^n \quad (2.1.6)$$

where $n = q(S_B r + S_A t) - d$. We thus have to calculate $g_{r,t}(u)$ up to given order in $r+t$ to obtain the free energy density.

It is worth noting that when q is odd and at least one of S_A, S_B is non-integral; $g_{r,t}(u)$ is not a polynomial in u but in $z = \sqrt{u}$.

In the following sections, we shall sketch the general theory and connection with thermodynamics (as it has been done before; Yousif, 1983), and give results for our particular model of mixed spins on the three loose-packed lattices: honeycomb, hydrogen peroxide and diamond. The final section is devoted to the application of the star-triangle (Y-Δ) transformation (Fisher, 1959) in determining the critical point of our mixed spin model on the hydrogen peroxide lattice.

2.2 Direct method of evaluation of free energy

A primitive method of derivation of $g_{r,t}$ polynomials (and hence the free energy) is to consider the configuration as the number of spins on both sublattices change. Here, a few examples on the honeycomb lattice are given to illustrate the method. We have $q=3$, $S_A=1/2$, $S_B=1$. Thus for excited spin states $x=1$, $y=1,2$; and we find $r=N_1^A$, $t=N_1^B + 2N_2^B$ and $d=N_{1,1}^{AB} + 2N_{1,2}^{AB}$, via (2.1.4b). Also

$$q (S_B r + S_A t) - d = 3 (r + t/2) - d = \frac{1}{2} (6r + 3t - 2d)$$

is the power of u in (2.1.4a) giving $(6r+3t-2d)$ as the power of z .

We consider the expansion of $\ln \Lambda(\mu, \nu, u)$ up to order $r+t=2$. We then have, from (2.1.5),

$$\begin{aligned} \ln \Lambda(\mu, \nu, u) = & g_{1,0}(z) \mu + g_{0,1}(z) \nu + g_{2,0}(z) \mu^2 \\ & + g_{1,1}(z) \mu \nu + g_{0,2}(z) \nu^2 . \end{aligned}$$

$g_{1,0}(z)$: $r=1$, $t=0$. Thus $N_1^A=1$ and $N_1^B=N_2^B=0$ and hence $d=0$, as there are no excited spins on the B sublattice to produce bonds. With $N/2$ spins on each sublattice, there are $N/2$ number of ways to perturb one spin on the A sublattice. The coefficient of N in $\sum_{r,t,d} \Omega_N(r,t,d) z^{6r+3t-2d} = \frac{1}{2} N z^6$, is thus $z^6/2$ which is just $g_{1,0}(z)$.

$g_{0,1}(z)$: $r=0$, $t=1$. Thus $N_1^A=0$ and $N_1^B=1$, $N_2^B=0$ and hence $d=0$. Again there will be $N/2$ ways of picking the excited spin on B sublattice. Similar arguments as above yield $g_{0,1}(z) = z^3/2$.

$g_{2,0}(z)$: $r=2$, $t=0$. Thus $N_1^A=2$ and $N_1^B=N_2^B=0$ and hence $d=0$. There are $\frac{1}{2}(N/2)(N/2-1)$ ways of choosing two excited spins, in the same state, on sublattice A, which implies $g_{2,0}(z) = -z^{12}/4$ as the coefficient of N in $\sum_{r,t,d} \Omega_N(r,t,d) z^{6r+3t-2d}$.

$g_{1,1}(z)$: $r=1$, $t=1$. Thus $N_1^A=1$ and $N_1^B=1$, $N_2^B=0$ and d can either be 1 or 0; according to whether the excited spins are nearest neighbours or not ($N_{1,1}^{AB}=1$ or 0).

(i) $d=0$. There will be $N/2$ ways of choosing the excited spin on the ^A sublattice. In order to create no bonds we have to exclude its three nearest neighbours, so over all we get $(N/2)(N/2-3)$. The contribution to $g_{1,1}(z)$ is therefore $-3z^9/2$.

(ii) $d=1$. This corresponds to selecting the excited spin on A sublattice in $N/2$ ways such that the excited spin on the B sublattice resides on one of its three nearest neighbours. Thus, the total number of ways of achieving this configuration is $3N/2$, giving contribution $3z^7/2$ to $g_{1,1}(z)$.

From (i) and (ii) we obtain, $g_{1,1}(z) = 3z^7/2 - 3z^9/2$.

$g_{0,2}(z)$: $r=0$, $t=2$. Thus $N_1^A=0$ and $N_1^B=2$, $N_2^B=0$ or $N_1^B=0$, $N_2^B=1$. Clearly $d=0$ in both cases.

(i) $N_1^B=2$, $N_2^B=0$. There are $\frac{1}{2}(N/2)(N/2-1)$ ways of achieving this configuration, yielding contribution $-z^6/4$.

(ii) $N_1^B=0$, $N_2^B=1$. Clearly there are $N/2$ ways of perturbing one spin on the B sublattice to form the $\gamma=2$ state, yielding the term $z^6/2$.

From (i) and (ii) we find, $g_{0,2}(z) = -z^6/4 + z^6/2 = z^6/4$.

In this manner we can obtain polynomials $g_{r,t}$ up to any desired order and write down the free energy expansion to that order. This method can be applied to any loose-packed lattice and is straightforward in principle. However, for higher orders of $r+t$, configurations become more complex and so do the calculations. Thus to have more terms in our expansions we need to lay hands on a more powerful technique. This is the method of PGF's.

2.3 PGF's and their use in determining $\ln \Lambda$

This technique is a generalization of that available for single spin Ising models on loose-packed lattices (Sykes et al, 1965 for spin-1/2 and Sykes and Gaunt, 1973 for higher spins). It was first applied to mixed spin models by Bowers and Yousif (1984) for a number of loose-packed lattices.

For our particular mixed spin model we introduce the symbols 'y' to denote the first excited spin state on the A sublattice and 'x', 'X' to denote perturbed spins on the B sublattice, in the first and second states, respectively; and represent:

bonds between x and y by b,

bonds between X and y by b^2 .

In this notation we can generate representation of various configurations of spins and bonds. In order to express $\ln \Lambda$ in terms of (μ, ν, u) we thus have to find the mapping between (x, X, y, b) and (μ, ν, u) . To this end consider a cluster of spins on a certain loose-packed lattice with coordination number q , consisting of N_1^A spins on the A sublattice, N_1^B and N_2^B on the B sublattice, and $N_{1,1}^{AB}$, $N_{1,2}^{AB}$ bonds of various types. Thus from section 2.1 we have that, apart from the embedding constant, the contribution to the free energy of this cluster is

$$u^{q(r+t/2)-d} \mu^r \nu^t$$

where $r=N_1^A$, $t=N_1^B + 2N_2^B$ and $d=N_{1,1}^{AB} + 2N_{1,2}^{AB}$. This must be compared with $y^{N_1^A} x^{N_1^B} X^{N_2^B} b^d$ in our new notation. Hence defining the transformation

$$\begin{aligned} y &= \mu u^q, & x &= \nu u^{\frac{1}{2}q} \\ X &= \nu^2 u^q, & b &= 1/u \end{aligned} \quad (2.3.1)$$

will enable us to re-obtain $u^{q(r+t/2)-d} \mu^r \nu^t$ in a unique manner. This unique mapping shows that our notation is indeed adequate. Taking lattice embedding constants as well, our generating functions will provide all the necessary information as contained in equation (2.1.5).

PGF's are equivalent to the solution of the problem when the number of overturned spins in one sublattice is held constant. The advantage of this method over the direct one is that it enables us, given spin perturbations on one sublattice, to treat all configurations on the other sublattice simultaneously, as we shall see shortly.

From above, we have for the total generating function (GF) $F(x, X, y, b)$, which is clearly equivalent to $\ln \Lambda(\mu, \nu, u)$,

$$F(x, X, y, b) = \sum_{N_1^A, N_1^B, N_2^B, d} a[r, t, d] y^{N_1^A} x^{N_1^B} X^{N_2^B} b^d$$

where $a[r, t, d]$ is defined via (2.1.6). We can, thus, hold the number of y 's fixed and perturb spins on the B sublattice, so that

$$F(x, X, y, b) = \sum_{n \geq 0} y^n F_n(x, X, b) \quad (2.3.2)$$

with

$$F_n(x, X, b) = \sum_{N_1^B, N_2^B, d} a[r, t, d] x^{N_1^B} X^{N_2^B} b^d. \quad (2.3.3)$$

We can hold the number of x and X spins constant and vary those of y, in which case

$$F(x,X,y,b) = \sum_{n \geq 0} \sum_{\substack{\alpha, \beta \\ \text{s.t } \alpha + \beta = n}} x^\alpha X^\beta G_{\alpha, \beta}(y,b) \quad (2.3.4)$$

where

$$G_{\alpha, \beta}(y,b) = \sum_{N_1^A, d} a[r, \alpha + 2\beta, d] y^{N_1^A} b^d. \quad (2.3.5)$$

Note the double summation. This is because we fixed n spins on the B sublattice so that the total number of x and X spins has to add up to n, and in the second stage we varied the n for all positive integers.

Also, we can define from equation (2.3.4) the quantity

$$G_n(x,X,y,b) = \sum_{\substack{\alpha, \beta \\ \text{s.t } \alpha + \beta = n}} x^\alpha X^\beta G_{\alpha, \beta}(y,b) \quad (2.3.6)$$

so that

$$F(x,X,y,b) = \sum_{n \geq 0} G_n(x,X,y,b). \quad (2.3.7)$$

F_n and G_n are called PGF's. For further clarification of this technique, we give the following examples on the honeycomb lattice.

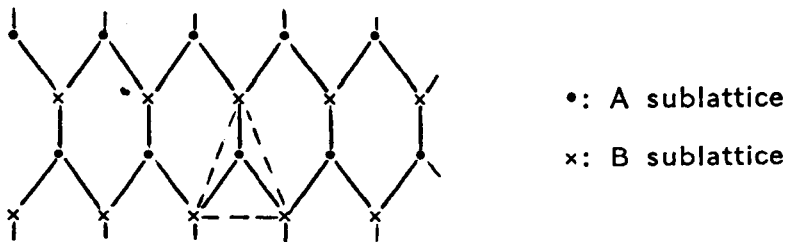
$F_0(x,X,b)$: This corresponds to configurations for which all perturbed spins are on the B sublattice and hence no bonds are created. If we perturb one spin on the B sublattice, it may be x or X, each occurring $N/2$ times; giving rise to the term $(x+X)/2$ as the coefficient of N. If we excite two spins on the B sublattice, they may be x^2 , xX or X^2 , occurring in $\frac{1}{2}(N/2)(N/2-1)$, $(N/2)(N/2-1)$, $\frac{1}{2}(N/2)(N/2-1)$ ways respectively; yielding the term $-(x+X)^2/4$ as the coefficient of N. A choice of three excited spins may give rise to x^3 , x^2X , xX^2 or X^3 , occurring respectively in $(1/3!)(N/2)(N/2-1)(N/2-2)$, $(1/2!)(N/2)(N/2-1)(N/2-2)$ and finally

$(1/3!)(N/2)(N/2-1)(N/2-2)$ ways; giving contribution $(x+X)^3/6$, and similarly for higher number of overturned spins on the B sublattice. Thus we have

$$F_0 = (x+X)/2 - (x+X)^2/4 + (x+X)^3/6 - \dots$$

$$= \frac{1}{2} \ln(1+x+X) .$$

$F_1(x, X, b)$: We now have one excited spin on the A sublattice and must consider the situation for increasing number of spins on B sublattice. The excited spin on A can be chosen in $N/2$ ways. It is surrounded by a triangular 'shadow' of three sites, in the sense that if any of these is perturbed a nearest neighbour bond will be formed.



If we 'select' α x-spins (i.e perturb α spins to form the x state) from the three sites in the shadow and β X-spins from the remaining $(3-\alpha)$ sites in the shadow, and ϵ x-spins from the remaining $(N/2-3)$ sites on B sublattice and finally η X-spins from $(N/2-3-\epsilon)$ remaining sites, we shall obtain the term (where $C_r^n = n!/r!(n-r)!$)

$$(N/2) C_\alpha^3 C_\beta^{3-\alpha} C_\epsilon^{N/2-3} C_\eta^{N/2-3-\epsilon}$$

$$(bx)^\alpha (b^2X)^\beta x^\epsilon X^\eta$$

which when summed over all $\alpha, \beta, \epsilon, \eta$'s yields

$$(N/2)(1+bx+b^2X)^3 (1+x+X)^{N/2-3} .$$

Thus taking the coefficient of N , we have

$$F_1 = \frac{1}{2} (1+bx+b^2X)^3 (1+x+X)^{-3} .$$

Such quantities can be written down directly by just considering the shadow patterns formed when spins on a given sublattice are perturbed. As an example we consider $F_2(x,X,b)$ below.

$F_2(x,X,b)$: This corresponds to two perturbed spins on the A sublattice, each forming a triangular shadow which can meet at a vertex or be completely separate, as shown in Fig(2.1). Embedding constants are given for each case.



(a) vertex-to-vertex: $\frac{1}{2}(N/2) \times 6$ (b) separated: $\frac{1}{2}(N/2)(N/2-7)$

Fig(2.1): Shadows cast by two overturned spins of sublattice A (denoted by •) on the honeycomb lattice.

As is evident from this diagram, for the case (a); we have four sites which belong to the shadow of exactly one perturbed spin and one site which belongs to the shadow of exactly two excited spins. The remaining $(N/2-5)$ sites on the B sublattice can be occupied by perturbed x , X spins or by non-perturbed spins. This configuration has the count of $3N/2$, yielding the contribution

$$(3/2)(1+bx+b^2X)^4 (1+b^2x+b^4X) (1+x+X)^{-5}$$

as the coefficient of N . Similarly for the case (b) we obtain the contribution

$$(-7/4)(1+bx+b^2X)^6 (1+x+X)^{-6} .$$

Hence

$$F_2 = (3/2)(1+bx+b^2X)^4 (1+b^2x+b^4X) (1+x+X)^{-5} \\ - (7/4)(1+bx+b^2X)^6 (1+x+X)^{-6} .$$

Following the code notation of Sykes et al (1965), $F_n(x, X, b)$ may be written as a sum, over all possible shadow patterns, of terms each of the form

$$\rho.(\lambda, \alpha_1, \alpha_2, \dots) = \\ \rho \prod_{m=1,2,\dots} (1+b^m x + b^{2m} X)^{\alpha_m} (1+x+X)^{-\lambda} \quad (2.3.8)$$

where $\lambda = \sum_m \alpha_m$ is the total number of sites on the entire shadow, and ρ is the coefficient of N in the embedding constant of the corresponding shadow pattern. Here α_m , which is the number of sites in the B sublattice belonging to exactly m shadows, is restricted by the coordination number q of the lattice. In this code language, the PGF's F_n of our mixed spin model are identical with those of standard Ising ferromagnetic model (Sykes et al, 1965) whose general term is given by

$$\rho \prod_{m=1,2,\dots} (1+b^m x)^{\alpha_m} (1+x)^{-\lambda}$$

denoted by the same code $\rho.(\lambda, \alpha_1, \alpha_2, \dots)$. Having noted this it was possible to use published codes for PGF's F_n of spin-1/2 model (Sykes et al, 1965;1973, Betts et al, 1974) for the three lattices of interest, namely honeycomb, hydrogen peroxide and diamond, as data for our mixed spin model.

Let us now calculate the generating function F using PGF's $G_n(x, X, y, b)$ defined by (2.3.6,7).

$G_0(x, X, y, b)$: This corresponds to no overturned spins on the B sublattice and hence no bonds are formed. Similar procedures to the one used for $F_0(x, X, b)$ yields $G_0(y, b) \equiv G_0(x, X, y, b) = \frac{1}{2} \ln(1+y)$.

$G_1(x, X, y, b)$: Equation (2.3.6) implies $G_1 = xG_{1,0} + XG_{0,1}$. Now

(i) $G_{1,0}(y, b)$ corresponds to one excited spin on the B sublattice, in the x state, which can be selected in $N/2$ ways and whose three nearest neighbour sites may be occupied by perturbed y-spins or by non-perturbed spins. This implies the factor $(1+by)^3$ straight away, where 1 denotes occupation by non-perturbed spins. The remaining $(N/2-3)$ sites on the B sublattice may again be occupied by perturbed y-spins or not occupied by perturbed spins at all; yielding the factor $(1+y)^{N/2-3}$, as no bonds are formed. Thus, we have $G_{1,0} = \frac{1}{2}(1+by)^3(1+y)^{-3}$ as the coefficient of N in the contribution of $(N/2)(1+by)^3(1+y)^{N/2-3}$ to G_1 .

(ii) $G_{0,1}(y, b)$ corresponds to one X-spin on the B sublattice which can be created in $N/2$ ways. Clearly we get the same factor as above but with b replaced by b^2 , as bonds between X and y spins yield b^2 . Thus $G_{0,1} = \frac{1}{2}(1+b^2y)^3(1+y)^{-3}$. Hence G_1 can be written down immediately from (i) and (ii).

Unfortunately, spin-1/2 codes are not so useful for the PGF's G_n , as the relation between F and G_n via (2.3.6) is more complex. Here, sublattice B is being decorated with x and X-spins and configurations decorated only with x-spins will remain identical with those of the spin-1/2 model. So these known spin-1/2 Ising results do provide a starting point. In the code language, PGF's G_n can be written as a sum, over all possible decorated shadow patterns, of terms each of the form (where $\lambda = \sum_{m,l} \alpha_{m,l}$)

$$\rho \tau x^\alpha X^\beta (\lambda, \alpha_{1,0}, \alpha_{0,1}, \dots) = \prod_{m,l} (1+b^{m+2l}y)^{\alpha_{m,l}} (1+y)^{-\lambda} \quad (2.3.9)$$

with $\alpha+\beta \leq n$. In (2.3.9) $\alpha_{m,l}$ is the number of sites in A sublattice which belong to the shadow of 'm' x-spins and 'l' X-spins, and τ is the symmetry number of decoration (1 for x^2 and X^2 , 2 for xX , 3 for x^2X and xX^2 , etc.) .

There is also another shorter code notation for the G_n PGF's. Since different $\alpha_{m,l}$'s (e.g $\alpha_{0,1}$ and $\alpha_{2,0}$) may give rise to the same power of b in the expansion of a code (as given by (2.3.9)), we can replace the bracket code in (2.3.9) by

$$(\lambda, \alpha_1, \alpha_2, \dots) = \prod_{m=1,2,\dots} (1+b^m y)^{\alpha_m} (1+y)^{-\lambda} \quad (2.3.10)$$

with $\lambda = \sum_m \alpha_m$, which is similar to that of $F_n(x, X, b)$, as given by (2.3.10), in that each place in the bracket corresponds to a certain power of b. In equation (2.3.10), $\alpha_1 = \alpha_{1,0}$, $\alpha_2 = \alpha_{2,0} + \alpha_{0,1}$, \dots , $\alpha_k = \sum_{\substack{m,l \\ s.t. m+2l=k}} \alpha_{m,l}$.

The codes for PGF's G_n of the honeycomb and diamond lattices were obtained in the form (2.3.10) (Gaunt, private communications), and those for the hydrogen peroxide lattice remained to be calculated. In the manner outlined above, it was possible to derive G_n of orders 0 through 3 on the hydrogen peroxide lattice. As a further example to illustrate the technique and the code language, we shall derive the codes (as defined via (2.3.10)) for G_2 .

Hydrogen peroxide has a three-dimensional lattice structure with $q=3$. Its shadow lattice is the (three-dimensional) hypertriangular lattice ($q=6$), just as the triangular lattice constitutes the shadow

lattice of the honeycomb lattice. Hydrogen peroxide differs from the honeycomb lattice in that the plane of neighbours of \wedge vertex is rotated by 60° with respect to the plane of neighbours of the neighbouring vertex (Betts et al, 1974). Now from (2.3.6)

$$G_2(x, X, y, b) = x^2 G_{2,0} + xX G_{1,1} + X^2 G_{0,2} .$$

(i) $G_{2,0}(y, b)$: Here we have two perturbed x-spins on the B sublattice. Since each triangular shadow can meet only at a vertex (and at most three shadows can meet at each vertex); these two spins can either be well separated so that the shadows do not meet, in which case we obtain the contributing code to be (6,6), or they can be positioned such that the shadows meet at a vertex, giving contribution (5,4,1). The counts for each configuration can be read-off from the published codes for spin-1/2 Ising model on the hydrogen peroxide lattice (Betts et al, 1974). Thus $G_{2,0}(y, b) = (-7/4)(6,6) + (3/2)(5,4,1)$.

(ii) $G_{1,1}(y, b)$: This corresponds to one x and one X-spin perturbed on the B sublattice. Again the two configurational cases, as for (i), arise; yielding the codes (6,3,3) and (5,2,2,1) for each case respectively. Taking embedding constants into account as well gives $G_{1,1}(y, b) = 3(5,2,2,1) - (7/2)(6,3,3)$.

(iii) $G_{0,2}(y, b)$: This implies two excited X-spins on B sublattice. Similarly, we obtain the codes (6,0,6) and (5,0,4,0,1) for each case, respectively; yielding $G_{0,2}(y, b) = (-7/4)(6,0,6) + (3/2)(5,0,4,0,1)$, when configurational counts are included.

We can thus write down an expression for G_2 in the code language, as required.

Finally in this section we briefly discuss the use of both kinds of PGF's in determining the free energy expansion. Clearly, given

PGF's of one kind (say F_n) to order n_F , exact information on all spin perturbation of up to n_F spins is available. This is because the information is exact to order n_F on one sublattice and to all orders on the other. Thus, by expanding PGF F_0 to degree n_F in x and X , F_1 to degree n_F-1 , ..., F_n to degree 0 and making substitutions (2.3.1), one obtains more than enough information (as each X now becomes v^2) to determine all the polynomials $g_{r,t}$ with $r+t \leq n_F$. The use of both PGF's should therefore provide a useful check as the resulting polynomials should be identical through order $\min(n_F, n_G)$, n_G being the order up to which PGF's G_n are given. Moreover, due to sublattice symmetry, we have that the expansion of $y^i F_i$ at order j in x and X , is identical with that of G_j at order i in y . This is because for any fixed i spins on the A sublattice the term of order j in x and X corresponds to j spins on the B sublattice and vice versa. We shall refer to this as the principle of symmetry of PGF's. This principle enables us to obtain more terms in our expansion of the free energy, when simultaneous use of both PGF's is made. In fact, one now has exact information on all spin perturbations of up to $n_F + n_G + 1$ spins. This can be extracted from the following procedure: The total GF, which is equivalent to $\ln \Lambda$, is $F_0 + yF_1 + y^2F_2 + \dots + y^{n_F} F_{n_F} + y^{n_F+1} F_{n_F+1} + \dots + y^k F_k$, through order k , in which we have to expand F_0 to degree k , F_1 to degree $k-1$, ..., F_{n_F+1} to degree $k-n_F-1$, ... and finally F_k to degree 0 in x and X . The difficulty is that we have only the first n_F PGF's. But, using the principle of symmetry of PGF's, one notes that the expansion of F_{n_F+1} to degree $k-n_F-1$ in x and X is equivalent to the expansion of $(G_0 + G_1 + \dots + G_{k-n_F-1})$ at degree n_F+1 in y ; ...; and the expansion of F_k to degree 0 in x and X is equivalent to that of G_0 at degree k in

y. Thus in order to use up all the G_n we must have $k - n_F - 1 = n_G$, whence $k = n_F + n_G + 1$.

Procedures of the above kind have been used for all the three lattices of interest. Details are tabulated below.

Lattice	n_F	n_G	$r+t \leq$
Honeycomb	10	5	16
Hydrogen peroxide	11	3	15
Diamond	8	5	14

Table 2.1

Polynomials $g_{r,t}$ have been worked out by Yousif (1983) for the honeycomb lattice only through order $r+t \leq 10$, because of his improper use of the symmetry principle of PGF's (in his case $n_G=3$ and $n_F=10$, so the maximum achievable order was $r+t \leq 14$). In the next section we give the polynomials $g_{r,t}$ through orders listed in table 2.1, except for the honeycomb lattice, for which results are presented from order 10 through 16. Those of order 0 through 10 can be found in related literature (Yousif, 1983).

2.4 Some results: Free energy polynomials

Polynomials $g_{r,t}$, which are obtained simply by picking coefficients of $\mu^r \nu^t$ in the free energy expansion, are listed in table 2.2.

Table 2.2: Low-temperature polynomials $g_{r,t}(u)$ for two- and three-dimensional lattices. For honeycomb and hydrogen peroxide lattices, u is replaced by $z = \sqrt{u}$.

<u>Honeycomb Lattice</u>		
<u>$r + t = 11:$</u>		
<u>r</u>	<u>t</u>	<u>$g_{r,t}(z)$</u>
0	11	$1/22 z^{33}$
1	10	$- 9/22 z^{24} + 27/2 z^{26} + 9 z^{28} - 63 z^{30} + 54 z^{32} + 6 z^{34}$ $- 15 z^{36}$
2	9	$6 z^{17} - 147/2 z^{19} + 245/2 z^{21} + 945 z^{23} - 7695/2 z^{25}$ $+ 7089/2 z^{27} + 10233/2 z^{29} - 24867/2 z^{31} + 7435 z^{33}$ $+ 1581/2 z^{35} - 4119/2 z^{37} + 454 z^{39}$
3	8	$3 z^{14} + 3/2 z^{16} + 489/2 z^{18} - 975 z^{20} - 5031 z^{22}$ $+ 51019/2 z^{24} + 5238 z^{26} - 214614 z^{28} + 992573/2 z^{30}$ $- 948255/2 z^{32} + 111279 z^{34} + 155451 z^{36} - 131721 z^{38}$ $+ 33741 z^{40} - 2571/2 z^{42}$
4	7	$15/2 z^{15} + 45 z^{17} + 879/2 z^{19} + 135 z^{21} - 14865 z^{23}$ $+ 942 z^{25} + 190155 z^{27} - 188928 z^{29} - 2932875/2 z^{31}$ $+ 5191152 z^{33} - 7914789 z^{35} + 6579132 z^{37} - 2896353 z^{39}$ $+ 461661 z^{41} + 87351 z^{43} - 59295/2 z^{45}$
5	6	$3/2 z^{16} + 21/2 z^{18} + 267/2 z^{20} + 891/2 z^{22} - 3028 z^{24}$ $- 35433/2 z^{26} + 94911/2 z^{28} + 182643 z^{30} - 513735/2 z^{32}$ $- 6160203/2 z^{34} + 26132417/2 z^{36} - 49185573/2 z^{38}$ $+ 26663061 z^{40} - 34983253/2 z^{42} + 6721257 z^{44}$ $- 1332516 z^{46} + 186853/2 z^{48}$
6	5	$3/2 z^{21} + 33/2 z^{23} - 45 z^{25} - 632 z^{27} - 4557 z^{29}$ $+ 67899/2 z^{31} - 36476 z^{33} + 391401/2 z^{35} - 2420481 z^{37}$ $+ 10007461 z^{39} - 42907497/2 z^{41} + 54931467/2 z^{43}$ $- 21830261 z^{45} + 10552107 z^{47} - 5655591/2 z^{49}$ $+ 638053/2 z^{51}$

Table 2.2 continued

<u>r</u>	<u>t</u>	<u>$g_{r,t}(z)$</u>
7	4	$39 z^{30} - 969/2 z^{32} + 8895/2 z^{34} - 41529/2 z^{36}$ $+ 189045/2 z^{38} - 542706 z^{40} + 2207751 z^{42} - 5441481 z^{44}$ $+ 16565517/2 z^{46} - 15772965/2 z^{48} + 9166029 z^{50}$ $- 1486686 z^{52} + 412143/2 z^{54}$
8	3	$- 218 z^{39} + 2565 z^{41} - 19098 z^{48} + 99596 z^{45}$ $- 326214 z^{47} + 654570 z^{49} - 804300 z^{51} + 590670 z^{53}$ $- 238095 z^{55} + 40524 z^{57}$
9	2	$217 z^{48} - 2079 z^{50} + 8262 z^{52} - 16890 z^{54} + 18630 z^{56}$ $- 21087/2 z^{58} + 4807/2 z^{60}$
10	1	$- 18 z^{57} + 135/2 z^{59} - 165/2 z^{61} + 33 z^{63}$
11	0	$1/22 z^{66}$

$r + t = 12:$

<u>r</u>	<u>6</u>	<u>$g_{r,t}(z)$</u>
0	12	$- 1/12 z^{36}$
1	11	$9/2 z^{27} + 9/2 z^{29} - 54 z^{31} + 63 z^{33} + 12 z^{35} - 45 z^{37}$ $15 z^{39}$
2	10	$3/2 z^{18} - 30 z^{20} + 423/4 z^{22} + 465 z^{24} - 5985/2 z^{26}$ $+ 3753 z^{28} + 23013/4 z^{30} - 18486 z^{32} + 13905 z^{34}$ $+ 2820 z^{36} - 33003/4 z^{38} + 3609 z^{40} - 453/4 z^{42}$
3	9	$7/2 z^{15} - 9 z^{17} + 261 z^{19} - 2965/2 z^{21} - 4311 z^{23}$ $+ 38295 z^{25} - 196391/6 z^{27} - 255564 z^{29} + 811746 z^{31}$ $- 940202 z^{33} + 439047/2 z^{35} + 546885 z^{37}$ $- 1122881/2 z^{39} + 380367/2 z^{41} - 4176 z^{43} - 20942/2 z^{45}$
4	8	$51/2 z^{16} + 78 z^{18} + 795 z^{20} - 1209 z^{22} - 67677/2 z^{24}$ $+ 48426 z^{26} + 423402 z^{28} - 1060479 z^{30} - 1937745 z^{32}$ $- 12259149 z^{34} - 47144259/2 z^{36} + 23520756 z^{38}$ $- 96474747/8 z^{40} + 1647801 z^{42} + 2613237/2 z^{44}$ $- 615678 z^{46} + 586971/8 z^{48}$

Table 2.2 continued

<u>r</u>	<u>t</u>	<u>$g_{r,t}(z)$</u>
5	7	$21/2 z^{17} + 165/2 z^{19} + 564 z^{21} + 1725/2 z^{23} - 17370 z^{25}$ $- 1109661/2 z^{27} + 596481/2 z^{29} + 1192797/2 z^{31}$ $- 3080247 z^{33} - 9849045/2 z^{35} + 91478103/2 z^{37}$ $- 223615389/2 z^{39} + 148690428 z^{41} - 119989953 z^{43}$ $+ 117262425/2 z^{45} - 15861069 z^{47} + 3504591/2 z^{49}$ $+ 54381/2 z^{51}$
6	6	$1/2 z^{18} + 117/2 z^{22} + 159 z^{24} - 768 z^{26} - 21129/2 z^{28}$ $- 17833/2 z^{30} + 255048 z^{32} - 342729/2 z^{34}$ $- 1682375/2 z^{36} - 33279669/4 z^{38} + 58424082 z^{40}$ $- 159454725 z^{42} + 497101155/2 z^{44} - 972728919/4 z^{46}$ $+ 151691418 z^{48} - 58188876 z^{50} + 24658419/2 z^{52}$ $- 1072004 z^{54}$
7	5	$6 z^{27} - 387/2 z^{29} + 747/2 z^{31} - 9369/2 z^{33}$ $+ 133581/2 z^{35} - 258204 z^{37} + 1535487/2 z^{39}$ $- 10150071/2 z^{41} + 51475005/2 z^{43} - 74656749 z^{45}$ $+ 265243485/2 z^{47} - 151125345 z^{49} + 222547959/2 z^{51}$ $- 102437463/2 z^{53} + 26756169/2 z^{55} - 3014559/2 z^{57}$
8	4	$- 813/4 z^{36} + 3030 z^{38} - 23538 z^{40} + 124800 z^{42}$ $- 5368575/8 z^{44} + 3193650 z^{46} - 10420515 z^{48}$ $- 21974850 z^{50} - 240280875/8 z^{52} + 26488704 z^{54}$ $- 14559600 z^{56} + 4536678 z^{58} - 1223349/2 z^{60}$
9	3	$1943/2 z^{45} - 8595 z^{47} + 64197 z^{49} - 303072 z^{51}$ $+ 892179 z^{53} - 1642932 z^{55} + 3781041/2 z^{57} - 1320363 z^{59}$ $+ 1023957/2 z^{61} - 253682/3 z^{63}$
10	2	$- 855/2 z^{54} + 3906 z^{56} - 14715 z^{58} + 28710 z^{60}$ $- 121935/4 z^{62} + 16731 z^{64} - 14883/4 z^{66}$
11	1	$45/2 z^{63} - 165/2 z^{65} + 99 z^{67} - 39 z^{69}$
12	0	$- 1/24 z^{72}$

Table 2.2 continued

r + t = 13:

<u>r</u>	<u>t</u>	<u>$g_{r,t}(z)$</u>
0	13	$1/26 z^{39}$
1	12	$3/2 z^{30} - 27 z^{32} + 54 z^{34} + 14 z^{36} - 90 z^{38} + 45 z^{40}$ $+ 5/2 z^{42}$
2	11	$- 15/2 z^{21} + 99/2 z^{23} + 321/2 z^{25} - 3645/2 z^{27}$ $+ 3294 z^{29} + 9693/2 z^{31} - 43479/2 z^{33} + 20439 z^{35}$ $+ 12495/2 z^{37} - 43245/2 z^{39} + 22563/2 z^{41} - 759/2 z^{43}$ $- 747 z^{45}$
3	10	$3 z^{16} - 33/2 z^{18} + 483/2 z^{20} - 1695 z^{22}$ $- 2117 z^{24} + 43929 z^{26} - 163359/2 z^{28} - 228307 z^{30}$ $+ 2201625/2 z^{32} - 3138711/2 z^{34} + 398361 z^{36}$ $+ 1416300 z^{38} - 3478377/2 z^{40} + 709450 z^{42} + 31860 z^{44}$ $- 190791/2 z^{46} + 33595/2 z^{48}$
4	9	$57 z^{17} + 51 z^{19} + 1106 z^{21} - 8487/2 z^{23} - 58797 z^{25}$ $+ 175710 z^{27} + 1314549/2 z^{29} - 3006342 z^{31} - 371200 z^{33}$ $+ 45113529/2 z^{35} - 56441625 z^{37} + 134354709/2 z^{39}$ $- 39101175 z^{41} + 3076749 z^{43} + 20129889/2 z^{45}$ $- 5875416 z^{47} + 1199088 z^{49} - 100601/2 z^{51}$
5	8	$135/2 z^{18} + 603/2 z^{20} + 1311 z^{22} - 213 z^{24} - 65313 z^{26}$ $- 195831/2 z^{28} + 2499321/2 z^{30} + 611364 z^{32}$ $- 27079677/2 z^{34} + 15839037/2 z^{36} + 225735795/2 z^{38}$ $- 770558061/2 z^{40} + 628137825 z^{42} - 1214892765/2 z^{44}$ $+ 356718753 z^{46} - 116381097 z^{48} + 26535387/2 z^{50}$ $+ 2712840 z^{52} - 677442 z^{54}$
6	7	$9/2 z^{19} + 57 z^{21} + 807/2 z^{23} + 1491/2 z^{25} - 9708 z^{27}$ $- 138951/2 z^{29} + 204939/2 z^{31} + 1428327 z^{33}$ $- 1998480 z^{35} - 21925659/2 z^{37} + 1529471/2 z^{39}$ $+ 440226669/2 z^{41} - 1673207097/2 z^{43} + 1604346101 z^{45}$

Table 2.2 continued

<u>r</u>	<u>t</u>	<u>$g_{r,t}(z)$</u>
7	6	$- 1895633901 z^{47} + 1451553957 z^{49} - 715548927 z^{51}$ $+ 214610646 z^{53} - 34023972 z^{55} + 3860121/2 z^{57}$ $2 z^{24} + 117/2 z^{26} - 255 z^{28} - 5081/2 z^{30} - 10299/2 z^{32}$ $+ 60351/2 z^{34} + 1030053/2 z^{36} - 2237064 z^{38}$ $+ 5494947/2 z^{40} - 43242803/2 z^{42} + 178148589 z^{44}$ $- 1318428915/2 z^{46} + 2800336633/2 z^{48} - 1896496383 z^{50}$ $+ 1700089926 z^{52} - 1005770175 z^{54} + 376738317 z^{56}$ $- 160950153/2 z^{58} + 7384618 z^{60}$
8	5	$- 201/2 z^{33} + 1311 z^{35} - 16431/2 z^{37} + 167829/2 z^{39}$ $- 1073475/2 z^{41} + 4231875/2 z^{43} - 9739833 z^{45}$ $+ 49844313 z^{47} - 181114461 z^{49} + 426373053 z^{51}$ $- 1324317981/2 z^{53} + 1376495541/2 z^{55} - 949772667/2 z^{57}$ $+ 417721113/2 z^{59} - 52963623 z^{61} + 11762877/2 z^{63}$
9	4	$1807/2 z^{42} - 13746 z^{44} + 215745/2 z^{46} - 1298577/2 z^{48}$ $- 6934869/2 z^{50} - 14227857 z^{52} + 40076931 z^{54}$ $- 75534030 z^{56} + 189987633/2 z^{58} - 157415115/2 z^{60}$ $+ 82518711/2 z^{62} - 24803961/2 z^{64} + 1628146 z^{66}$
10	3	$- 1803 z^{51} + 25398 z^{53} - 183555 z^{55} + 799797 z^{57}$ $- 2173545 z^{59} + 7491825/2 z^{61} - 8178841/2 z^{63}$ $+ 5479155/2 z^{65} - 2055339/2 z^{67} + 165308 z^{69}$
11	2	$1557/2 z^{60} - 6831 z^{62} + 49335/2 z^{64} - 46365 z^{66}$ $- 51051/2 z^{70} + 11115/2 z^{72}$
12	1	$- 55/2 z^{69} + 99 z^{71} - 117 z^{73} + 91/2 z^{75}$
13	0	$1/26 z^{78}$
<u>$r + t = 14:$</u>		
<u>r</u>	<u>t</u>	<u>$g_{r,t}(z)$</u>
0	14	$1/28 z^{42}$

Table 2.2 continued

r	t	$g_{r,t}(z)$
1	13	$- 9 z^{33} + 27 z^{35} + 12 z^{37} - 105 z^{39} + 90 z^{41} + 15/2 z^{43} - 45/2 z^{45}$
2	12	$53/4 z^{24} + 33 z^{26} - 3435/4 z^{28} + 2281 z^{30} + 3015 z^{32} - 20268 z^{34} + 48813/2 z^{36} + 9528 z^{38} - 41685 z^{40} + 27965 z^{42} - 903/4 z^{44} - 5487 z^{46} + 5131/4 z^{48}$
3	11	$3/2 z^{17} - 33/2 z^{19} + 371/2 z^{21} - 3045/2 z^{23} + 297 z^{25} + 39356 z^{27} - 118719 z^{29} - 133146 z^{31} + 2495031/2 z^{33} - 4482075/2 z^{35} + 702057 z^{37} + 2854498 z^{39} - 4189548 z^{41} + 3968109/2 z^{43} + 306068 z^{45} - 1256013/2 z^{47} + 188613 z^{49} - 10650 z^{51}$
4	10	$195/2 z^{18} - 111 z^{20} + 1359 z^{22} - 8334 z^{24} - 80655 z^{26} + 397443 z^{28} + 2613579/4 z^{30} - 6018477 z^{32} + 22834251/4 z^{34} + 31878909 z^{36} - 111301557 z^{38} + 158844276 z^{40} - 417355983/4 z^{42} - 353649 z^{44} + 204031545/4 z^{46} - 35218227 z^{48} + 37440249/4 z^{50} - 359736 z^{52} - 688995/4 z^{54}$
5	9	$6 z^{17} + 240 z^{19} + 582 z^{21} + 3381/2 z^{23} - 12189/2 z^{25} - 358989/2 z^{27} + 627 z^{29} + 7459491/2 z^{31} - 6300151/2 z^{33} - 37724772 z^{35} + 158423565/2 z^{37} + 353798251/2 z^{39} - 2066088543/2 z^{41} + 2096937249 z^{43} - 4802967735/2 z^{45} + 3284705715/2 z^{47} - 602499615 z^{49} + 42763159 z^{51} + 53103912 z^{53} - 37504977/2 z^{55} + 3679405/2 z^{57}$
6	8	$69 z^{20} + 402 z^{22} + 3083 z^{24} - 15/2 z^{26} - 126489/2 z^{28} - 537245/2 z^{30} + 4368801/4 z^{32} + 11271663/2 z^{34} - 17003278 z^{36} - 95805153/2 z^{38} + 643199655/4 z^{40} + 930088553/2 z^{42} - 3195239523 z^{44} + 15526078005/2 z^{46} - 44034811737/4 z^{48} + 20133201945/2 z^{50}$

Table 2.2 continued

<u>r</u>	<u>t</u>	<u>$g_{r,t}(z)$</u>
		- 12057735141/2 z^{52} + 4564025387/2 z^{54} - 489649731 z^{56} + 42605622 z^{58} + 3459851/4 z^{60}
7	7	39/2 z^{23} + 141/2 z^{25} + 1317/2 z^{27} - 4596 z^{29} - 29808 z^{31} - 35511 z^{33} + 1526973/2 z^{35} + 2202819 z^{37} - 16710456 z^{39} + 12388023/2 z^{41} + 16894755/2 z^{43} + 711137262 z^{45} - 3949838445 z^{47} + 145672739649/14 z^{49} - 33575622027/2 z^{51} + 17945362221 z^{53} - 12980468829 z^{55} + 6266087736 z^{57} - 3835754715/2 z^{59} + 331190433 z^{61} - 333280755/14 z^{63}
8	6	- 25/2 z^{30} - 288 z^{32} - 4287/2 z^{34} + 17125 z^{36} - 23463/2 z^{38} + 722616 z^{40} - 6224004 z^{42} + 20290551 z^{44} - 142431225/2 z^{46} + 434367732 z^{48} - 3867903093/2 z^{50} + 5325373023 z^{52} - 9550787739 z^{54} + 1159745443 z^{56} - 19301699181/2 z^{58} + 5429346461 z^{60} - 1972396815 z^{62} + 416498376 z^{64} - 38630893 z^{66}
9	5	1257/2 z^{39} - 17127/2 z^{41} + 161265/2 z^{43} - 1299657/2 z^{45} + 3527049 z^{47} - 32355891/2 z^{49} + 78509533 z^{51} - 656173899/2 z^{53} + 1953576009/2 z^{55} - 3983899777/2 z^{57} + 2792993247 z^{49} - 5388452967/2 z^{61} + 3517166997/2 z^{63} - 1484400093/2 z^{65} + 365448987/2 z^{67} - 19907381 z^{69}
10	4	- 13593/4 z^{48} + 53004 z^{50} - 1776783/4 z^{52} + 2831142 z^{54} - 14271507 z^{56} + 52234776 z^{58} - 264354651/2 z^{60} + 228654558 z^{62} - 1076173923/4 z^{64} + 211648437 z^{66} - 213042687/2 z^{68} + 31010499 z^{70} - 15884661/4 z^{72}
11	3	4671 z^{57} - 66924 z^{59} + 463617 z^{61} - 1893342 z^{63} + 4834038 z^{65} - 15803997/2 z^{67} + 8261825 z^{69} - 10687677/2 z^{71} + 1948089 z^{73} - 306137 z^{75}
12	2	- 1331 z^{66} + 11286 z^{68} - 157509/4 z^{70} + 71786 z^{72} - 287937/4 z^{74} + 37674 z^{76} - 16107/2 z^{78}

Table 2.2 continued

<u>r</u>	<u>t</u>	<u>$g_{r,t}(z)$</u>
13	1	$33 z^{75} - 117 z^{77} + 273/2 z^{79} - 105/2 z^{81}$
14	0	$- 1/28 z^{84}$
<u>$r + t = 15:$</u>		
<u>r</u>	<u>t</u>	<u>$g_{r,t}(z)$</u>
0	15	$- 1/15 z^{45}$
1	14	$9 z^{36} + 6 z^{38} - 90 z^{40} + 105 z^{42} + 15 z^{44} - 135/2 z^{46}$ $+ 45/2 z^{48}$
2	13	$3 z^{27} - 555/2 z^{29} + 2439/2 z^{31} + 2583/2 z^{33} - 30213/2$ $z^{35} + 23679 z^{37} + 21081/2 z^{39} - 122799/2 z^{41} + 52110 z^{43}$ $+ 2895/2 z^{45} - 43269 z^{47} + 17073/2 z^{49} - 819/2 z^{51}$
3	12	$1/2 z^{18} - 9 z^{20} + 114 z^{22} - 2113/2 z^{24} + 1710 z^{26}$ $+ 54957/2 z^{28} - 126185 z^{30} - 24039/2 z^{32} + 1183362 z^{34}$ $- 2755810 z^{36} + 1180323 z^{38} + 9231861/2 z^{40} - 8177251$ $z^{42} + 8898921/2 z^{44} + 1304682 z^{46} - 5315509/2 z^{48}$ $+ 1072557 z^{50} - 80364 z^{52} - 50337/2 z^{54}$
4	11	$249/2 z^{19} - 417 z^{21} + 3537/2 z^{23} - 24237/2 z^{25}$ $- 89136 z^{27} + 670950 z^{29} + 161997 z^{31} - 18474615/2 z^{33}$ $+ 17842470 z^{35} + 63708765 z^{37} - 183307380 z^{39} +$ $318575673 z^{41} - 476058357/2 z^{43} - 43172193/2 z^{45}$ $+ 190189041 z^{47} - 303587427/2 z^{49} + 47084994 z^{51}$ $+ 770547 z^{53} - 3641118 z^{55} + 544518 z^{57}$
5	10	$3/2 z^{16} + 24 z^{18} + 579 z^{20} + 909/2 z^{22} + 609/2 z^{24}$ $- 18621 z^{26} - 765981/2 z^{28} + 596922 z^{30} + 16652193/2 z^{32}$ $- 37539249/2 z^{34} - 71896521 z^{36} + 576490281/2 z^{38}$ $+ 269516748/5 z^{40} - 4335051363/2 z^{42} + 5694190821 z^{44}$ $- 7713421434 z^{46} + 6043103517 z^{48} - 11937716592/5 z^{50}$ $- 138698439/2 z^{52} + 537938874 z^{54} - 235441713 z^{56}$ $+ 79292193/2 z^{58} - 8015286/5 z^{60}$

Table 2.2 continued

<u>r</u>	<u>t</u>	<u>$g_{r,t}(z)$</u>
6	9	$18 z^{19} + 390 z^{21} + 1590 z^{23} + 2352 z^{25} + 13441 z^{27}$ $- 257028 z^{29} - 656583 z^{31} + 5847679 z^{33} + 29029083/2 z^{35}$ $- 91100082 z^{37} - 182074505/2 z^{39} + 924039030 z^{41} -$ $270360189/2 z^{43} - 26508148787/3 z^{45} + 58199014047/2 z^{47}$ $- 99578446899/2 z^{49} + 53579669273 z^{51} - 75464981079/2$ $z^{53} + 16939199856 z^{55} - 4303876991 z^{57} + 693968067/2 z^{59}$ $+ 86487477 z^{61} - 98209241/6 z^{63}$
7	8	$57/2 z^{22} + 429/2 z^{24} + 915 z^{26} + 2937/2 z^{28} - 86925/2$ $z^{30} - 214176 z^{32} + 211566 z^{34} + 6274305 z^{36} + 1673970$ $z^{38} - 103057545 z^{40} + 153922887/2 z^{42} + 613949958 z^{44}$ $+ 1809325185/2 z^{46} - 16166754999 z^{48} + 113489214891/2$ $z^{50} - 110412522426 z^{52} + 278812807353/2 z^{54}$ $- 119856835614 z^{56} + 141057186159/2 z^{58} - 55298025651/2$ $z^{60} + 13491344121/2 z^{62} - 881757468 z^{64} + 82371585/2 z^{66}$
8	7	$18 z^{27} - 48 z^{29} + 435/2 z^{31} - 23799/2 z^{33} - 19863/2 z^{35}$ $+ 390795/2 z^{37} + 943047 z^{39} + 561852 z^{41} - 47074332 z^{43}$ $+ 303831825/2 z^{45} - 520142199/2 z^{47} + 4151602587/2 z^{49}$ $- 26755703487/2 z^{51} + 45706415190 z^{53} - 96527683668 z^{55}$ $+ 136669264887 z^{57} - 268432535853/2 z^{59} + 183781369041/2$ $z^{61} - 43005544905 z^{63} + 13068371427 z^{65} - 2306980056$ $z^{67} + 177341847 z^{69}$
9	6	$613/6 z^{36} - 3525/2 z^{38} + 62031/2 z^{40} - 168891 z^{42}$ $+ 1184964 z^{44} - 10731201 z^{46} + 109362837/2 z^{48}$ $- 411497031/2 z^{50} + 947712954 z^{52} - 26372143633/6 z^{54}$ $+ 29481521289/2 z^{56} - 33700997832 z^{58} + 106714225107/2$ $z^{60} - 118689370311/2 z^{62} + 92676315045/2 z^{64}$ $- 49788545937/2 z^{66} + 17520210129/2 z^{68} - 3630494553/2$

Table 2.2 continued

<u>r</u>	<u>t</u>	<u>$g_{r,t}(z)$</u>
		$z^{70} + 334929271/2 z^{72}$
10	5	$- 6171/2 z^{45} + 100305/2 z^{47} - 514251 z^{49} + 3747441 z^{51}$ $- 41047101/2 z^{53} + 1021159803/10 z^{55} - 465749229 z^{57}$ $+ 1673503821 z^{59} - 8675442567/2 z^{61} + 7948410195 z^{63}$ $- 102782444919/10 z^{65} + 9319558599 z^{67} - 5798773305 z^{69}$ $+ 2358389370 z^{71} - 1129022169/2 z^{73} + 602647221/10 z^{75}$
11	4	$11307 z^{54} - 368979/2 z^{56} + 3278517/2 z^{58} - 10505550 z^{60}$ $+ 49561479 z^{62} - 331636239/2 z^{64} + 386375979 z^{66}$ $- 1248938691/2 z^{68} + 695731608 z^{70} - 523848897 z^{72}$ $+ 509007213/2 z^{74} - 72010029 z^{76} + 18026385/2 z^{78}$
12	3	$- 11231 z^{63} + 159885 z^{65} - 1061940 z^{67} + 4112625 z^{69}$ $- 9985833 z^{71} + 15632331 z^{73} - 15764021 z^{75} + 9895158$ $z^{77} - 3518580 z^{79} + 541606 z^{81}$
13	2	$4323/2 z^{72} - 35607/2 z^{74} + 60372 z^{76} - 107289 z^{78}$ $+ 210483/2 z^{80} - 54054 z^{82} + 22743/2 z^{84}$
14	1	$- 39 z^{81} + 273/2 z^{83} - 315/2 z^{85} + 60 z^{87}$
15	0	$1/30 z^{90}$
<u>$r + t = 16:$</u>		
<u>r</u>	<u>t</u>	<u>$g_{r,t}(z)$</u>
0	16	$1/32 z^{48}$
1	15	$2 z^{39} - 45 z^{41} + 90 z^{43} + 35/2 z^{45} - 135 z^{47} + 135/2 z^{49}$ $+ 3 z^{51}$
2	14	$- 225/4 z^{30} + 441 z^{32} + 1281/4 z^{34} - 8760 z^{36} + 18765$ $z^{38} + 8358 z^{40} - 285783/4 z^{42} + 75789 z^{44} + 10125/2 z^{46}$ $- 56115 z^{48} + 125181/4 z^{50} - 1932 z^{52} - 1722 z^{54}$
3	13	$- 3 z^{21} + 48 z^{23} - 1113/2 z^{25} + 1754 z^{27} + 29421/2 z^{29}$ $- 103530 z^{31} + 80664 z^{33} + 933021 z^{35} - 5845875/2 z^{37}$ $+ 3583889/2 z^{39} + 6095247 z^{41} - 13258299 z^{43} + 8342996$ $z^{45} + 3682863 z^{47} - 16387629/2 z^{49} + 8137881/2 z^{51}$

Table 2.2 continued

<u>r</u>	<u>t</u>	<u>$g_{r,t}(z)$</u>
4	12	$ \begin{aligned} & - 529641/2 z^{53} - 671289/2 z^{55} + 67417 z^{57} \\ & 249/2 z^{20} - 714 z^{22} + 2508 z^{24} - 14523 z^{26} \\ & - 317619/2 z^{28} + 898784 z^{30} - 852456 z^{32} - 11141958 z^{34} \\ & + 276150215/8 z^{36} + 137 23737 z^{38} - 506908221/2 z^{40} \\ & + 550764801 z^{42} - 1904895177/4 z^{44} - 75909978 z^{46} \\ & + 1111346629/2 z^{48} - 507311112 z^{50} + 1390335177/8 z^{52} \\ & + 22362127 z^{54} - 35101215 z^{56} + 8877180 z^{58} - 1047969/2 \\ & z^{60} \end{aligned} $
5	11	$ \begin{aligned} & 6 z^{17} + 93/2 z^{19} + 1038 z^{21} - 1821/2 z^{23} - 7413/2 z^{25} \\ & - 31494 z^{27} - 1328625/2 z^{29} + 4368855/2 z^{31} + 28411125/2 \\ & z^{33} - 57715317 z^{35} - 84828626 z^{37} + 713074041 z^{39} \\ & - 1348394223/2 z^{41} - 6917981511/2 z^{43} + 25626452007/2 \\ & z^{45} - 20705997276 z^{47} + 18473761722 z^{49} \\ & - 15354281913/2 z^{51} - 2958101391/2 z^{53} + 7162929915/2 \\ & z^{55} - 3676382079/2 z^{57} + 400267353 z^{59} - 17114610 z^{61} \\ & - 8496693/2 z^{63} \end{aligned} $
6	10	$ \begin{aligned} & 6 z^{18} + 108 z^{20} + 1455 z^{22} + 7295/2 z^{24} - 23907/4 z^{26} \\ & - 121473/2 z^{28} - 2993765/4 z^{30} - 833532 z^{32} + 21594921 \\ & z^{24} + 34361825/2 z^{36} - 677184471/2 z^{38} + 262076739/2 \\ & z^{40} + 3121654919 z^{42} - 10875902133/2 z^{44} - 16094379039 \\ & z^{46} + 172003993561/2 z^{48} - 724098935019/4 z^{50} \\ & + 456082352673/2 z^{52} - 740923089025/4 z^{54} + 94965229917 \\ & z^{56} - 104851703979/4 z^{58} + 510389779 z^{60} + 8202187305/4 \\ & z^{62} - 1133305917/2 z^{64} + 46842014 z^{66} \end{aligned} $
7	9	$ \begin{aligned} & 37/2 z^{21} + 519/2 z^{23} + 3615/2 z^{25} + 3024 z^{27} - 13701 z^{29} \\ & - 257430 z^{31} - 920189 z^{33} + 7252263/2 z^{35} + 31429674 z^{37} \\ & - 98420087/2 z^{39} - 954949095/2 z^{41} + 1835140341/2 z^{43} \\ & + 3515902773 z^{45} - 15524659947/2 z^{47} - 41091986628 z^{49} \\ & + 231784206794 z^{51} - 559604983518 z^{53} + 833971255668 \\ & z^{55} - 1677206241945/2 z^{57} + 1164177139881/2 z^{59} \end{aligned} $

Table 2.2 continued

r	t	$g_{r,t}(z)$
8	8	$ \begin{aligned} & -275281723919 z^{61} + 168536159289 /_2 z^{63} - 14774751558 \\ & z^{65} + 2034796029 /_2 z^{67} + 28728560 z^{69} \\ & 9 /_2 z^{24} + 24 z^{26} + 351 z^{28} - 105 z^{30} - 31875 /_4 z^{32} \\ & - 274875 /_2 z^{34} + 116163 /_2 z^{36} + 5049471 /_2 z^{38} \\ & + 74707845 /_8 z^{40} - 41795487 z^{42} - 486964965 /_2 z^{44} \\ & + 1089688803 z^{46} - 401199081 z^{48} + 2841938460 z^{50} \\ & - 117459049329 /_2 z^{52} + 279293516826 z^{54} \\ & - 11461419709629 /_{16} z^{56} + 1188044777049 z^{58} \\ & - 2722395969189 /_2 z^{60} + 1102185125352 z^{62} \\ & - 1257610166499 /_2 z^{64} + 492207337815 /_2 z^{66} \\ & - 62281502859 z^{68} + 18033609729 /_2 z^{70} \\ & - 8767874529 /_{16} z^{72} \\ & - 83 z^{33} - 279 /_2 z^{35} - 7170 z^{37} + 31748 z^{39} \\ & + 762789 /_2 z^{41} - 1011099 z^{43} + 4946397 /_2 z^{45} \\ & - 175688805 /_2 z^{47} + 541239510 z^{49} - 1672499253 z^{51} \\ & + 13250860713 /_2 z^{53} - 73409675637 /_2 z^{55} \\ & + 148164675391 z^{57} - 392702075043 z^{59} \\ & + 1421644528941 /_2 z^{61} - 907841484108 z^{63} \\ & + 1658748442701 /_2 z^{65} - 1079373441561 /_2 z^{67} \\ & + 244216674649 z^{69} - 145800174771 /_2 z^{71} + 12858010878 \\ & z^{73} - 1008835664 z^{75} \end{aligned} $
9	7	$ \begin{aligned} & - 2273 /_2 z^{42} + 49083 /_2 z^{44} - 514965 /_2 z^{46} \\ & + 1828682 z^{48} - 57214383 /_4 z^{50} + 182904759 /_2 z^{52} \\ & - 423609270 z^{54} + 1833862938 z^{56} - 33038057481 /_4 z^{58} \\ & + 62946897453 /_2 z^{60} - 176297290719 /_2 z^{62} + 176469849528 \\ & z^{64} - 253576746091 z^{66} + 524685931815 /_2 z^{68} \\ & - 193901071212 z^{70} + 99915159305 z^{72} - 68176963659 /_2 \\ & z^{74} + 6914220018 z^{76} - 630181679 z^{78} \end{aligned} $
10	6	$ \begin{aligned} & - 2273 /_2 z^{42} + 49083 /_2 z^{44} - 514965 /_2 z^{46} \\ & + 1828682 z^{48} - 57214383 /_4 z^{50} + 182904759 /_2 z^{52} \\ & - 423609270 z^{54} + 1833862938 z^{56} - 33038057481 /_4 z^{58} \\ & + 62946897453 /_2 z^{60} - 176297290719 /_2 z^{62} + 176469849528 \\ & z^{64} - 253576746091 z^{66} + 524685931815 /_2 z^{68} \\ & - 193901071212 z^{70} + 99915159305 z^{72} - 68176963659 /_2 \\ & z^{74} + 6914220018 z^{76} - 630181679 z^{78} \end{aligned} $

Table 2.2 continued

<u>r</u>	<u>t</u>	<u>$g_{r,t}(z)$</u>
11	5	$+ 13545 z^{51} - 496227/2 z^{53} + 2570403 z^{55} - 36823275/2 z^{57} + 105175989 z^{59} - 1056424479/2 z^{61} + 4431989001/2 z^{63} - 7091816292 z^{65} + 16565931525 z^{67} - 55835002509/2 z^{69} + 33794236905 z^{71} - 29082118026 z^{73} + 34715413629/2 z^{75} - 13658132763/2 z^{77} + 3184695849/2 z^{79} - 166603662 z^{81}$
12	4	$- 275805/8 z^{60} + 590736 z^{62} - 5422395 z^{64} + 34026729 z^{66} - 1206621405/8 z^{68} + 469480011 z^{70} - 1024284976 z^{72} + 1566187623 z^{74} - 3334015581/2 z^{76} + 1208954565 z^{78} - 1138986537/2 z^{80} + 157086072 z^{82} - 77020619/4 z^{84}$
13	3	$25146 z^{69} - 351780 z^{71} + 4495491/2 z^{73} - 8329321 z^{75} + 38809407/2 z^{77} - 29299998 z^{79} + 28653625 z^{81} - 17526015 z^{83} + 6097260 z^{85} - 921366 z^{87}$
14	2	$- 13455/4 z^{78} + 27027 z^{80} - 357903/4 z^{82} + 155610 z^{84} - 299565/2 z^{86} + 75684 z^{88} - 15699 z^{90}$
15	1	$91/2 z^{87} - 315/2 z^{89} + 180 z^{91} - 68 z^{93}$
16	0	$- 1/32 z^{96}$

Hydrogen Peroxide Lattice

$r + t = 1:$

<u>r</u>	<u>t</u>	<u>$g_{r,t}(z)$</u>
0	1	$1/2 z^3$
1	0	$1/2 z^6$

$r + t = 2:$

<u>r</u>	<u>t</u>	<u>$g_{r,t}(z)$</u>
0	2	$1/4 z^6$
1	1	$3/2 z^7 - 3/2 z^9$

Table 2.2 continued

<u>r</u>	<u>t</u>	<u>$g_{r,t}(z)$</u>
2	0	$-1/4 z^{12}$

r + t = 3:

<u>r</u>	<u>t</u>	<u>$g_{r,t}(z)$</u>
0	3	$-1/3 z^9$
1	2	$3 z^8 - 9/2 z^{10} + 3/2 z^{12}$
2	1	$3/2 z^{11} - 9/2 z^{13} + 3 z^{15}$
3	0	$1/6 z^{18}$

r + t = 4:

<u>r</u>	<u>t</u>	<u>$g_{r,t}(z)$</u>
0	4	$1/8 z^{12}$
1	3	$7/2 z^9 - 9 z^{11} + 9/2 z^{13} + z^{15}$
2	2	$3/2 z^{10} + 6 z^{12} - 117/4 z^{14} + 33 z^{16} - 45/4 z^{18}$
3	1	$1/2 z^{15} - 9/2 z^{17} + 9 z^{19} - 5 z^{21}$
4	0	$-1/8 z^{24}$

r + t = 5:

<u>r</u>	<u>t</u>	<u>$g_{r,t}(z)$</u>
0	5	$1/10 z^{15}$
1	4	$3 z^{10} - 21/2 z^{12} + 9 z^{14} + 3 z^{16} - 9/2 z^{18}$
2	3	$6 z^{11} + 15/2 z^{13} - 187/2 z^{15} + 321/2 z^{17} - 195/2 z^{19} + 17 z^{21}$
3	2	$1/2 z^{12} + 9/2 z^{16} - 59 z^{18} + 144 z^{20} - 261/2 z^{22} + 81/2 z^{24}$
4	1	$-3/2 z^{21} + 9 z^{23} - 15 z^{25} + 15/2 z^{27}$
5	0	$1/10 z^{30}$

r + t = 6:

<u>r</u>	<u>t</u>	<u>$g_{r,t}(z)$</u>
0	6	$-1/6 z^{18}$
1	5	$3/2 z^{11} - 9 z^{13} + 21/2 z^{15} + 6 z^{17} - 27/2 z^{19} + 9/2 z^{21}$
2	4	$15 z^{12} - 6 z^{14} - 189 z^{16} + 465 z^{18} - 1635/4 z^{20}$

Table 2.2 continued

<u>r</u>	<u>t</u>	<u>$g_{r,t}(z)$</u>
		$+ 117 z^{22} + 27/4 z^{24}$
3	3	$3 z^{13} + 17/2 z^{15} - 15 z^{17} - 297 z^{19} + 1035 z^{21}$ $- 1335 z^{23} + 735 z^{25} - 305/2 z^{27}$
4	2	$- 3/2 z^{18} + 6 z^{20} - 243/4 z^{22} + 270 z^{24} - 1935/4$ $z^{26} + 378 z^{28} - 108 z^{30}$
5	1	$3 z^{27} - 15 z^{29} + 45/2 z^{31} - 21/2 z^{33}$
6	0	$- 1/12 z^{36}$
<u>r + t = 7:</u>		
<u>r</u>	<u>t</u>	<u>$g_{r,t}(z)$</u>
0	7	$1/14 z^{21}$
1	6	$1/2 z^{12} - 9/2 z^{14} + 9 z^{16} + 7 z^{18} - 27 z^{20} + 27/2 z^{22}$ $+ 3/2 z^{24}$
2	5	$24 z^{13} - 93/2 z^{15} - 513/2 z^{17} + 945 z^{19} - 2205/2 z^{21}$ $+ 819/2 z^{23} + 201/2 z^{25} - 147/2 z^{27}$
3	4	$33/2 z^{14} + 39 z^{16} - 481/2 z^{18} - 690 z^{20} + 8565/2 z^{22}$ $- 7533 z^{24} + 12201/2 z^{26} - 4485/2 z^{28} + 535/2 z^{30}$
4	3	$6 z^{17} - 39/2 z^{19} + 5/2 z^{21} - 993/2 z^{23} + 5997/2 z^{25}$ $- 13283/2 z^{27} + 14121/2 z^{29} - 7263/2 z^{31} + 1443/2 z^{33}$
5	2	$9/2 z^{24} - 81/2 z^{26} + 270 z^{28} - 855 z^{30} + 2565/2 z^{32}$ $- 903 z^{34} + 483/2 z^{36}$
6	1	$- 5 z^{33} + 45/2 z^{35} - 63/2 z^{37} + 14 z^{39}$
7	0	$1/14 z^{42}$
<u>r + t = 8:</u>		
<u>r</u>	<u>t</u>	<u>$g_{r,t}(z)$</u>
0	8	$1/16 z^{24}$
1	7	$- 3/2 z^{15} + 9/2 z^{17} + 6 z^{19} - 63/2 z^{21} + 27 z^{23}$ $+ 9/2 z^{25} - 9 z^{27}$
2	6	$57/2 z^{14} - 96 z^{16} - 897/4 z^{18} + 1413 z^{20} - 4365/2 z^{22}$ $+ 985 z^{24} + 2181/4 z^{26} - 588 z^{28} + 119 z^{30}$

Table 2.2 continued

r	t	$g_{r,t}(z)$
3	5	$55 z^{15} + 129/2 z^{17} - 2085/2 z^{19} - 495/2 z^{21} + 22935/2 z^{23} - 27786 z^{25} + 29684 z^{27} - 30435/2 z^{29} + 5925/2 z^{31} + 60 z^{33}$
4	4	$6 z^{16} + 42 z^{18} - 567/4 z^{20} - 465 z^{22} - 909 z^{24} + 16893 z^{26} - 401205/8 z^{28} + 69441 z^{30} - 101439/2 z^{32} + 18657 z^{34} - 21225/8 z^{36}$
5	3	$3 z^{21} - 81/2 z^{23} + 135 z^{25} - 727 z^{27} + 5100 z^{29} - 17340 z^{31} + 60011/2 z^{33} - 27825 z^{35} + 26409/2 z^{37} - 5031/2 z^{39}$
6	2	$- 57/4 z^{30} + 153 z^{32} - 3285/4 z^{34} + 2170 z^{36} - 2898 z^{38} + 1890 z^{40} - 959/2 z^{42}$
7	1	$15/2 z^{39} - 63/2 z^{41} + 42 z^{43} - 18 z^{45}$
8	0	$- 1/16 z^{48}$

 $r + t = 9:$

r	t	$g_{r,t}(z)$
0	9	$- 1/9 z^{27}$
1	8	$3/2 z^{18} + 3 z^{20} - 27 z^{22} + 63/2 z^{24} + 9 z^{26} - 27 z^{28} + 9 z^{30}$
2	7	$24 z^{15} - 255/2 z^{17} - 189/2 z^{19} + 3231/2 z^{21} - 6615/2 z^{23} + 1836 z^{25} + 3303/2 z^{27} - 4809/2 z^{29} + 819 z^{31} - 12 z^{33}$
3	6	$135 z^{16} - 25 z^{18} - 2697 z^{20} + 3468 z^{22} + 20637 z^{24} - 73458 z^{26} + 100500 z^{28} - 65176 z^{30} + 30297/2 z^{32} + 2871 z^{34} - 2807/2 z^{36}$
4	5	$42 z^{17} + 198 z^{19} - 936 z^{21} - 6369/2 z^{23} + 15201 z^{25} + 104481/2 z^{27} - 477399/2 z^{29} + 427410 z^{31} - 407292 z^{33} + 425745/2 z^{35} - 110403/2 z^{37} + 4950 z^{39}$
5	4	$3/2 z^{18} + 81/2 z^{22} - 546 z^{24} + 966 z^{26} - 2871 z^{28}$

Table 2.2 continued

<u>r</u>	<u>t</u>	<u>$g_{r,t}(z)$</u>
6	3	$+ 80775/2 z^{30} - 178269 z^{32} + 751627/2 z^{34}$ $+ 291714 z^{38} - 103005 z^{40} + 29733/2 z^{42}$ $- 37/2 z^{27} + 186 z^{29} - 1959/2 z^{31} + 12117/2 z^{33}$ $- 55503/2 z^{35} + 72156 z^{37} - 106547 z^{39} + 89301 z^{41}$ $- 79281/2 z^{43} + 14471/2 z^{45}$
7	2	$81/2 z^{36} - 861/2 z^{38} + 2016 z^{40} - 4746 z^{42} + 5838$ $z^{44} - 3591 z^{46} + 873 z^{48}$
8	1	$- 21/2 z^{45} + 42 z^{47} - 54 z^{49} + 45/2 z^{51}$
9	0	$1/18 z^{54}$

$r + t = 10$:

<u>r</u>	<u>t</u>	<u>$g_{r,t}(z)$</u>
0	10	$1/20 z^{30}$
1	9	$z^{21} - 27/2 z^{23} + 27 z^{25} + 21/2 z^{27} - 54 z^{29} + 27 z^{31} + 2 z^{33}$
2	8	$15 z^{16} - 114 z^{18} + 54 z^{20} + 1413 z^{22} - 15975/4 z^{24}$ $+ 2781 z^{26} + 3420 z^{28} - 6384 z^{30} + 6003/2 z^{32} + 78 z^{34}$ $- 1083/4 z^{36}$
3	7	$243 z^{17} - 405 z^{19} - 9531/2 z^{21} + 26217/2 z^{23}$ $+ 45999/2 z^{25} - 293363/2 z^{27} + 256473 z^{29} - 202401 z^{31}$ $+ 48928 z^{33} + 29448 z^{35} - 39897/2 z^{37} + 6003/2 z^{39}$
4	6	$196 z^{18} + 588 z^{20} - 4818 z^{22} - 9232 z^{24} + 239973/4 z^{26}$ $+ 65712 z^{28} - 3078663/4 z^{30} + 1822248 z^{32} - 8741511/4$ $z^{34} + 1467600 z^{36} - 2096091/4 z^{38} + 76032 z^{40} + 747$ z^{42}
5	5	$27/2 z^{19} + 183/2 z^{21} - 4245 z^{25} + 10677/2 z^{27} + 16632$ $z^{29} + 277041/2 z^{31} - 2152737/2 z^{33} + 14512464/5 z^{35}$ $- 8424087 z^{37} + 3608187 z^{39} - 3629259/2 z^{41} + 489051 z^{43}$ $- 530403/10 z^{45}$
6	4	$- 37/4 z^{24} + 66 z^{26} - 798 z^{28} + 4146 z^{30} - 52485/4 z^{32}$

Table 2.2 continued

<u>r</u>	<u>t</u>	<u>$g_{r,t}(z)$</u>
		$+ 77844 z^{34} - 816319/2 z^{36} + 1200342 z^{38} - 4104093 z^{40} + 2115843 z^{42} - 5199615/4 z^{44} + 437823 z^{46} - 248103/4 z^{48}$
7	3	$145/2 z^{33} - 777 z^{35} + 5295 z^{37} - 59395/2 z^{39} + 109011 z^{41} - 240555 z^{43} + 317688 z^{45} - 246348 z^{47} + 206955/2 z^{49} - 36333/2 z^{51}$
8	2	$- 399/4 z^{42} + 1008 z^{44} - 8589/2 z^{46} + 9324 z^{48} - 21573/2 z^{50} + 6336 z^{52} - 5949/4 z^{54}$
9	1	$14 z^{51} - 54 z^{53} + 135/2 z^{55} - 55/2 z^{57}$
10	0	$- 1/20 z^{60}$
<u>$r + t = 11$:</u>		
<u>r</u>	<u>t</u>	<u>$g_{r,t}(z)$</u>
0	11	$1/22 z^{33}$
1	10	$- 9/2 z^{24} + 27/2 z^{26} + 9 z^{28} - 63 z^{30} + 54 z^{32} + 6 z^{34} - 15 z^{36}$
2	9	$6 z^{17} - 147/2 z^{19} + 245/2 z^{21} + 945 z^{23} - 7695/2 z^{25} + 7089/2 z^{27} + 10233/2 z^{29} - 24867/2 z^{31} + 7435 z^{33} + 1581/2 z^{35} - 4119/2 z^{37} + 454 z^{39}$
3	8	$681/2 z^{18} - 1089 z^{20} - 11925/2 z^{22} + 28088 z^{24} + 5823 z^{26} - 226539 z^{28} + 1035755/2 z^{30} - 491589 z^{32} + 116046 z^{34} + 158190 z^{36} - 268659/2 z^{38} + 69003/2 z^{40} - 2715/2 z^{42}$
4	7	$630 z^{19} + 966 z^{21} - 17199 z^{23} - 7755 z^{25} + 221547 z^{27} - 171315 z^{29} - 3415167/2 z^{31} + 11463975/2 z^{33} - 8558217 z^{35} + 14079735/2 z^{37} - 6187263/2 z^{39} + 1013067/2 z^{43} - 29985 z^{45}$
5	6	$243/2 z^{20} + 1431/2 z^{22} - 4079/2 z^{24} - 46365/2 z^{26} + 87837/2 z^{28} + 201582 z^{30} - 181977/2 z^{32} - 3980157 z^{34}$

Table 2.2 continued

<u>r</u>	<u>t</u>	<u>$g_{r,t}(z)$</u>
		$+ 30247247/2 z^{36} - 54726615/2 z^{38} + 58103613/2 z^{40}$ $- 37652461/2 z^{42} + 7187199 z^{44} - 1424076 z^{46}$ $+ 101015 z^{48}$
6	5	$33 z^{28} - 111 z^{25} + 5/2 z^{27} - 16101/2 z^{29} + 43221 z^{31}$ $- 72041 z^{33} + 405375 z^{35} - 6419787/2 z^{37} + 23603345/2$ $z^{39} - 48140937/2 z^{41} + 2994057 z^{43} - 46895299/2 z^{45}$ $+ 22424655/2 z^{47} - 5967417 z^{49} + 335234 z^{51}$
7	4	$105/2 z^{30} - 693 z^{32} + 5826 z^{34} - 28338 z^{36} + 265545/2$ $z^{38} - 684060 z^{40} + 2556393 z^{42} - 6014385 z^{44}$ $+ 8914437 z^{46} - 8349420 z^{48} + 4799790 z^{50} - 3090969/2$ $z^{52} + 426219/2 z^{54}$
8	3	$- 481/2 z^{39} + 5895 z^{41} - 21663 z^{43} + 108857 z^{45}$ $- 346500 z^{47} + 682920 z^{49} - 829815 z^{51} + 605025 z^{53}$ $- 485397/2 z^{55} + 82335/2 z^{57}$
9	2	$217 z^{48} - 2079 z^{50} + 8262 z^{52} - 16890 z^{54} + 18630 z^{56}$ $- 21087/2 z^{58} + 4807/2 z^{60}$
10	1	$- 18 z^{57} + 135/2 z^{59} + 65/2 z^{61} + 33 z^{63}$
11	0	$1/22 z^{66}$

$r + t = 12:$

<u>r</u>	<u>t</u>	<u>$g_{r,t}(z)$</u>
0	12	$- 1/12 z^{36}$
1	11	$9/2 z^{27} + 9/2 z^{29} - 54 z^{31} + 63 z^{33} + 12 z^{35} - 45 z^{37}$ $+ 15 z^{39}$
2	10	$3/2 z^{18} - 30 z^{20} + 423/4 z^{22} + 465 z^{24} - 5985/2 z^{26}$ $+ 3753 z^{28} + 23013/4 z^{30} - 18486 z^{32} + 13905 z^{34}$ $+ 2820 z^{36} - 33003/4 z^{38} + 3069 z^{40} - 453/4 z^{42}$
3	9	$369 z^{19} - 3687/2 z^{21} - 10161/2 z^{23} + 85725/2 z^{25}$

Table 2.2 continued

<u>r</u>	<u>t</u>	<u>$g_{r,t}(z)$</u>
4	8	$ \begin{aligned} & - 108145/3 z^{27} - 541557/2 z^{29} + 851454 z^{31} - 978156 \\ & z^{33} + 227178 z^{35} + 563040 z^{37} - 1153983/2 z^{39} \\ & + 195939 z^{41} - 4950 z^{43} - 41965/6 z^{45} \\ & 1554 z^{20} + 126 z^{22} - 88851/2 z^{24} + 40320 z^{26} \\ & + 530901 z^{28} - 1171926 z^{30} - 2371329 z^{32} + 13801779 \\ & z^{34} - 51782361/2 z^{36} + 25510941 z^{38} - 104352003/8 z^{40} \\ & + 1874235 z^{42} + 2643111/2 z^{44} - 634743 z^{46} + 609543/8 \\ & z^{48} \end{aligned} $
5	7	$ \begin{aligned} & 666 z^{21} + 6285/2 z^{23} - 17103 z^{25} - 88740 z^{27} \\ & + 312270 z^{29} + 842628 z^{31} - 6280521/2 z^{33} - 7840629 \\ & z^{35} + 111220551/2 z^{37} + 128698146 z^{39} + 166621998 z^{41} \\ & - 132406467 z^{43} + 64196187 z^{45} - 17384583 z^{47} \\ & + 3945585/2 z^{49} + 15969 z^{51} \end{aligned} $
6	6	$ \begin{aligned} & 33 z^{22} + 330 z^{24} - 552 z^{26} - 8310 z^{28} - 156605/4 z^{30} \\ & + 328431 z^{32} - 262407 z^{34} + 63609 z^{36} - 27528147/2 z^{38} \\ & + 74655495 z^{40} - 188649454 z^{42} + 282981537 z^{44} \\ & - 270573891 z^{46} + 166295459 z^{48} - 63189648 z^{50} \\ & + 13320591 z^{52} - 4631993/4 z^{54} \end{aligned} $
7	5	$ \begin{aligned} & 39/2 z^{27} - 693/2 z^{29} + 3213/2 z^{31} - 13089 z^{33} \\ & + 102858 z^{35} - 782847/2 z^{37} + 2765931/2 z^{39} - 15228951/2 \\ & z^{41} + 32958090 z^{43} - 88420080 z^{45} + 301006893/2 z^{47} \\ & - 334148913/2 z^{49} + 120910539 z^{51} - 54994632 z^{53} \\ & + 28489491/2 z^{55} - 3181535/2 z^{57} \end{aligned} $
8	4	$ \begin{aligned} & - 1101/4 z^{36} + 4089 z^{38} - 31635 z^{40} + 173175 z^{42} \\ & - 7146111/8 z^{44} + 3910140 z^{46} - 11999673 z^{48} \\ & + 24359220 z^{50} - 260016075/8 z^{52} + 28210611 z^{54} \\ & - 15335793 z^{56} + 4740957 z^{58} - 1271085/2 z^{60} \end{aligned} $

Table 2.2 continued

r	t	$g_{r,t}(z)$
9	3	$4381/6 z^{45} - 19665/2 z^{47} + 71820 z^{49} - 328944 z^{51}$ $+ 946233 z^{53} - 1715697 z^{55} + 3908091/2 z^{57} - 1355211$ $z^{59} + 522918 z^{61} - 516373/6 z^{63}$
10	2	$- 855/2 z^{54} + 3906 z^{56} - 14715 z^{58} + 28710 z^{60}$ $- 121935/4 z^{62} + 16731 z^{64} - 14883/4 z^{66}$
11	1	$45/2 z^{63} - 165/2 z^{65} + 99 z^{67} - 39 z^{69}$
12	0	$- 1/24 z^{72}$

$r + t = 13:$

r	t	$g_{r,t}(z)$
0	13	$1/26 z^{39}$
1	12	$3/2 z^{30} - 27 z^{32} + 54 z^{34} + 14 z^{36} - 90 z^{38} + 45 z^{40}$ $+ 5/2 z^{42}$
2	11	$- 15/2 z^{21} + 99/2 z^{23} + 321/2 z^{25} - 5645/2 z^{27}$ $+ 3294 z^{29} + 9693/2 z^{31} - 43479/2 z^{33} + 20439 z^{35}$ $+ 12495/2 z^{37} + 43245/2 z^{39} + 22563/2 z^{41} - 759/2 z^{43}$ $- 747 z^{45}$
3	10	$315 z^{20} - 2223 z^{22} - 2225 z^{24} + 49500 z^{26} - 181665/2$ $z^{28} - 483227/2 z^{30} + 1160541 z^{32} - 1639440 z^{34}$ $+ 817695/2 z^{36} + 1471212 z^{38} - 3596841/2 z^{40} + 734767$ $z^{42} + 29025 z^{44} - 96525 z^{46} + 17072 z^{48}$
4	9	$2996 z^{21} - 4284 z^{23} - 85734 z^{25} + 200451 z^{27} + 1752129/2$ $z^{29} - 3540924 z^{31} - 687136 z^{33} + 51613875/2 z^{35}$ $- 125638695/2 z^{37} + 147347109/2 z^{39} - 85320657/2 z^{41}$ $+ 7418961/2 z^{43} + 1048334 z^{45} - 12334815/2 z^{47}$ $+ 2536083/2 z^{49} - 55705 z^{51}$
5	8	$2724 z^{22} + 8817 z^{24} - 169491/2 z^{26} - 220608 z^{28}$ $+ 1512126 z^{30} + 1513167 z^{32} - 32518197/2 z^{34} + 3679116$ $z^{36} + 14502006 z^{38} - 916081419/2 z^{40} + 1445329347/2 z^{42}$

Table 2.2 continued

r	t	$g_{r,t}(z)$
6	7	$ \begin{aligned} & - 686131185 z^{44} + 798540561/2 z^{46} - 130650231 z^{48} \\ & + 15816981 z^{50} + 2595003 z^{52} - 1392759/2 z^{54} \\ & 330 z^{23} + 2736 z^{25} - 11869/2 z^{27} - 87645 z^{29} \\ & - 95253/2 z^{31} + 3987239/2 z^{33} - 1969938 z^{35} \\ & - 21622581/2 z^{37} - 38598461/2 z^{39} + 311817171 z^{41} \\ & - 1046941245 z^{43} + 3812859875/2 z^{45} - 2186968227 z^{47} \\ & + 3287232609/2 z^{49} - 1601604371/2 z^{51} + 238815981 z^{53} \\ & - 75880197/2 z^{55} + 4394683/2 z^{57} \end{aligned} $
7	6	$ \begin{aligned} & 13/2 z^{24} + 711/2 z^{28} - 4767 z^{30} + 4830 z^{32} - 128631/2 \\ & z^{34} + 1896467/2 z^{36} - 6811431/2 z^{38} + 7246065 z^{40} \\ & - 88907715/2 z^{42} + 258791973 z^{44} - 843434853 z^{46} \\ & + 1683628747 z^{48} - 2198624802 z^{50} + 1924530405 z^{52} \\ & - 2240111435/2 z^{54} + 414789279 z^{56} - 87930996 z^{58} \\ & + 16070259/2 z^{60} \end{aligned} $
8	5	$ \begin{aligned} & - 186 z^{33} + 5139/2 z^{35} - 3908/2 z^{37} + 304833/2 z^{39} \\ & - 1693233/2 z^{41} + 6969237/2 z^{45} - 31236909/2 z^{45} \\ & + 139399947/2 z^{47} - 457743861/2 z^{49} - 1014106071/2 z^{51} \\ & - 1516446855/2 z^{53} + 1537153527 z^{55} - 1042240887/2 z^{57} \\ & + 452643813/2 z^{59} - 113724633/2 z^{61} + 6271635 z^{63} \end{aligned} $
9	4	$ \begin{aligned} & 2419/2 z^{42} - 36981/2 z^{44} + 147654 z^{46} - 885552 z^{48} \\ & + 4463919 z^{50} - 17146773 z^{52} + 46007625 z^{54} \\ & - 83930220 z^{56} + 206503605/2 z^{58} - 84244677 z^{60} \\ & + 43676028 z^{62} - 13021515 z^{64} + 3397979/2 z^{66} \end{aligned} $
10	3	$ \begin{aligned} & - 4101/2 z^{51} + 57627/2 z^{53} - 203355 z^{55} + 863949 z^{57} \\ & - 2302740 z^{59} + 7829415/2 z^{61} - 8466337/2 z^{63} \\ & + 5633595/2 z^{65} - 1051479 z^{67} + 337051/2 z^{69} \end{aligned} $
11	2	$ \begin{aligned} & 1557/2 z^{60} - 6831 z^{62} + 49335/2 z^{64} - 46365 z^{66} \\ & + 47718 z^{68} - 51051/2 z^{70} + 11115/2 z^{72} \end{aligned} $

Table 2.2 continued

r	t	$g_{r,t}(z)$
12	1	$- 55/2 z^{69} + 99 z^{71} - 117 z^{73} + 91/2 z^{75}$
13	0	$1/26 z^{78}$
$r + t = 14:$		
r	t	$g_{r,t}(z)$
0	14	$1/28 z^{42}$
1	13	$- 9 z^{33} + 27 z^{35} + 12 z^{37} - 105 z^{39} + 90 z^{41} + 15/2 z^{43} - 45/2 z^{45}$
2	12	$+ 53/4 z^{24} - 33 z^{26} - 3435/4 z^{28} + 2281 z^{30} + 3015 z^{32} - 20268 z^{34} + 48813/2 z^{36} + 9528 z^{38} - 41685 z^{40} + 27965 z^{42} - 903/4 z^{44} - 5487 z^{46} + 5131/4 z^{48}$
3	11	$205 z^{21} - 2035 z^{23} + 1881/2 z^{25} + 88441/2 z^{27} - 265941/2 z^{29} - 138258 z^{31} + 1321950 z^{33} - 4707657/2 z^{35} + 720756 z^{37} + 5970515/2 z^{39} - 4353030 z^{41} + 2060640 z^{43} + 305213 z^{45} - 1282347/2 z^{47} + 386397/2 z^{49} - 22191/2 z^{51}$
4	10	$4662 z^{22} - 14022 z^{24} - 251073/2 z^{26} + 515808 z^{28} + 3683997/4 z^{30} - 7357806 z^{32} + 25970037/4 z^{34} + 36915294 z^{36} - 250522659/2 z^{38} + 175835214 z^{40} - 457849881/4 z^{42} + 332046 z^{44} + 217264311/4 z^{46} - 37560732 z^{48} + 40254885/4 z^{50} - 441948 z^{52} - 689949/4 z^{54}$
5	9	$15/2 z^{21} + 8439 z^{23} + 29499/2 z^{25} - 293772 z^{27} - 519387/2 z^{29} + 10269249/2 z^{31} - 3848389/2 z^{33} - 50163228 z^{35} + 87466149 z^{37} + 493175791/2 z^{39} - 2531037225/2 z^{41} + 4940673861/2 z^{43} - 5539027425/2 z^{45} + 3747485409/2 z^{47} - 1380615729/2 z^{49} + 57943693 z^{51} + 109265427/2 z^{53} - 19860039 z^{55} + 1973210 z^{57}$

Table 2.2 continued

r	t	$g_{r,t}(z)$
6	8	$2300 z^{24} + 14580 z^{26} - 231369/4 z^{28} + 494802 z^{30}$ $+ 768534 z^{32} + 9110826 z^{34} - 73637961/4 z^{36}$ $- 64784946 z^{38} + 280771791/2 z^{40} + 796297296 z^{42}$ $- 16982884287/4 z^{44} + 9623688216 z^{46} - 13159094833 z^{48}$ $+ 11765740440 z^{50} - 27800540577/4 z^{52} + 2614999023 z^{54}$ $- 2257202409/4 z^{56} + 51438273 z^{58} + 2069393/4 z^{60}$
7	7	$78 z^{25} + 1707/2 z^{27} + 2457/2 z^{29} - 48225 z^{31} - 48149$ $z^{33} + 648687/2 z^{35} + 5575572 z^{37} - 24611297 z^{39}$ $+ 44150217/2 z^{41} - 100357812 z^{43} + 2511454643/2 z^{45}$ $- 5516409006 z^{47} + 186187457319/14 z^{49} - 40895356331/2$ $z^{51} + 21200730456 z^{53} - 30041642181/2 z^{55} + 14296752313$ $z^{57} - 2167813596 z^{59} + 372717645 z^{61} - 375837227/14 z^{63}$ $- 62 z^{30} + 630 z^{32} - 17541/2 z^{34} + 51450 z^{36} - 942855/4$ $z^{38} + 1996980 z^{40} - 44553943/4 z^{42} + 37828506 z^{44}$ $- 582977271/4 z^{46} + 718104560 z^{48} - 10865174913/4 z^{50}$ $+ 6839499618 z^{52} - 46524544463/4 z^{54} + 13643465676 z^{56}$ $- 44337897015/4 z^{58} + 6129017682 z^{60} - 8794114005/4 z^{62}$ $- 459990426 z^{64} - 169582317/4 z^{66}$
8	6	$2217/2 z^{39} - 33393/2 z^{41} + 154068 z^{43} - 1095603 z^{45}$ $+ 11495463/2 z^{47} - 52719927/2 z^{49} + 118057888 z^{51}$ $- 444663360 z^{53} + 2452978737/2 z^{55} - 4755221185/2 z^{57}$ $+ 6443422095/2 z^{59} - 3034160178 z^{61} + 1946263176 z^{63}$ $- 1621596327/2 z^{65} + 395304405/2 z^{67} - 42744067/2 z^{69}$
9	5	$- 18183/4 z^{48} + 71955 z^{50} - 2434275/4 z^{52} + 3773127 z^{54}$ $- 35947719/2 z^{56} + 62325054 z^{58} - 302889015/2 z^{60}$ $+ 254578896 z^{62} - 1174040373/4 z^{64} + 227510712 z^{66}$ $- 226510713/2 z^{68} + 32697600 z^{70} - 16641651/4 z^{72}$
10	4	

Table 2.2 continued

<u>r</u>	<u>t</u>	<u>$g_{r,t}(z)$</u>
11	3	$10629/2 z^{57} - 150579/2 z^{59} + 509949 z^{61} - 4076259/2 z^{63}$ $+ 5117178 z^{65} - 8263002 z^{67} + 8562983 z^{69} - 5502783 z^{71}$ $+ 3992703/2 z^{73} - 312572 z^{75}$
12	2	$- 1331 z^{66} + 11286 z^{68} - 157509/4 z^{70} + 71786 z^{72}$ $- 287937/4 z^{74} + 37674 z^{76} - 16107/2 z^{78}$
13	1	$33 z^{75} - 117 z^{77} + 273/2 z^{79} - 105/2 z^{81}$
14	0	$- 1/28 z^{84}$

$r + t = 15:$

<u>r</u>	<u>t</u>	<u>$g_{r,t}(z)$</u>
0	15	$- 1/15 z^{45}$
1	14	$9 z^{36} + 6 z^{38} - 90 z^{40} + 105 z^{42} + 15 z^{44} - 135/2 z^{46}$ $+ 45/2 z^{48}$
2	13	$3 z^{27} - 555/2 z^{29} + 2439/2 z^{31} + 2583/2 z^{33} - 30213/2$ $z^{35} + 23679 z^{37} - 21081/2 z^{39} - 122799/2 z^{41} + 52110$ $z^{43} + 2895/2 z^{45} - 43269/2 z^{47} + 17073/2 z^{49} - 819/2 z^{51}$
3	12	$201/2 z^{22} - 1375 z^{24} + 5439/2 z^{26} + 30366 z^{28}$ $- 284241/2 z^{30} - 5379 z^{32} + 2519511/2 z^{34} - 5828127/2$ $z^{36} + 1223838 z^{38} + 4852617 z^{40} - 17059961/2 z^{42}$ $+ 4627149 z^{44} + 2670957/2 z^{46} - 2734419 z^{48} - 1105752$ $z^{50} + 170463/2 z^{52} - 25207 z^{54}$
4	11	$5886 z^{23} - 27972 z^{25} - 275121/2 z^{27} + 1875651/2 z^{29}$ $+ 519129/2 z^{31} - 23099289/2 z^{33} + 42682941/2 z^{35}$ $+ 74119185/2 z^{37} - 416498445/2 z^{39} + 711340335/2 z^{41}$ $- 524468547/2 z^{43} - 47132679/2 z^{45} + 206086188 z^{47}$ $- 164040822 z^{49} + 102613335/2 z^{51} + 622323/2 z^{53}$ $- 7479459/2 z^{55} + 1134081/2 z^{57}$
5	10	$3/2 z^{20} + 75/2 z^{22} + 41559/2 z^{24} + 10215/2 z^{26}$ $- 1532103/2 z^{28} + 882915/2 z^{30} + 12795141 z^{32}$

Table 2.2 continued

r	t	$g_{r,t}(z)$						
6	9	$ \begin{aligned} & - 21687624 z^{34} - 104312958 z^{36} + 714235521/2 z^{38} \\ & + 657636813/5 z^{40} - 5460328875/2 z^{42} + 13697734059/2 \\ & z^{44} - 18113689263/2 z^{46} + 7004124204 z^{48} \\ & - 27771711609/10 z^{50} - 26753031 z^{52} + 577090665 z^{54} \\ & - 256108743 z^{56} + 43691322 z^{58} - 18722307/10 z^{60} \\ & 30 z^{23} + 22305/2 z^{25} + 106925/2 z^{27} - 360486 z^{29} \\ & - 1832982 z^{31} + 13713017/2 z^{33} + 58445925/2 z^{35} \\ & - 230122977/2 z^{37} - 174510547 z^{39} + 2225869623/2 z^{41} \\ & + 529843587 z^{43} - 37755226337/3 z^{45} + 37587749238 z^{47} \\ & - 61544202267 z^{49} + 64518783665 z^{51} - 44723597952 z^{53} \\ & + 39903940509/2 z^{55} - 5123408885 z^{57} + 928797843/2 \\ & z^{59} + 83455710 z^{61} - 51690751/3 z^{63} \end{aligned} $						
		7	8	$ \begin{aligned} & 1020 z^{26} + 9171 z^{28} - 16165/2 z^{30} - 402681 z^{32} \\ & - 300741 z^{34} + 13269707/2 z^{36} + 39350859/2 z^{38} \\ & - 313780551/2 z^{40} + 20486245/2 z^{42} + 855521889/2 z^{44} \\ & + 3141032040 z^{46} - 50356378607/2 z^{48} + 154630780287/2 \\ & z^{50} - 282701692689/2 z^{52} + 343788984991/2 z^{54} \\ & - 144145297827 z^{56} + 166793746389/2 z^{58} - 64698460721/2 \\ & z^{60} + 7860609111 z^{62} - 2067278409/2 z^{64} + 99790719/2 z^{66} \end{aligned} $				
				8	7	$ \begin{aligned} & 210 z^{29} - 657 z^{31} - 99 z^{33} - 100878 z^{35} + 947883/2 z^{37} \\ & - 1271003/2 z^{39} + 25222443/2 z^{41} - 190885527/2 z^{43} \\ & + 575653195/2 z^{45} - 787317459 z^{47} + 4467657243 z^{49} \\ & - 42676948019/2 z^{51} + 127622314203/2 z^{53} \\ & - 250835331153/2 z^{55} + 339565902833/2 z^{57} \\ & - 1617176003205 z^{59} + 216652200219/2 z^{61} - 49896445388 \\ & z^{63} + 14990047122 z^{65} - 5252617239/2 z^{67} + 402338423/2 \\ & z^{69} \end{aligned} $		
						9	6	$ 3169/6 z^{36} - 17841/2 z^{38} + 178935/2 z^{40} - 1122667/2 $

Table 2.2 continued

<u>r</u>	<u>t</u>	<u>$g_{r,t}(z)$</u>
		$z^{42} + 3638331 z^{44} - 22715766 z^{46} + 102912923 z^{48}$ $- 400145151 z^{50} + 1707748791 z^{52} - 40834380235/6 z^{54}$ $+ 20417653014 z^{56} - 86935233327/2 z^{58} + 131308829641/2$ $z^{60} - 14133889169/2 z^{62} + 53884904220 z^{64}$ $- 28438840499 z^{66} + 19746259359/2 z^{68} - 4049860395/2$ $z^{70} + 185376380 z^{72}$
10	5	$- 5460 z^{45} + 185307/2 z^{47} - 1807605/2 z^{49} + 12471885 z^{51}$ $- 33643641 z^{53} + 1607837103/10 z^{55} - 1347769203/2 z^{57}$ $+ 4456868229/2 z^{59} - 5427702027 z^{61} + 9518203464 z^{63}$ $- 59643654642/5 z^{65} + 21142358991/2 z^{67} - 12930836529/2$ $z^{69} + 2595067782 z^{71} - 614816388 z^{73} + 325539753/5 z^{75}$
11	4	$30453/2 z^{54} - 251901 z^{56} + 2223342 z^{58} - 27429369/2 z^{60}$ $+ 122933745/2 z^{62} - 196485399 z^{64} + 884248629/2 z^{66}$ $- 696446751 z^{68} + 761369895 z^{70} - 565204068 z^{72}$ $- 5976174637/22 z^{74} - 1676803983/22 z^{76} + 18954429/2 z^{78}$
12	3	$- 25465/2 z^{63} + 357093/2 z^{65} - 2323365/2 z^{67} + 8830855/2$ $z^{69} - 21127821/2 z^{71} + 32709105/2 z^{73} - 32712225/2 z^{75}$ $+ 20405931/2 z^{77} - 3610815 z^{79} + 553761 z^{81}$
13	2	$4323/2 z^{72} - 35607/2 z^{74} + 60372 z^{76} - 107289 z^{78}$ $+ 210483/2 z^{80} - 54034 z^{82} + 22843/2 z^{84}$
14	1	$- 39 z^{81} + 273/2 z^{83} - 315/2 z^{85} + 60 z^{87}$
15	0	$1/30 z^{90}$

Diamond Lattice

$r + t = 1$:

<u>r</u>	<u>t</u>	<u>$g_{r,t}(u)$</u>
0	1	$1/2 u^2$
1	0	$1/2 u^4$

Table 2.2 continued

r + t = 2:

<u>r</u>	<u>t</u>	<u>$g_{r,t}(u)$</u>
0	2	$1/4 u^4$
1	1	$2 u^5 - 2 u^6$
2	0	$- 1/4 u^8$

r + t = 3:

<u>r</u>	<u>t</u>	<u>$g_{r,t}(u)$</u>
0	3	$- 1/3 u^6$
1	2	$5 u^6 - 8 u^7 + 3 u^8$
2	1	$3 u^8 - 8 u^9 + 5 u^{10}$
3	0	$1/6 u^{12}$

r + t = 4:

<u>r</u>	<u>t</u>	<u>$g_{r,t}(u)$</u>
0	4	$1/8 u^8$
1	3	$8 u^7 - 20 u^8 + 12 u^9$
2	2	$3 u^8 + 18 u^9 - 75 u^{10} + 82 u^{11} - 28 u^{12}$
3	1	$2 u^{11} - 12 u^{12} + 20 u^{13} - 10 u^{14}$
4	0	$- 1/8 u^{16}$

r + t = 5:

<u>r</u>	<u>t</u>	<u>$g_{r,t}(u)$</u>
0	5	$1/10 u^{10}$
1	4	$19/2 u^8 - 32 u^9 + 30 u^{10} - 15/2 u^{12}$
2	3	$18 u^9 + 42 u^{10} - 340 u^{11} + 558 u^{12} - 350 u^{13} + 72 u^{14}$
3	2	$2 u^{10} + 33 u^{12} - 248 u^{13} + 517 u^{14} - 432 u^{15} + 128 u^{16}$
4	1	$1/2 u^{14} - 8 u^{15} + 30 u^{16} - 40 u^{17} + 35/2 u^{18}$
5	0	$1/10 u^{20}$

r + t = 6:

<u>r</u>	<u>t</u>	<u>$g_{r,t}(u)$</u>
0	6	$- 1/6 u^{12}$
1	5	$8 u^9 - 38 u^{10} + 48 u^{11} - 30 u^{13} + 12 u^{14}$

Table 2.2 continued

r	t	$g_{r,t}(u)$
2	4	$63 u^{10} + 24 u^{11} - 1945/2 u^{12} + 2240 u^{13} - 2037 u^{14}$ $+ 744 u^{15} - 123/2 u^{16}$
3	3	$18 u^{11} + 36 u^{12} + 66 u^{13} - 1920 u^{14} + 16646/3 u^{15}$ $- 6648 u^{16} + 3654 u^{17} - 2264/3 u^{18}$
4	2	$1/2 u^{12} - 8 u^{14} + 60 u^{15} - 935/2 u^{16} + 1540 u^{17}$ $- 2303 u^{18} + 1608 u^{19} - 425 u^{20}$
5	1	$- 2 u^{18} + 20 u^{19} - 60 u^{20} + 70 u^{21} - 28 u^{22} - 1/12 u^{24}$

$r + t = 7:$

r	t	$g_{r,t}(u)$
0	7	$1/14 u^{14}$
1	6	$5 u^{10} - 32 u^{11} + 57 u^{12} - 75 u^{14} + 48 u^{15} - 3 u^{16}$
2	5	$150 u^{11} - 171 u^{12} - 1932 u^{13} + 6265 u^{14} - 7546 u^{15}$ $+ 3810 u^{16} - 408 u^{17} - 168 u^{18}$
3	4	$123 u^{12} + 240 u^{13} - 924 u^{14} - 7584 u^{15} + 66911/2 u^{16}$ $- 54288 u^{17} + 43290 u^{18} - 16736 u^{19} + 4847/2 u^{20}$
4	3	$6 u^{13} + 95/2 u^{14} - 146 u^{15} + 442 u^{16} - 6290 u^{17}$ $+ 26572 u^{18} - 49950 u^{19} + 48126 u^{20} - 23300 u^{21}$ $+ 8985/2 u^{22}$
5	2	$- 2 u^{16} + 65 u^{18} - 584 u^{19} + 2705 u^{20} - 6384 u^{21}$ $+ 7840 u^{22} - 4800 u^{23} + 1160 u^{24}$
6	1	$5 u^{22} - 40 u^{23} + 105 u^{24} - 112 u^{25} + 42 u^{26}$
7	0	$1/14 u^{28}$

$r + t = 8:$

r	t	$g_{r,t}(u)$
0	8	$1/16 u^{16}$
1	7	$2 u^{11} - 20 u^{12} + 48 u^{13} - 120 u^{15} + 120 u^{16} - 12 u^{17}$ $- 18 u^{18}$
2	6	$270 u^{12} - 672 u^{13} - 2692 u^{14} + 13104 u^{15} - 20342 u^{16}$

Table 2.2 continued

<u>r</u>	<u>t</u>	<u>$g_{r,t}(u)$</u>
		$+ 13020 u^{17} - 1206 u^{18} - 2100 u^{19} + 618 u^{20}$
3	5	$6 u^{12} + 552 u^{13} + 588 u^{14} - 7422 u^{15} - 14782 u^{16}$ $+ 131354 u^{17} - 284616 u^{18} + 300432 u^{19} - 166204 u^{20}$ $+ 43722 u^{21} - 3630 u^{22}$
4	4	$105 u^{14} + 492 u^{15} - 1508 u^{16} - 1650 u^{17} - 33673 u^{18}$ $+ 231034 u^{19} - 1131829/2 u^{20} + 713986 u^{21} - 497198 u^{22}$ $+ 181098 u^{23} - 53543/2 u^{24}$
5	3	$18 u^{16} - 14 u^{17} - 416 u^{18} + 2134 u^{19} - 15680 u^{20}$ $+ 79186 u^{21} - 209216 u^{22} + 305586 u^{23} - 251486 u^{24}$ $+ 109560 u^{25} - 19672 u^{26}$
6	2	$5 u^{20} + 18 u^{21} - 443 u^{22} + 3010 u^{23} - 10605 u^{24}$ $+ 20580 u^{25} - 22078 u^{26} + 12276 u^{27} - 2763 u^{28}$
7	1	$- 10 u^{26} + 70 u^{27} - 168 u^{28} + 168 u^{29} - 60 u^{30}$
8	0	$- 1/16 u^{32}$
<u>r + t = 9:</u>		
<u>r</u>	<u>t</u>	<u>$g_{r,t}(u)$</u>
0	9	$- 1/9 u^8$
1	8	$1/2 u^{12} - 8 u^{13} + 30 u^{14} - 285/2 u^{16} + 192 u^{17} - 30 u^{18}$ $- 72 u^{19} + 30 u^{20}$
2	7	$378 u^{13} - 1467 u^{14} - 2420 u^{15} + 21329 u^{16} - 42378 u^{17}$ $+ 33432 u^{18} - 2016 u^{19} - 12348 u^{20} + 6204 u^{21} - 714 u^{22}$
3	6	$2 u^{12} + 36 u^{13} + 1782 u^{14} - 44 u^{15} - 29637 u^{16} + 5328$ $u^{17} + 1080995/3 u^{18} - 1064592 u^{19} + 1428891 u^{20}$ $- 3063980/3 u^{21} + 368967 u^{22} - 46596 u^{23} - 3142 u^{24}$
4	5	$24 u^{14} + 842 u^{15} + 2853 u^{16} - 13142 u^{17} - 31280 u^{18}$ $- 38022 u^{19} + 1184450 u^{20} - 3983570 u^{21} + 12865449/2$ $u^{22} - 5884780 u^{23} + 3098151 u^{24} - 865120 u^{25}$ $+ 193739/2 u^{26}$

Table 2.2 continued

<u>r</u>	<u>t</u>	<u>$g_{r,t}(u)$</u>
5	4	$51 u^{16} + 276 u^{17} - 17 u^{18} - 813 u^{19} + 41705/2 u^{20}$ $- 144544 u^{21} + 1010520 u^{22} - 3316892 u^{23} + 11853191/2$ $u^{24} - 6225860 u^{25} + 3855763 u^{26} - 1304234 u^{27}$ $+ 185627 u^{28}$
6	3	$18 u^{19} - 147 u^{20} - 60 u^{21} + 3777 u^{22} - 29670 u^{23}$ $+ 165886 u^{24} - 568260 u^{25} + 1160370 u^{26} - 4286720/3$ $u^{27} + 1043775 u^{28} - 417036 u^{29} + 210761/3 u^{30}$
7	2	$- 7 u^{24} - 152 u^{25} + 2037 u^{26} - 11088 u^{27} + 32802 u^{28}$ $- 55776 u^{29} + 54222 u^{30} - 27984 u^{31} + 5946 u^{32}$
8	1	$35/2 u^{30} - 112 u^{31} + 252 u^{32} - 240 u^{33} + 165/2 u^{34}$
9	0	$1/18 u^{36}$

r + t = 10:

<u>r</u>	<u>t</u>	<u>$g_{r,t}(u)$</u>
0	10	$1/20 u^{20}$
1	9	$- 2 u^{14} + 12 u^{15} - 120 u^{17} + 228 u^{18} - 48 u^{19} - 180 u^{20}$ $+ 120 u^{21} - 10 u^{22}$
2	8	$423 u^{14} - 2268 u^{15} - 2475/4 u^{16} + 27508 u^{17} - 70903 u^{18}$ $+ 68208 u^{19} - 1659 u^{20} - 46032 u^{21} + 31842 u^{22}$ $- 6000 u^{23} - 2001/4 u^{24}$
3	7	$12 u^{13} + 108 u^{14} + 4392 u^{15} - 5460 u^{16} - 79896 u^{17}$ $139248 u^{18} + 694698 u^{19} - 3020660 u^{20} + 5082444 u^{21}$ $- 4475524 u^{22} + 1995038 u^{23} - 261888 u^{24} - 100470 u^{25}$ $+ 27958 u^{26}$
4	6	$12 u^{14} + 216 u^{15} + 4529 u^{16} + 10138 u^{17} - 86576 u^{18}$ $- 152494 u^{19} + 555506 u^{20} + 3661076 u^{21} - 19190020 u^{22}$ $+ 39603156 u^{23} - 45567298 u^{24} + 31259146 u^{25}$ $- 12480640 u^{26} + 2575162 u^{27} - 191913 u^{28}$
5	5	$36 u^{16} + 684 u^{17} + 3486 u^{18} - 5308 u^{19} - 86468 u^{20}$ $+ 137364 u^{21} - 437554 u^{22} + 6867054 u^{23} - 30915530 u^{24}$

Table 2.2 continued

<u>r</u>	<u>t</u>	<u>$g_{r,t}(u)$</u>
6	4	$+ 344402482/5 u^{25} - 90026100 u^{26} + 72504730 u^{27}$ $- 35435130 u^{28} + 9617788 u^{29} - 5527742/5 u^{30}$ $18 u^{18} + 24 u^{19} + 533/2 u^{20} - 2532 u^{21} - 11325 u^{22}$ $+ 98468 u^{23} - 548634 u^{24} + 3301960 u^{25} - 12959975 u^{26}$ $+ 30423528 u^{27} - 44218428 u^{28} + 40423452 u^{29}$ $- 22691784 u^{30} + 7155612 u^{31} - 1941301/2 u^{32}$
7	3	$6 u^{22} - 152 u^{23} + 694 u^{24} + 1882 u^{25} - 36150 u^{26}$ $+ 250428 u^{27} - 1078812 u^{28} + 2931288 u^{29} - 5044734 u^{30}$ $+ 5482560 u^{31} - 3647622 u^{32} + 1356854 u^{33} - 216242 u^{34}$
8	2	$- 27/4 u^{28} + 712 u^{29} - 7084 u^{30} + 32928 u^{31} - 86163 u^{32}$ $+ 133056 u^{33} - 119964 u^{34} + 58344 u^{35} - 47289/4 u^{36}$
9	1	$- 28 u^{34} + 168 u^{35} - 360 u^{36} + 330 u^{37} - 110 u^{38}$
10	0	$- 1/20 u^{40}$

$r + t = 11:$

<u>r</u>	<u>t</u>	<u>$g_{r,t}(u)$</u>
0	11	$1/22 u^{22}$
1	10	$3 u^{16} - 75 u^{18} + 192 u^{19} - 57 u^{20} - 288 u^{21} + 300 u^{22}$ $- 40 u^{23} - 35 u^{24}$
2	9	$378 u^{15} - 2691 u^{16} + 2140 u^{17} + 28215 u^{18} - 97202 u^{19}$ $+ 114618 u^{20} - 124302 u^{22} + 109140 u^{23} - 26541 u^{24}$ $- 6648 u^{25} + 2893 u^{26}$
3	8	$42 u^{14} + 192 u^{15} + 8712 u^{16} - 22332 u^{17} - 158466 u^{18}$ $+ 533820 u^{19} + 830406 u^{20} - 6724260 u^{21} + 14253484 u^{22}$ $- 15121028 u^{23} + 15838677/2 u^{24} - 816200 u^{25} - 1153500$ $u^{26} + 507360 u^{27} - 115137/2 u^{28}$
4	7	$108 u^{15} + 1125 u^{16} + 17462 u^{17} + 37433/2 u^{18} - 407444$ $u^{19} - 201188 u^{20} + 4118014 u^{21} + 9906757/2 u^{22}$ $- 66506442 u^{23} + 179370829 u^{24} - 254323024 u^{25}$

Table 2.2 continued

<u>r</u>	<u>t</u>	<u>$f_{r,t}(u)$</u>
		$+ 215799526 u^{26} - 110364918 u^{27} + 31459576 u^{28}$
		$- 3851628 u^{29} + 5909 u^{30}$
5	6	$33 u^{16} + 432 u^{17} + 6342 u^{18} + 24162 u^{19} - 91215 u^{20}$
		$- 615040 u^{21} + 1143230 u^{22} + 1901842 u^{23} + 24128369$
		$u^{24} - 186590440 u^{25} + 535334333 u^{26} - 861442066 u^{27}$
		$+ 863058870 u^{28} - 549858696 u^{29} + 215858385 u^{30}$
		$- 47164466 u^{31} + 4305925 u^{32}$
6	5	$24 u^{18} + 338 u^{19} + 1911 u^{20} + 90 u^{21} - 48171 u^{22}$
		$- 168044 u^{23} + 1297134 u^{24} - 4705630 u^{25} + 32582883$
		$u^{26} - 162210678 u^{27} + 459209568 u^{28} - 796423024 u^{29}$
		$+ 887855817 u^{30} - 641600316 u^{31} + 291090464 u^{32}$
		$- 75361368 u^{33} + 8479002 u^{34}$
7	4	$3 u^{20} - 116 u^{22} + 818 u^{23} - 7326 u^{24} + 9118 u^{25}$
		$+ 168309 u^{26} - 1396318 u^{27} + 16790277/2 u^{28} - 37033692$
		$u^{29} + 107821764 u^{30} - 204931282 u^{31} + 513083493/2 u^{32}$
		$- 210226514 u^{33} + 108680885 u^{34} - 3218622 u^{35}$
		$+ 4163788 u^{36}$
8	3	$- 97/2 u^{26} + 724 u^{27} - 1808 u^{28} - 22560 u^{29} + 517659/2$
		$u^{30} - 1462692 u^{31} + 5200440 u^{32} - 12046500 u^{33}$
		$+ 36617295/2 u^{34} - 18073264 u^{35} + 11152328 u^{36}$
		$- 3907644 u^{37} + 1187095/2 u^{38}$
9	2	$82 u^{32} - 2448 u^{33} + 20286 u^{34} - 84000 u^{35} + 200610 u^{36}$
		$- 287760 u^{37} + 244431 u^{38} - 113256 u^{39} + 22055 u^{40}$
10	1	$42 u^{38} - 240 u^{39} + 495 u^{40} - 440 u^{41} + 143 u^{42}$
11	0	$1/22 u^{44}$
<u>r + t = 12:</u>		
<u>r</u>	<u>t</u>	<u>$f_{r,t}(u)$</u>
0	12	$- 1/12 u^{24}$

Table 2.2 continued

<u>r</u>	<u>t</u>	<u>$g_{r,t}(u)$</u>
1	11	$- 30 u^{19} + 120 u^{20} - 48 u^{21} - 342 u^{22} + 480 u^{23} - 100 u^{24} - 140 u^{25} + 60 u^{26}$
2	10	$270 u^{16} - 2496 u^{17} + 4508 u^{18} + 22720 u^{19} - 110691 u^{20} + 161520 u^{21} - 420 u^{22} - 258192 u^{23} + 276915 u^{24} - 80958 u^{25} - 40395 u^{26} + 28226 u^{27} - 3707 u^{28}$
3	9	$100 u^{15} + 162 u^{16} + 14436 u^{17} - 57372 u^{18} - 236502 u^{19} + 1322136 u^{20} + 180752/3 u^{21} - 11900538 u^{22} + 32576778 u^{23} - 123941762/3 u^{24} + 24885090 u^{25} - 1247004 u^{26} - 7652568 u^{27} + 4378392 u^{28} - 851202 u^{29} + 21762 u^{30}$
4	8	$1233/2 u^{16} + 3708 u^{17} + 51163 u^{18} - 8864 u^{19} - 1427174 u^{20} + 594092 u^{21} + 16229003 u^{22} - 13756264 u^{23} - 666495897/4 u^{24} + 62057232 u^{25} - 1088779167 u^{26} + 1111219756 u^{27} - 688190604 u^{28} + 240963152 u^{29} - 33975303 u^{30} - 3568156 u^{31} + 4843135/4 u^{32}$
5	7	$6 u^{16} + 384 u^{17} + 3600 u^{18} + 38508 u^{19} + 98424 u^{20} - 777542 u^{21} - 3026706 u^{22} + 974054 u^{23} + 22560880 u^{24} + 5538222 u^{25} - 750618742 u^{26} + 2975737744 u^{27} - 5911629492 u^{28} + 719588800 u^{29} - 5668819956 u^{30} + 2884832652 u^{31} - 902906682 u^{32} + 153467228 u^{33} - 10132586 u^{34}$
6	6	$49 u^{18} + 366 u^{19} + 5814 u^{20} + 23962 u^{21} - 41853 u^{22} - 682698 u^{23} - 945585 u^{24} + 12503586 u^{25} - 24217035 u^{26} + 169034410 u^{27} - 1246077537 u^{28} + 4484696778 u^{29} - 9391782285 u^{30} + 12591718398 u^{31} - 11206092729 u^{32} + 19820781898/3 u^{33} - 2480109594 u^{34} + 535322472 u^{35} - 150851455/3 u^{36}$
7	5	$6 u^{20} + 98 u^{21} + 672 u^{22} - 1250 u^{23} - 6824 u^{24} - 110774 u^{25} + 56116 u^{26} + 3841896 u^{27} - 23183244 u^{28}$

Table 2.2 continued

<u>r</u>	<u>t</u>	<u>$g_{r,t}(u)$</u>
		$+ 129993780 u^{29} - 644014416 u^{30} + 2150558746 u^{31}$ $- 4685989780 u^{32} + 6818385206 u^{33} - 6710675896 u^{34}$ $+ 4424439950 u^{35} - 1874840310 u^{36} + 461777106 u^{37}$ $- 50231082 u^{38}$
8	4	$- 97/4 u^{24} + 24 u^{25} + 1234 u^{26} - 13364 u^{27} + 60079 u^{28}$ $+ 54112 u^{29} - 2118424 u^{30} + 15933388 u^{31} - 321434787 u^{32}$ $+ 280949812 u^{33} - 671628936 u^{34} + 1098040232 u^{35}$ $- 1225836795 u^{36} + 919397812 u^{37} - 443327086 u^{38}$ $+ 124225312 u^{39} - 15378679 u^{40}$
9	3	$222 u^{30} - 2370 u^{31} - 1950 u^{32} + 491648/3 u^{33} - 1384110$ $u^{34} + 6594408 u^{35} - 20320300 u^{36} + 41819580 u^{37}$ $- 57775014 u^{38} + 158470070/3 u^{39} - 30634890 u^{40}$ $+ 10203648 u^{41} - 4459390/3 u^{42}$
10	2	$- 327 u^{36} + 6900 u^{37} - 50430 u^{38} + 191268 u^{39} - 425535$ $u^{40} + 575718 u^{41} - 465905 u^{42} + 207350 u^{43} - 39039 u^{44}$
11	1	$- 60 u^{42} + 330 u^{43} - 660 u^{44} + 572 u^{45} - 182 u^{46}$
12	0	$- 1/24 u^{48}$
<u>$r + t = 13$:</u>		
<u>r</u>	<u>t</u>	<u>$g_{r,t}(u)$</u>
0	13	$1/26 u^{26}$
1	12	$- 15/2 u^{20} + 48 u^{21} - 30 u^{22} - 288 u^{26} + 570 u^{24} - 160$ $u^{25} - 350 u^{26} + 240 u^{27} - 45/2 u^{28}$
2	11	$150 u^{17} - 1827 u^{18} + 5268 u^{19} + 13769 u^{20} - 105182 u^{21}$ $+ 193230 u^{22} - 8976 u^{23} + 428442 u^{24} + 564750 u^{25}$ $- 190026 u^{26} - 153300 u^{27} + 143418 u^{28} - 31966 u^{29} - 866$ u^{30}
3	10	$180 u^{16} - 144 u^{17} + 20622 u^{18} - 111192 u^{19} - 255097 u^{20}$ $+ 2478468 u^{21} - 2521057 u^{22} - 16586212 u^{23}$

Table 2.2 continued

<u>r</u>	<u>t</u>	<u>$g_{r,t}(u)$</u>
		$+ 61975188 u^{24} - 94144704 u^{25} + 64876863 u^{26} + 1021416$ $u^{27} + 35114475 u^{28} + 24366804 u^{29} - 6185553 u^{30} + 12324$ $u^{31} + 166569 u^{32}$
4	9	$25 u^{16} + 2304 u^{17} + 7794 u^{18} + 120870 u^{19} - 191263 u^{20}$ $- 3892220 u^{21} + 12777559/2 u^{22} + 43830814 u^{23}$ $- 110482345 u^{24} - 276636550 u^{25} + 1729131018 u^{26}$ $- 372631416 u^{27} + 4511768181 u^{28} - 3280080858 u^{29}$ $+ 26522485345/2 u^{30} - 169794248 u^{31} - 80823862 u^{32}$ $+ 34527916 u^{33} - 368631213 u^{34}$
5	8	$3 u^{16} + 60 u^{17} + 3027 u^{18} + 19524 u^{19} + 324927/2 u^{20}$ $+ 225048 u^{21} - 4409859 u^{22} - 10016480 u^{23} + 125323213/2$ $u^{24} + 87952788 u^{25} - 427275001 u^{26} - 1844489348 u^{27}$ $+ 12279966615 u^{28} - 30703532844 u^{29} - 4246685288 u^{31}$ $+ 26453970792 u^{32} - 10582034292 u^{33} + 2503233492 u^{34}$ $- 283641220 u^{35} + 6393328 u^{36}$
6	7	$2 u^{17} + 18 u^{18} + 696 u^{19} + 5515 u^{20} + 54426 u^{21} + 167805$ $u^{22} - 741332 u^{23} - 6120351 u^{24} + 1504602 u^{25} + 96875498$ $u^{26} - 123608250 u^{27} + 298613298 u^{28} - 5992916480 u^{29}$ $+ 3027452267 u^{30} - 78216281674 u^{31} + 125494519336 u^{32}$ $- 1341446402088 u^{33} + 97502905825 u^{34} - 47606274364 u^{35}$ $+ 148862723 u^{36} - 2670647666 u^{37} + 205788304 u^{38}$
7	6	$39 u^{20} + 126 u^{21} + 3354 u^{22} + 14224 u^{23} - 18980 u^{24}$ $- 375424 u^{25} - 1312279 u^{26} + 3252068 u^{27} + 46419590 u^{28}$ $- 238291988 u^{29} + 1130606935 u^{30} - 6600475620 u^{31}$ $+ 26687193725 u^{32} - 68478806992 u^{33} + 116466615694 u^{34}$ $- 135621660020 u^{35} + 109145646130 u^{36} - 59833479722 u^{37}$ $+ 21344603400 u^{38} - 4464534364 u^{39} + 414600098 u^{40}$
8	5	$12 u^{23} + 141 u^{24} - 266 u^{25} - 15107/2 u^{26} + 28476 u^{27}$

Table 2.2 continued

<u>r</u>	<u>t</u>	<u>$g_{r,t}(u)$</u>
		$- 270218 u^{28} + 1148868 u^{29} + 4737668 u^{30} - 61370010 u^{31}$ $+ 399020474 u^{32} - 2022120650 u^{33} + 7601272070 u^{34}$ $- 19930452292 u^{35} + 36299450222 u^{36} - 46250900476 u^{37}$ $+ 82314887535/2 u^{38} - 25097630234 u^{39} + 10043521 u^{40}$ $- 2349358436 u^{41} + 246454916 u^{42}$
9	4	$116 u^{28} + 158 u^{29} - 12459 u^{30} + 103806 u^{31} - 561519/2$ $u^{32} - 1545234 u^{33} + 21073192 u^{34} - 131890836 u^{35}$ $+ 1109413305/2 u^{36} - 1632418062 u^{37} + 3379697101 u^{38}$ $- 4926018786 u^{39} + 5019304095 u^{40} - 3498416334 u^{41}$ $+ 1589449452 u^{42} - 424208728 u^{43} + 50456626 u^{44}$
10	3	$- 733 u^{34} + 4980 u^{35} + 48875 u^{36} - 856672 u^{37} + 5895582$ $u^{38} - 24572196 u^{39} + 67821270 u^{40} - 127325154 u^{41}$ $+ 163034157 u^{42} - 139997572 u^{43} + 77075141 u^{44}$ $- 24580010 u^{45} + 3452332 u^{46}$
11	2	$960 u^{40} - 16896 u^{41} + 112596 u^{42} - 398640 u^{43} + 838035$ $u^{44} - 1081080 u^{45} + 840411 u^{46} - 361504 u^{47} + 66118 u^{48}$
12	1	$165/2 u^{46} - 440 u^{47} + 858 u^{48} - 728 u^{49} + 455/2 u^{50}$
13	0	$1/26 u^{52}$
<u>$r + t = 14:$</u>		
<u>r</u>	<u>t</u>	<u>$g_{r,t}(u)$</u>
0	14	$1/28 u^{28}$
1	13	$12 u^{22} - 12 u^{23} - 180 u^{24} + 480 u^{25} - 190 u^{26} - 560 u^{27}$ $+ 600 u^{28} - 90 u^{29} - 60 u^{30}$
2	12	$63 u^{18} - 1032 u^{19} + 8735/2 u^{20} + 5544 u^{21} - 83503 u^{22}$ $+ 196632 u^{23} - 57537/2 u^{24} - 579288 u^{25} + 930345 u^{26}$ $- 363384 u^{27} - 836241/2 u^{28} + 488488 u^{29} - 147249 u^{30}$ $- 13984 u^{31} + 19779/2 u^{32}$
3	11	$252 u^{17} - 774 u^{18} + 25922 u^{19} - 173964 u^{20} - 157062 u^{21}$

Table 2.2 continued

<u>r</u>	<u>t</u>	<u>$g_{r,t}(u)$</u>
		$+ 37124114 u^{22} - 7376930 u^{23} - 17207838 u^{24} + 99396710 u^{25} - 182714448 u^{26} + 144724590 u^{27} + 11552178 u^{28} - 121963380 u^{29} + 99435402 u^{30} - 29710230 u^{31} - 2141256 u^{32} + 3020706 u^{33} - 422292 u^{34}$
4	10	$21/2 u^{16} + 100 u^{17} + 6302 u^{18} + 9000 u^{19} + 485199/2 u^{20} - 763722 u^{21} - 8521571 u^{22} + 26048602 u^{23} + 84598156 u^{24} - 399831628 u^{25} - 142113726 u^{26} + 3809753320 u^{27} - 20962677843/2 u^{28} + 14998092342 u^{29} - 12586596387 u^{30} + 5675863214 u^{31} - 471258074 u^{32} - 872722560 u^{33} + 447383602 u^{34} - 82936724 u^{35} + 8172131/2 u^{36}$
5	9	$30 u^{17} + 540 u^{18} + 16020 u^{19} + 71240 u^{20} + 504420 u^{21} + 48864 u^{22} - 18563796 u^{23} - 18311670 u^{24} + 295531190 u^{25} + 84243392 u^{26} - 2676098502 u^{27} - 872794280 u^{28} + 37868848064 u^{29} - 125052677400 u^{30} + 219991140402 u^{31} - 245283030198 u^{32} + 180855907590 u^{33} - 87019866504 u^{34} + 25361152720 u^{34} - 3518381904 u^{36} - 48715918 u^{37} + 50975700 u^{38}$
6	8	$1/2 u^{16} + 36 u^{18} + 202 u^{19} + 7716 u^{20} + 47862 u^{21} + 332698 u^{22} + 691332 u^{23} - 14189583/2 u^{24} - 36626720 u^{25} + 69738606 u^{26} + 583118544 u^{27} - 997465176 u^{28} - 1922227372 u^{29} - 15138526521 u^{30} + 145154249496 u^{31} - 1933159727525/4 u^{32} + 931633545084 u^{33} - 1179743196663 u^{34} + 1025006633574 u^{35} - 614746482447 u^{36} + 248806104518 u^{37} - 64095144118 u^{38} + 9266884944 u^{39} - 2178635691/4 u^{40}$
7	7	$6 u^{19} + 20 u^{20} + 640 u^{21} + 5232 u^{22} + 45970 u^{23} + 180700 u^{24} - 537058 u^{25} - 5888758 u^{26} - 9778628 u^{27} + 76507170 u^{28} + 352657758 u^{29} - 1949476228 u^{30} + 6112993102 u^{31}$

Table 2.2 continued

<u>r</u>	<u>t</u>	<u>$g_{r,t}(u)$</u>
		- 42016868854 u^{32} + 221667140530 u^{33} - 691634205440 u^{34} + 9703825192882/7 u^{35} - 1894483748242 u^{36} + 1814115472308 u^{37} - 1221018227010 u^{38} + 56641266888 u^{39} - 172251774262 u^{40} + 30817376460 u^{41} - 17117002982/7 u^{42}
8	6	15 u^{22} + 18 u^{23} + 924 u^{24} + 6126 u^{25} - 9794 u^{26} - 185804 u^{27} - 1118429/4 u^{28} - 1176616 u^{29} + 17756040 u^{30} + 83735784 u^{31} - 998696355 u^{32} + 5527033728 u^{33} - 28889012022 u^{34} + 122499727704 u^{35} - 365340212908 u^{36} + 756045832448 u^{37} - 1103375739239 u^{38} + 1147475543454 u^{39} - 847456959117 u^{40} + 434899552170 u^{41} - 147534875976 u^{42} + 29744254924 u^{43} - 10785183587/4 u^{44}
9	5	6 u^{26} + 84 u^{27} - 1996 u^{28} - 656 u^{29} + 84906 u^{30} - 730634 u^{31} + 4072562 u^{32} - 4257558 u^{33} - 97312672 u^{34} + 880485360 u^{35} - 4999388856 u^{36} + 2103264588 u^{37} - 64537133416 u^{38} + 142654508874 u^{39} - 227169636280 u^{40} + 260540815390 u^{41} - 213282010044 u^{42} + 121619843140 u^{43} - 45914301704 u^{44} + 10316864982 u^{45} - 1044543166 u^{46}
10	4	- 707/2 u^{32} - 3860 u^{33} + 86228 u^{34} - 535220 u^{35} + 381420 u^{36} + 17400872 u^{37} - 158603511 u^{38} + 833505640 u^{39} - 3015768360 u^{40} + 7775874964 u^{41} - 14407251859 u^{42} + 19166687644 u^{43} - 36240274941/2 u^{44} + 11872637720 u^{45} - 5123965424 u^{46} + 1309974576 u^{47} - 150283006 u^{48}
11	3	1840 u^{38} - 1624 u^{39} - 303798 u^{40} + 3551130 u^{41} - 21088584 u^{42} + 79099350 u^{43} - 200061576 u^{44} + 348891114 u^{45} - 419819400 u^{46} + 342100902 u^{47} - 180181430 u^{48} + 55338452 u^{49} - 7526376 u^{50}
12	2	- 2376 u^{44} + 37224 u^{45} - 231044 u^{46} + 773916 u^{47}

Table 2.2 continued

<u>r</u>	<u>t</u>	<u>$g_{r,t}(u)$</u>
		- 3106389/2 u^{48} + 1925924 u^{49} - 1447264 u^{50} + 60465656 u^{51} - 215683/2 u^{52}
13	1	- 110 u^{50} + 572 u^{51} - 1092 u^{52} + 910 u^{53} - 280 u^{54}
14	0	- 1/28 u^{56}

2.5 Thermodynamic functions and their series expansions

Having obtained the polynomials $g_{r,t}$ on the three lattices of interest, we can immediately write down the corresponding expression for the Gibbsian free energy density via equations (2.1.3,5). Expressions for thermodynamic functions can thus be obtained from the Gibbsian free energy per spin in the standard manner.

In this section, we shall study the thermodynamic quantities of interest, namely the magnetisation in a non-zero field, the spontaneous magnetisation, the zero-field susceptibility and the zero-field specific heat capacity, in both uniform and staggered fields, denoted by H and H^\dagger , respectively (see section 1.2). For the sake of brevity, we shall only derive expressions for the magnetisations, and list the remaining functions. The interested reader can find the full derivations in Yousif, 1983.

For our particular model we shall take $m_A = S_A = 1/2$ and $m_B = S_B = 1$, so that $m_A/S_A = m_B/S_B$.

(i) Magnetisation: Magnetisation $M(T,H)$ in uniform field H ($=H_A=H_B$) is given by

$$M(T,H) = -(\partial G(T,H)/\partial H)_T .$$

Defining the sublattice magnetisations

$$M_A = -(\partial G/\partial H_A)_T , \quad M_B = -(\partial G/\partial H_B)_T$$

we have from (2.1.3)

$$\begin{aligned} M_A &= \frac{1}{2} m_A + kT (\partial/\partial H_A) \ln \Lambda(\mu, \nu, u) \\ &= \frac{1}{2} m_A - 2m_A \mu (\partial/\partial \mu) \ln \Lambda(\mu, \nu, u) \end{aligned}$$

and on using (2.1.5), this gives

$$M_A(\mu, \nu, u) = \frac{1}{2} m_A - 2m_A \sum_{r,t} r g_{r,t}(u) \mu^r \nu^t .$$

Similarly we obtain for M_B

$$M_B(\mu, \nu, u) = \frac{1}{2} m_B - m_B \sum_{r,t} t g_{r,t}(u) \mu^r \nu^t$$

yielding for the uniform magnetisation $M = M_A + M_B$ (see (1.2.1))

$$M(\mu, \nu, u) = \frac{1}{2} (m_A + m_B) - \sum_{r,t} (2m_A r + m_B t) g_{r,t}(u) \mu^r \nu^t .$$

Here, of course, $\mu = \exp(-2\beta m_A H)$ and $\nu = \exp(-\beta m_B H)$. Now, the magnetisation in staggered field $H^\dagger (=H_A = -H_B)$ is similarly given by

$$M^\dagger(T, H^\dagger) = -(\partial G(T, H^\dagger) / \partial H^\dagger)_T = M_A - M_B .$$

Hence, from above

$$M^\dagger(\mu, \nu, u) = \frac{1}{2} (m_A - m_B) - \sum_{r,t} (2m_A r - m_B t) g_{r,t}(u) \mu^r \nu^t$$

with $\mu = \exp(-2\beta m_A H^\dagger)$, $\nu = \exp(\beta m_B H^\dagger)$. For our particular choice of $m_A = 1/2$ and $m_B = 1$, these expressions reduce to

$$M(\mu, u) = 3/4 - \sum_{r,t} (r+t) g_{r,t}(u) \mu^{r+t} \quad (2.5.1)$$

where $\mu = \exp(-\beta H)$, and

$$M^\dagger(\mu, u) = -1/4 - \sum_{r,t} (r-t) g_{r,t}(u) \mu^{r-t} \quad (2.5.2)$$

where $\mu = \exp(-\beta H^\dagger)$. In equations (2.5.1,2) $u = \exp(-2\beta J)$. These equations could have been written in terms of ν equivalently ($\mu = \nu$ in uniform and $\mu = 1/\nu$ in staggered fields).

From (2.5.1,2) we obtain expressions for the uniform and the staggered critical isotherms as

$$M(\mu, u_C) = 3/4 - \sum_{r,t} (r+t) g_{r,t}(u_C) \mu^{r+t} \quad (2.5.3)$$

and

$$M^\dagger(\mu, u_C) = -1/4 - \sum_{r,t} (r-t) g_{r,t}(u_C) \mu^{r-t} \quad (2.5.4)$$

respectively, where $u=u_C$ is the critical point; and also expressions for the spontaneous uniform and staggered magnetisations:

$$M_0(u) = 3/4 - \sum_{r,t} (r+t) g_{r,t}(u) \quad (2.5.5)$$

and

$$M_0^\dagger(u) = -1/4 - \sum_{r,t} (r-t) g_{r,t}(u) \quad (2.5.6)$$

respectively. Equations (2.5.5,6) follow because $\mu=1$ in zero field. Defining the high field polynomials $L_n(u)$ by

$$L_n(u) = \sum_{\substack{r,t \\ s.t. r+t=n}} g_{r,t}(u) \quad (2.5.7)$$

equations (2.5.3,5) may be re-written as

$$M(\mu, u_C) = 3/4 - \sum_{n>0} n L_n(u_C) \mu^n \quad (2.5.8)$$

and

$$M_0(u) = 3/4 - \sum_{n>0} n L_n(u) \quad (2.5.9)$$

respectively.

(ii) Susceptibility in zero field: We have, for our particular choice of magnetic moments per spin,

$$\chi_0(u) = \sum_{n>0} n^2 L_n(u) \quad (2.5.10)$$

$$x_0^\dagger(u) = \sum_{r,t} (r-t)^2 g_{r,t}(u) \quad (2.5.11)$$

where $x_0(u)$ and $x_0^\dagger(u)$ denote the (reduced) uniform and staggered susceptibilities in zero field, respectively.

(iii) Specific heat in zero field: Denoting the reduced zero-field specific heat capacity by $C_0(u)$ (there is no distinction between the uniform and the staggered), we have

$$C_0(u) = \sum_{r,t} \sum_{n>0} n^2 a_n[r,t,d] u^n \quad (2.5.12)$$

again for our particular choice of m_A and m_B . The coefficients a_n can be obtained directly from $g_{r,t}$ via the defining relationship (2.1.6).

These thermodynamic functions are listed below for convenience.

$$\begin{aligned} M_0(u) &= 3/4 - \sum_{n>0} n L_n(u) \\ M_0^\dagger(u) &= -1/4 - \sum_{r,t} (r-t) g_{r,t}(u) \\ x_0(u) &= \sum_{n>0} n^2 L_n(u) \\ x_0^\dagger(u) &= \sum_{r,t} (r-t)^2 g_{r,t}(u) \\ C_0(u) &= \sum_{r,t} \sum_{n>0} n^2 a_n[r,t,d] u^n \\ M_C(\mu) &= 3/4 - \sum_{n>0} n L_n(u_C) \mu^n \\ M_C^\dagger(\mu) &= -1/4 - \sum_{r,t} (r-t) g_{r,t}(u_C) \mu^{r-t} . \end{aligned} \quad (2.5.13)$$

The high field polynomials $L_n(u)$ have also been calculated for the three lattices under consideration, through corresponding orders of $g_{r,t}(u)$, but since more information is contained in polynomials $g_{r,t}$ and also because of reasons of space, the $L_n(u)$ are not presented in this thesis.

Before proceeding; we make an important note. As seen from equations (2.5.13), spontaneous magnetisations, zero-field susceptibilities and the zero-field specific heat are all power series in the variable u (or z). Thus in our series expansions for these functions, the maximum power of u which we are convinced is not repeated in higher undetermined orders of $L_n(u)$ (or $g_{r,t}(u)$), must be found; so that we have all the contributions to each power and hence the series will be exact to that maximum power. The pattern of polynomials $g_{r,t}(u)$ listed in table 2.2 suggests, for this maximum power, the values 17; 20; 16 for the honeycomb, hydrogen peroxide and the diamond lattices, respectively.

Clearly, the series expansions for the uniform and staggered critical isotherms (although the latter will not be considered in this thesis) do not present such problems as above, since they form series in the variable μ and contributions to μ_λ^n (say) come from $L_n(u_C)$, so the expansion up to the existing order of $L_n(u_C)$ is indeed exact.

We are now in a position to calculate the initial terms of the low-temperature series expansions for the spontaneous magnetisations, zero-field susceptibilities and the zero-field specific heat on all the three lattices of interest. These are listed in table 2.3. The discussion of the (uniform) isotherm is delayed until the next chapter, where we obtain information about the values of the critical point on all the lattices. As seen from table 2.3, contrary to our expectation (see section 1.4), for the three-dimensional lattices under consideration, only the uniform susceptibility series for the hydrogen peroxide lattice has coefficients which are of one sign (up to the given order).

Table 2.3: Low-temperature series expansions for: spontaneous magnetisations $M_0(u)$, $M_0^\dagger(u)$; zero field susceptibilities $\chi_0(u)$, $\chi_0^\dagger(u)$ and the zero-field specific heat $C_0(u)$ of the honeycomb, hydrogen peroxide and diamond lattices. For the honeycomb and the hydrogen peroxide lattices expansions are in powers of $z = \sqrt{u}$.

Honeycomb Lattice

$$M_0(z) = 3/4 - 1/2 z^3 - z^6 - 3 z^7 - 9 z^8 - 10 z^9 - 15/2 z^{10} - 15/2 z^{11}$$

$$- 153/2 z^{12} - 201 z^{13} - 303 z^{14} - 207 z^{15} - 426 z^{16} - 3945/2 z^{17}$$

$$M_0^\dagger(z) = - 1/4 + 1/2 z^3 + 3 z^8 + 6 z^9 + 9/2 z^{10} - 15/2 z^{11} + 9/2 z^{12}$$

$$+ 66 z^{13} + 156 z^{14} + 102 z^{15} - 54 z^{16} + 375/2 z^{17}$$

$$\chi_0(z) = 1/2 z^3 + 3/2 z^6 + 6 z^7 + 27 z^8 + 47 z^9 + 117/2 z^{10} + 147/2 z^{11}$$

$$+ 931/2 z^{12} + 1425 z^{13} + 2904 z^{14} + 3858 z^{15} + 8100 z^{16}$$

$$+ 50655/2 z^{17}$$

$$\chi_0^\dagger(z) = 1/2 z^3 + 3/2 z^6 + 3 z^8 + 11 z^9 + 45/2 z^{10} - 9/2 z^{11} - 29/2 z^{12}$$

$$+ 123 z^{13} + 540 z^{14} + 732 z^{15} + 324 z^{16} + 819/2 z^{17}$$

$$C_0(z) = 9/2 z^3 + 27 z^6 + 147/2 z^7 + 192 z^8 + 135 z^9 + 1926 z^{12}$$

$$+ 9633/2 z^{13} + 4851 z^{14} - 7605/2 z^{15} - 2304 z^{16} + 47685 z^{17}$$

Hydrogen Peroxide Lattice

$$M_0(z) = 3/4 - 1/2 z^3 - z^6 - 3 z^7 - 9 z^8 - 10 z^9 - 15/2 z^{10} - 15/2 z^{11}$$

$$- 72 z^{12} - 174 z^{13} - 204 z^{14} + 39/2 z^{15} - 33/2 z^{16} - 2511/2 z^{17}$$

$$- 3711 z^{18} - 3438 z^{19} + 5217/2 z^{20}$$

$$M_0^\dagger(z) = - 1/4 + 1/2 z^3 + 3 z^8 + 6 z^9 + 9/2 z^{10} - 15/2 z^{11} + 3 z^{12}$$

$$+ 57 z^{13} + 123 z^{14} + 57/2 z^{15} - 357/2 z^{16} - 15/2 z^{17} + 1231 z^{18}$$

$$+ 2331 z^{19} + 297/2 z^{20}$$

Table 2.3 continued

$$\begin{aligned}
 \chi_o(z) &= 1/2 z^3 + 3/2 z^6 + 6 z^7 + 27 z^8 + 47 z^9 + 117/2 z^{10} + 147/2 z^{11} \\
 &\quad + 425 z^{12} + 1179 z^{13} + 1953 z^{14} + 2979/2 z^{15} + 5877/2 z^{16} \\
 &\quad + 27717/2 z^{17} + 39643 z^{18} + 55248 z^{19} + 37275 z^{20} \\
 \chi_o^\dagger(z) &= 1/2 z^3 + 3/2 z^6 + 3 z^8 + 11 z^9 + 45/2 z^{10} - 9/2 z^{11} - 19 z^{12} \\
 &\quad + 93 z^{13} + 417 z^{14} + 867/2 z^{15} - 483/2 z^{16} - 1251/2 z^{17} + 3255 \\
 &\quad z^{18} + 10962 z^{19} + 11259 z^{20} \\
 C_o(z) &= 9/2 z^3 + 27 z^6 + 147/2 z^7 + 192 z^8 + 135 z^9 + 1854 z^{12} \\
 &\quad + 8619/2 z^{13} + 2793 z^{14} - 17505/2 z^{15} - 10368 z^{16} + 37281 z^{17} \\
 &\quad + 121500 z^{18} + 92055/2 z^{19} - 353400 z^{20}
 \end{aligned}$$

Diamond Lattice

$$\begin{aligned}
 M_o(u) &= 3/4 - 1/2 u^2 - u^4 - 4 u^5 - 10 u^6 - 8 u^7 + 5/2 u^8 - 74 u^9 \\
 &\quad - 541/2 u^{10} - 18 u^{11} + 1451/2 u^{12} - 2142 u^{13} - 19171/2 u^{14} \\
 &\quad + 4668 u^{15} + 81697/2 u^{16} \\
 M_o^\dagger(u) &= - 1/4 + 1/2 u^2 + 4 u^6 + 8 u^7 - 21/2 u^8 - 14 u^9 + 249/2 u^{10} \\
 &\quad + 198 u^{11} - 1089/2 u^{12} - 650 u^{13} + 9707/2 u^{14} + 6468 u^{15} \\
 &\quad - 53897/2 u^{16} \\
 \chi_o(u) &= 1/2 u^2 + 3/2 u^4 + 8 u^5 + 34 u^6 + 56 u^7 + 41/2 u^8 + 346 u^9 \\
 &\quad + 3685/2 u^{10} + 1994 u^{11} - 5451/2 u^{12} + 14170 u^{13} + 187539/2 \\
 &\quad u^{14} + 59236 u^{15} - 285077 u^{16} \\
 \chi_o^\dagger(u) &= 1/2 u^2 + 3/2 u^4 + 2 u^6 + 24 u^7 + 25/2 u^8 - 102 u^9 + 181/2 \\
 &\quad + u^{10} + 1154 u^{11} + 517/2 u^{12} - 6422 u^{13} + 8531/2 u^{14} + 62020 \\
 &\quad u^{15} - 3741 u^{16} \\
 C_o(u) &= 2 u^2 + 12 u^4 + 50 u^5 + 96 u^6 - 104 u^8 + 1296 u^9 + 3410 u^{10} \\
 &\quad - 5566 u^{11} - 18000 u^{12} + 60502 u^{13} + 175042 u^{14} - 394500 u^{15} \\
 &\quad - 1130320 u^{16}
 \end{aligned}$$

2.6 Y-Δ transformation and the hydrogen peroxide lattice

In this final section we employ the Y-Δ transformation (Fisher, 1959) to determine the critical point, z_C , of our mixed spin hydrogen peroxide lattice.

The Y-Δ transformation was first applied to mixed spin system by Yousif (1983), who; as a result; obtained the exact critical point of the mixed spin honeycomb lattice. It is this exact value (see the next chapter) which we will be using when analysing the thermodynamic series expansions on the honeycomb lattice.

Applying the Y-Δ transformation, we can 'remove' the spin-1 objects from the mixed spin hydrogen peroxide lattice (for a description of the lattice refer to section 2.3), in the standard manner, to get the spin-1/2 hypertriangular lattice. This yields the same formula obtained by Yousif (1983)

$$u_{ht} = z_{hp}^2 (1+z_{hp} +z_{hp}^2)/(1+z_{hp}^3+z_{hp}^6) \quad (2.6.1)$$

where $u_{ht} = \exp(-4\beta J_{ht})$, for the hypertriangular lattice and $z_{hp} = \sqrt{u_{hp}} = \exp(-\beta J_{hp})$, for the hydrogen peroxide lattice variable. Therefore, if the critical point u_C , of the spin-1/2 hypertriangular lattice, is found; we can obtain the critical point of the mixed spin hydrogen peroxide via (2.6.1). With the hypertriangular lattice being three-dimensional too, no exact solution for its critical point is possible (as yet). However, we can apply the Y-Δ transformation once more; this time to the spin-1/2 hydrogen peroxide lattice, whose critical point has been estimated by the method of high-temperature expansions (Betts and Chan, 1974), to obtain the same spin-1/2 hypertriangular lattice, yielding

$$u_{ht} = \bar{z}_{hp} / (1 - \bar{z}_{hp} + \bar{z}_{hp}^2) \quad (2.6.2)$$

with $u_{ht} = \exp(-4\beta J_{ht})$ [as before] and $\bar{z}_{hp} = \sqrt{u_{hp}} = \exp(-2\beta J_{hp})$, for the spin-1/2 hydrogen peroxide lattice variable.

Equation (2.6.6) is the equivalent of (2.6.1) and is the well known $Y-\Delta$ relationship for the ferromagnetic Ising model (Wannier, 1945). Now substitution of the critical point $\bar{z}_C = 0.317401 \pm 0.000010$ (Betts and Chan, 1974), for the spin-1/2 hydrogen peroxide lattice, in (2.6.2) yields an estimate for the hypertriangular critical point:

$$u_C = 0.405188 \pm 0.000015 .$$

Using this estimate, equation (2.6.1) finally solves to give the following singularities: $z_C = 0.512920 \pm 0.000017$, 1.94962 ± 0.000017 , -0.648597 ± 0.000017 , -1.54179 ± 0.000017 and $(-0.136078 \pm 0.000017) \pm i(0.990698 \pm 0.000017)$. Since $z_{hp} = \exp(-\beta J_{hp})$, the region of physical interest is $0 < z_{hp} < 1$ for $J_{hp} > 0$ (ferromagnetic) and $z_{hp} > 1$ for $J_{hp} < 0$ (ferrimagnetic). We, therefore, conclude that the 'physical' singularities are $z_C = 0.512920 \pm 0.000017$ and $z_N = 1.94962 \pm 0.000017$ which correspond to the Curie and the Ne'el points, respectively, of the mixed spin hydrogen peroxide lattice. These happily satisfy the symmetry condition $k_C = -k_N$, where $k = \beta J_{hp}$.

In the series analysis of the next chapter, we shall take $z_C = 0.512920$ as the best estimate for the Curie point of the mixed spin hydrogen peroxide lattice. (Remember we are studying the Hamiltonian (1.3.1) with $J > 0$, which can be interpreted ferrimagnetically, if required).

CHAPTER 3

LOW-TEMPERATURE CRITICAL BEHAVIOUR

3.1 Introduction

In this chapter, we shall study the critical behaviour of various thermodynamic functions obtained in section 2.5 of the previous chapter. As mentioned there, these thermodynamic functions are all power series, about zero, in some variable (μ or u), and have the general form

$$F(u) = \sum_{r=0}^{\infty} a_r u^r \quad (3.1.1)$$

where only the first n coefficients are known. An important assumption is that at a critical point u_C , the function $F(u)$ of interest has a power-law singularity of the form (see also section 1.2)

$$F(u) \sim A(u_C) (1-u/u_C)^{-\lambda}, \quad u \rightarrow u_C^- \quad (3.1.2)$$

where $A(u_C)$ is the so-called critical amplitude, and λ is the critical exponent (or index) at $u=u_C$ (in this thesis, we do not consider the former). Thus the investigation of appropriate singularities of our power series will provide information about the critical behaviour of the corresponding thermodynamic quantities.

It is well known that the radius of convergence of $F(u)$, as given by (3.1.1), is

$$R = \lim_{r \rightarrow \infty} |a_r|^{-1/r}. \quad (3.1.3)$$

Since the series converges for $|u| < R$ and diverges for $|u| > R$; there must exist at least one singularity of $F(u)$ on the circle of convergence $|u| = R$. Unfortunately, the series are often slowly convergent, so that in practice R can not be estimated from its coefficients using (3.1.3). Other methods, therefore, have to be employed to locate the singularities. The methods most widely used in the analysis of singularities of the form (3.1.2) are the ratio (Domb and Sykes, 1957 ; Domb, 1960 ; Fisher, 1967) and the Pade' approximant (PA) (Baker, 1961 ; Fisher, 1967 ; Guant and Guttmann, 1974) methods; the latter, being more powerful, is employed for the analysis of our series expansions, as these series generally do not fulfil the requirements of the ratio method (see section 3.2(i)). For this reason, we shall discuss the ratio method in less detail and rather give its general features. The Pade' approximant is, however, explained more fully (see the following section). The interested reader can find a more detailed description of both methods in the references cited above.

In subsequent sections, a detailed investigation of relevant critical properties is undertaken. Also, a separate section is devoted to the study of the uniform field critical isotherm exponent, where Guant's method (Gaunt, 1967) is briefly described and the actual numerical series expansion for $M_C(\mu)$ is given.

3.2 Series analysis: Ratio and Pade' approximant methods

Let us, to begin with, note some fundamental characteristics of such singularities as (3.1.2). Singularities nearest the origin will dominate the behaviour for large r . If the dominant singularity is on the positive real axis, the coefficients will eventually all have the same sign, whereas for the dominant singularities on the negative real axis, the coefficients must eventually alternate in sign. Dominant

singularities on the complex plane (which must occur in pairs, as the coefficients are real) indicate more irregular behaviour of coefficients. Our thermodynamic functions often have two 'physical' singularities (corresponding to the Curie' and Ne'el points) which may or may not be dominant. Sometimes the dominant singularity is a non-physical one. Also, the presence of nearby singularities disturbs the rate of convergence of the series.

We are in a position to briefly describe the ratio and the Pade' approximant methods.

(i) Ratio method: This method is used to determine the location and nature of a singularity which lies on the real axis and is dominant. In this method, we have to 'guess' the form of the coefficients for large r .

Suppose that the dominant singularity is on the positive real axis and thus the coefficients are all of one sign (if they alternate in sign, one replaces u by $-u$). From equation (3.1.3), with $R > 0$, $a_r \sim R^{-r} f(r)$ for large r , where $f(r)$ has to obey $\lim_{r \rightarrow \infty} \{f(r)\}^{1/r} = 1$. It can be seen that the choice of

$$f(r) = A C_r^{g+r} = A (r+1)(r+2)\dots(r+g)/g!$$

satisfies $\lim_{r \rightarrow \infty} \{f(r)\}^{1/r} = 1$, and yields (by Appell's comparison theorem, Dienes; 1957) for $g > -1$ and real u , singularities of the form (3.1.2):

$$F(u) \sim A (1-u/R)^{-(1+g)}, \quad u \rightarrow R^-$$

and so A and g directly determine the critical amplitude and exponent, respectively, at the singularity $u=R$. With this choice for $f(r)$, the ratios $\mu_r = a_r/a_{r-1} \sim R^{-1}(1+g/r)$ for large r , should vary linearly

with $1/r$ as $r \rightarrow \infty$. Thus, if the first few coefficients are known, the initial estimates are often obtained from the sequences

$$l_r = r\mu_r - (r-1)\mu_{r-1} \rightarrow 1/R, \text{ as } r \rightarrow \infty \quad (3.2.1)$$

$$g_r = r(R'\mu_r - 1) \rightarrow g, \text{ as } r \rightarrow \infty \quad (3.2.2)$$

with R' in (3.2.2) obtained from (3.2.1) for given r . Another way to estimate g is to use the best estimate of R which is available, in (3.2.2). These sequences can therefore be extrapolated to obtain best estimates of R and g . For loose-packed lattices, the use of alternate pairs of ratios usually leads to more regular sequences, although we do not give details here.

The ratio method is used to find the singularities one by one. Having found the most dominant singularity, we can 'subtract it off' and proceed to locate the next-most dominant singularity and so on, provided they all lie on the real axis.

Our thermodynamic functions do not generally satisfy the requirements of this method in that they do not have coefficients of one sign (neither do they alternate in sign) and also the ratios μ_r , for the available larger r , do not vary linearly with $1/r$, so that extrapolation can not be formed.

(ii) Pade' approximant method: The shortcomings of the ratio method are that it can only deal with one singularity at a time and only if it lies on the real axis and is dominant. Pade' approximants, however, enable several singularities anywhere on the complex plane to be studied simultaneously and, besides, no particular choice of functions has to be made. This is a method of 'analytic continuation', by which we continue the series function up to the physical boundary, or be-

yond (if there is no natural boundary). This analytic continuation is, of course, unique.

The method consists of forming rational function approximations to a given series. Suppose we have $F(u)$ through order n in u , as by equation (3.1.1). Let

$$\begin{aligned}
 [N,D] &= P_N(u)/Q_D(u) \\
 &= \frac{p_0 + p_1u + p_2u^2 + \dots + p_Nu^N}{1 + q_1u + q_2u^2 + \dots + q_Du^D} \quad (3.2.3)
 \end{aligned}$$

where $P_N(u)$ and $Q_D(u)$ are polynomials in u , of degree N and D , respectively. We call $[N,D]$ a Pade' approximant of order $N+D$. We want to approximate our series function of interest $F(u)$, in such a manner that the expansion of (3.2.3), up to order $N+D$, coincides with that of $F(u)$ through $N+D$. Of course, we must have $N+D \leq n$, for all the possible Pade' approximants of various order. This requires

$$F(u) - [N,D] = O(u^{N+D+1})$$

i.e

$$F(u) Q_D(u) - P_N(u) = O(u^{N+D+1}) .$$

Thus, we have that the coefficients of u at orders 0 through $N+D$ in the expansion of $Q_D(u)F(u) - P_N(u)$, must vanish. By picking coefficients of u , at orders $N+1$ through $N+D$, we obtain D equations for D unknowns q_1, q_2, \dots, q_D which must be solved simultaneously. Substituting their solution into the remaining $N+1$ equations obtained by picking coefficients of u of orders 0 through N , then yields the coefficients p_0 to p_N .

In these equations, if one of the matrices is singular, the corresponding Pade' approximant does not exist. Also, care must be taken if low accuracy is to be avoided, since the set of equations is often 'ill conditioned' in the sense that a small change in the variables leads to large changes in 'right hand sides' of the equations.

In the above manner, we form Pade' approximants of various orders ($\leq n$), whose results are displayed in the well known Pade' table with D labelling the rows and N the columns; the extrapolation techniques are then employed yielding final estimates. Pade' approximants can represent simple poles exactly and consequently the convergence in a region where $F(u)$ has such a pole is normally extremely rapid (Essam and Fisher, 1963). We therefore form PA's to the following functions obtained from $F(u)$, which possess simple poles near the critical point.

(a) Since our thermodynamic power series possess singularities of the kind (3.1.2), we have that for the logarithmic derivative

$$(d/du) \ln F(u) \sim -\lambda/(u-u_C) \quad , \quad u \rightarrow u_C^- \quad (3.2.4)$$

which has a simple pole at $u=u_C$ with residue $-\lambda$. Thus by examining the poles of successive approximants in the neighbourhood of u_C (the smallest root of the denominator is usually taken to be u_C) and also the residues at these points, a sequence of estimates of both u_C and λ may be obtained.

(b) If the exact value, or best estimate, of λ is available; we can form PA's to

$$\{F(u)\}^{1/\lambda} \sim A^{1/\lambda} (1-u/u_C)^{-1} \quad , \quad u \rightarrow u_C^- \quad (3.2.5)$$

which also has a simple pole, in the neighbourhood of which convergence will be rapid. This yields estimates for u_C and A .

(c) Given a realistic estimate for u_C , or its exact value, we can obtain estimates for the critical exponent λ , by forming PA's to the series

$$(u-u_C)(d/du) \{F(u)\} \sim -\lambda, \quad u \rightarrow u_C^- \quad (3.2.6)$$

and evaluating them at u_C .

There are many more functions (such as higher order analogues of (a)-(c)) to which PA's may be formed (Bowers and Woolf, 1969), but they yield poorer rates of convergence in our case.

3.3 Pade' analysis of critical points

As mentioned in section 2.6, the exact value of critical point of the mixed spin honeycomb lattice, $z_C = 0.4688638599\dots$, as obtained by Yousif (1983); is used for analysing the thermodynamic functions on that lattice. Moreover, we derived an estimate, $z_C = 0.512920$, for the critical point of the mixed spin hydrogen peroxide lattice. In this section, we shall show that this value checks with the estimates obtained using the Pade' analysis technique, and also give an estimate for the critical point u_C , of the diamond lattice via the same technique.

Preliminary examination of PA's to the logarithmic derivative shows that the spontaneous magnetisation $M_0(u)$ provides a smoother sequence of estimates than any other zero-field thermodynamic quantity. Also, method (b) of the previous section, with λ given by the well known values suggested by the universality hypothesis, has been initially examined for different $F(u)$; but the smoothness and conver-

gence of estimates is not as satisfactory, which is contrary to the case of high-temperature expansion analysis (Yousif, 1983). Table 3.1 shows the results for the hydrogen peroxide and diamond lattices, respectively. As before, u is replaced by z for the hydrogen peroxide lattice.

As seen from this table, the value $z_C = 0.512920$ estimated for the hydrogen peroxide lies within the range prescribed by the Pade' table: $z_C = 0.528 \pm 0.016$, from the last three orders of estimates.

Also, we estimate for the critical point u_C , of the diamond lattice, from the last three orders of Pade' results, that

$$u_C = 0.419 \pm 0.002$$

where the central value will be used as the critical point. Below, all the three values of the critical point are listed for quick reference.

$$\begin{aligned} z_C &= 0.4688638599 && \text{(honeycomb)} \\ z_C &= 0.512920 && \text{(hydrogen peroxide)} \\ u_C &= 0.419 && \text{(diamond)} . \end{aligned} \tag{3.3.1}$$

We mention, in passing, that the above critical point for the honeycomb has been checked using Pade' analysis by Yousif (1983).

Table 3.1: Estimate for u_c provided by evaluating PA's $[N,D]$, to the series $d/du \ln M_0(u)$ on the hydrogen peroxide and the diamond lattice.

Hydrogen Peroxide Lattice

$\begin{matrix} N \\ D \end{matrix}$	7	8	9	10	11	12	13
7	0.49820	0.48353	0.51029	-	0.51420	0.51570	0.55697
8	0.53287	0.54276	0.55306	0.52480	0.52024	0.51224	
9	0.54146	1.1583	0.54344	0.51884	0.52411		
10	0.54971	0.54220	0.53542	0.53442			
11	0.52107	0.51669	0.53419				
12	0.51770	0.52078					
13	-						

Diamond Lattice

$\begin{matrix} N \\ D \end{matrix}$	5	6	7	8	9	10	11
5	0.41456	0.40978	0.40563	0.41584	0.41936	0.42148	0.41717
6	0.41271	0.41425	0.41595	0.41727	0.41752	0.41910	
7	0.42306	0.42056	0.41983	0.41753	0.41726		
8	0.41989	0.41933	0.42066	0.41945			
9	0.41942	0.41991	0.41799				
10	0.41069	0.41871					
11	-						

3.4 Analysis of zero-field thermodynamic series functions

In this section, we shall try to find reasonable estimates of critical (zero-field) exponents of both uniform and staggered thermodynamic functions of section 2.5 .

First let us consider the uniform and staggered components of spontaneous magnetisation on the basis of relations

$$\begin{aligned} M_0(u) &\sim (u_C - u)^\beta, \quad u \rightarrow u_C^- \\ M_0^+(u) &\sim (u_C - u)^{\beta^+}, \quad u \rightarrow u_C^- \end{aligned}$$

respectively, as given in section 1.2 of the review chapter. In order to obtain estimates for the uniform and staggered exponents β and β^+ , we form PA's to the series $(u_C - u)(d/du) \ln M_0(u)$ and $(u_C - u)(d/du) \ln M_0^+(u)$ (see section 3.2(ii)), respectively, where the critical points u_C (or Z_C) are given by (3.3.1) of the previous section.

On the hydrogen peroxide lattice, we have changed the expansion variable from z to x (by analogy with Fox and Guttman, 1973), where

$$z = x/(2-x) \tag{3.4.1}$$

or equivalently, $x = 1 - \tanh(\beta J/2)$. This transformation happens to improve both the rate of convergence and smoothness of our estimates for β and β^+ (and only for the case of the hydrogen peroxide lattice). The transformed critical point x_C , is obtained by solving (3.4.1) for x , with $z = z_C = 0.512920$, on the basis of the assumption of the uniqueness of the critical point. This yields $x_C = 0.678053$.

Table 3.2 lists various PA estimates for β on all the three lattices under consideration. These show rapid convergence and the last three orders of PA's yield, with few exceptions,

$$\begin{aligned}\beta &= 0.126 \pm 0.001 \quad (\text{honeycomb}) \\ \beta &= 0.301 \pm 0.014 \quad (\text{hydrogen peroxide}) \\ \beta &= 0.298 \pm 0.024 \quad (\text{diamond})\end{aligned}\tag{3.4.2}$$

which include the values suggested by universality for two-dimensional (honeycomb) and three-dimensional (hydrogen peroxide and diamond) lattices (see section 1.2). The value estimated for honeycomb is in good agreement with that of Yousif (1983), in spite of his shorter series expansions (see also section 2.3).

The results of Pade' analysis for β^\dagger are similarly displayed in table 3.3. Again, from the last few orders of PA's, with few exceptions, one estimates

$$\begin{aligned}\beta^\dagger &= 0.1245 \pm 0.0015 \quad (\text{honeycomb}) \\ \beta^\dagger &= 0.302 \pm 0.015 \quad (\text{hydrogen peroxide}) \\ \beta^\dagger &= 0.299 \pm 0.030 \quad (\text{diamond})\end{aligned}\tag{3.4.3}$$

which are, over all, in good agreement with (3.4.2). The above analysis provides evidence for the equality of β and its staggered counterpart β^\dagger , which is, not surprisingly, the case as M_0 and M_0^\dagger are just linear combinations of \wedge_{sub} lattice magnetisations (Bowers, 1981).

Next, we consider the uniform and staggered zero-field susceptibilities. Tables 3.4 and 3.5 list the corresponding Pade' estimates, respectively, obtained on the basis of relations (see section 1.2)

$$\begin{aligned}x_0(u) &\sim (u_C - u)^{-\delta'} \quad , \quad u \rightarrow u_C^- \\ x_0^\dagger(u) &\sim (u_C - u)^{-\delta'^\dagger} \quad , \quad u \rightarrow u_C^-\end{aligned}$$

for the uniform and staggered critical exponents ν' and ν'^{\dagger} of the corresponding zero-field susceptibilities. As seen from table 3.4, estimates of ν' converge very slowly on all the three lattices and are quite irregular, preventing us from obtaining a satisfactory final estimate for ν' . This is due to the presence of non-physical singularities inside the 'physical disc' $|u| \leq u_C$, which slows down the rate of convergence of our results. Transformation (3.4.1) failed to improve matters; and other transformations (such as the one given by Fox and Guttmann, 1973 for spin-1 Ising model) have also been employed to map the non-physical singularities outside the physical disc, which regrettably did not work. In spite of all these, table 3.4 suggests something round about 1.3 in three dimensions for ν' .

This problem is certainly no easier for the case of the staggered critical exponent ν'^{\dagger} , as is evident from table 3.5, since it gives ranges of estimates which are very different from those obtained for ν' , contradicting the general belief that $\nu' = \nu'^{\dagger}$ (Bowers, 1981). Also, estimates for ν'^{\dagger} evaluated on the hydrogen peroxide do not agree sufficiently enough with those evaluated on the diamond lattice; as they should, in view of the universality. But the fact that the estimates seem quite converged (especially for the three-dimensional lattices) remains puzzling. We, therefore, feel that no reasonable estimate for ν'^{\dagger} can be obtained for our model, at present.

Finally, in the same respect, the analysis of the zero-field specific heat capacity on the basis of relation

$$C_0(u) \sim (u_C - u)^{-\alpha'}, \quad u \rightarrow u_C^-$$

failed to provide any useful estimate for the critical exponent α' , because of the high irregularity of the Padé estimates due to the

presence of non-physical singularities inside the physical disc. Again, various transformations (see above) have been applied to improve the rate of convergence, without any success. Because of their high irregularity, we shall not present the Pade' estimates for α' here.

Table 3.2: Estimates for β provided by evaluating $[N,D]$ PA's to the series $(u_c - u) (d/du) \ln M_0(u)$, with $u = u_c$, on the two- and three-dimensional lattice. The transformation $z = x/(2-x)$ has been applied to the hydrogen peroxide lattice to yield improved results.

Honeycomb Lattice, $z_c = 0.468864$

$\begin{matrix} N \\ D \end{matrix}$	6	7	8	9	10	11
6	0.14045	0.12360	0.12324	-0.00986	0.21503	0.12608
7	0.13833	0.12442	0.12502	0.12560	0.12457	
8	0.11520	0.12476	0.12665	0.12502		
9	0.10993	0.12505	0.12476			
10	0.13723	0.11632				
11	0.13492					

Hydrogen Peroxide Lattice, $x_c = 0.678053$

$\begin{matrix} N \\ D \end{matrix}$	7	8	9	10	11	12	13
7	0.32662	0.32184	0.31127	-3.1738	-3.9423	2.5486	0.28681
8	0.32217	0.33420	0.44817	0.28233	-1.5091	0.28693	
9	0.31554	0.44816	0.31483	0.29294	0.28233		
10	0.30899	0.29081	0.29374	0.31483			
11	0.30525	0.29336	0.29081				
12	0.30111	0.30525					
13	0.29912						

Diamond Lattice, $u_c = 0.419$

$\begin{matrix} N \\ D \end{matrix}$	5	6	7	8	9	10	11
5	0.30290	0.29233	0.39217	0.44531	0.50929	0.31586	0.32122
6	0.30776	0.30596	0.30511	0.59952	0.58499	0.29579	
7	0.30496	0.30413	0.30382	0.30502	0.30988		
8	0.30433	0.30374	0.30412	0.30458			
9	0.30402	0.30431	0.30447				
10	0.31110	0.30453					
11	0.27426						

Table 3.3: Estimates for β^\dagger provided by evaluating $[N,P]$ PA's to the series $(u_c - u) (d/du) \ln M_0^\dagger(u)$, with $u = u_c$, on the two- and three-dimensional lattices. The transformation $z = x/2-x$ has been applied to the hydrogen peroxide lattice to yield improved results.

Honeycomb Lattice, $z_c = 0.468864$

D \ N	6	7	8	9	10	11
6	0.12190	0.12445	0.12419	0.11928	0.10821	0.12510
7	0.12212	0.12408	0.12428	0.12415	0.12463	
8	0.12273	0.12466	0.12044	0.12430		
9	0.12255	0.12569	0.12468			
10	0.12101	0.12274				
11	0.12310					

Hydrogen Peroxide Lattice, $x_c = 0.678053$

D \ N	7	8	9	10	11	12	13
7	0.29139	0.31554	0.31700	-3.8510	-3.0379	0.21485	0.28435
8	0.32236	0.31706	0.31581	0.28684	-2.3461	0.28440	
9	0.31621	0.33915	0.30171	0.29994	0.28684		
10	0.30720	0.29922	0.30007	0.31714			
11	0.30384	0.30001	0.29922				
12	0.30137	0.30384					
13	0.30075						

Table 3.3 continued

Diamond Lattice, $u_c = 0.419$

$\begin{array}{c} N \\ \backslash \\ D \end{array}$	5	6	7	8	9	10	11
5	0.30712	0.30598	0.58097	0.34033	0.29584	0.26916	0.29239
6	0.30522	0.30938	0.30486	0.33901	0.44936	0.30873	
7	0.30165	0.30342	0.30492	0.30486	0.31635		
8	0.30491	0.28800	0.31220	0.30466			
9	0.30837	0.31609	0.28484				
10	0.31048	0.30815					
11	0.32845						

Table 3.4: Estimates for γ' provided by evaluating $[N,D]$ PA's to the series $(u_c - u) (d/du) \ln \chi_o(u)$, with $u = u_c$, on the two- and three-dimensional lattices.

Honeycomb Lattice, $z_c = 0.468864$

$\begin{array}{c} N \\ \backslash \\ D \end{array}$	4	5	6	7	8	9
5	2.1012	1.7709	1.8016	0.51738	57.246	60.976
6	1.8752	1.7997	1.7720	1.1746	0.86007	
7	1.8202	1.8845	3.4333	64.173		
8	1.5072	1.5647	-33.266			
9	1.5811	1.1560				
10	1.1760					

Table 3.4 continued

Hydrogen Peroxide Lattice, $z_c = 0.512920$

D \ N	6	7	8	9	10	11
6	1.6298	-0.04092	2.7434	154.69	76.541	97.622
7	-25.326	0.79409	2.1181	3.2502	122.36	
8	1.3382	1.3164	1.4384	2.5152		
9	1.3569	1.3342	1.3240			
10	1.3376	1.6747				
11	1.3037					

Diamond Lattice, $u_c = 0.419$

D \ N	4	5	6	7	8	9
5	1.9491	1.0511	0.66063	30.070	73.719	-18.559
6	1.2133	1.3057	1.2514	1.3647	-129.29	
7	1.2459	1.26619	1.2859	1.3018		
8	1.2730	1.2244	1.3100			
9	1.2838	1.3446				
10	1.3104					

Table 3.5: Estimates for γ^{\dagger} provided by evaluating $[N,D]$ PA's to the series $(u_c - u) (d/du) \ln \chi_0^{\dagger}(u)$, with $u_c = u$, on the two- and three-dimensional lattices

Honeycomb Lattice, $z_c = 0.468864$

D \ N	4	5	6	7	8	9
5	0.52614	0.53067	0.56521	0.57013	2.3123	1.4273
6	0.53080	0.52571	0.57117	0.56424	0.58564	
7	0.59301	0.58413	1.2757	0.61131		
8	0.58288	0.59175	0.62285			
9	0.66668	0.61147				
10	0.53633					

Table 3.5 continued

Hydrogen Peroxide Lattice, $z_c = 0.512920$

D \ N	6	7	8	9	10	11
6	0.83848	0.78599	0.76901	2.1607	-2.0306	0.82944
7	0.82381	0.77817	0.78400	0.78834	0.80130	
8	0.80244	0.79344	0.79195	0.78387		
9	0.79812	0.79142	0.79344			
10	0.79516	0.79807				
11	0.80526					

Diamond Lattice, $u_c = 0.419$

D \ N	4	5	6	7	8	9
5	0.48719	0.46157	0.40099	0.49973	0.46671	1.0266
6	0.46777	0.47514	0.51903	0.22786	0.47700	
7	0.49717	0.44967	0.46268	0.50787		
8	0.47296	0.46672	0.44889			
9	0.46606	0.47286				
10	0.52240					

3.5 Uniform field critical isotherm

We have, from (2.5.13), the series expansions for the uniform field critical isotherm $M_C(\mu)$. Using the values of the critical points for our three lattices of interest (as given by (3.3.1)), we obtain the basic power series

$$M_C(\mu) = 3/4 - \sum_{n>0} d_n \mu^n \quad (3.5.1)$$

for the uniform critical isotherm. The critical exponent δ is defined via the relation

$$M_C(H) \sim H^{1/\delta} \quad \text{as } H \rightarrow 0^+, T=T_C$$

as mentioned in the introductory chapter. In terms of variables u and μ (or ν), we have, since $\mu = \exp(-\beta m_A H/S_A)$ in a uniform field H ,

$$M_C(\mu) \sim (1 - \mu)^{1/\delta} \quad \text{as } \mu \rightarrow 1^-, u=u_C \quad (3.5.2)$$

having used the fact that, as $\mu \rightarrow 1^-$

$$-\ln \mu = (1-\mu) + (1-\mu)^2/2 + (1-\mu)^3/3 + \dots \approx 1-\mu .$$

Thus equation (3.5.2) can be equivalently used to define δ .

In this section, we shall analyse the series (3.5.1) on the basis of relation (3.5.2), to evaluate estimates for the critical exponent δ . This analysis is performed using two different methods. The first being the Pade' approximant approach, where procedure (c) of section 3.2(ii) is employed. Here, PA's are formed to the series $(1-\mu)(d/d\mu) \ln M_C(\mu)$, at $\mu=1$. The second method used in our analysis is the Gaunt's method (Gaunt, 1967). Before proceeding to explain this technique, we give the series for $M_C(\mu)$ on all the three lattices of interest by listing the coefficients d_n in table 3.6 . As one can

see, the available coefficients d_n , are positive for all lattices, as is the case for the spin-1/2, spin-1 and mixed spin (Gaunt and Sykes, 1972 ; Fox and Guttman, 1972 ; Yousif, 1983) Ising ferromagnets.

Gaunt's method: In this method, we again work with the logarithmic derivative of $M_C(\mu)$. This leads to most consistent results for spin-1/2 (Gaunt, 1967 ; Gaunt and Sykes, 1972) and spin-1 (Fox and Gaunt, 1970;1972) and mixed spin (Yousif, 1983) Ising ferromagnets. Thus (3.5.2) yields

$$\begin{aligned} -\mu(d/d\mu) \ln M_C(\mu) &= \sum_{n>0} C_n \mu^n \sim \mu/\delta(1-\mu) \\ &= \mu/\delta + \mu^2/\delta + \mu^3/\delta + \dots \end{aligned} \quad (3.5.3)$$

where C_n are positive for all the lattices under consideration. The coefficients C_n should, therefore, approach $1/\delta$ as $n \rightarrow \infty$ (Gaunt, 1967).

The results of these two methods are displayed in tables 3.7 and 3.8 . From Pade' analysis of table 3.7; we estimate, using the last two orders (with few exceptions)

$$\begin{aligned} \delta &= 15.25 \pm 0.55 \quad (\text{honeycomb}) \\ \delta &= 5.3 \pm 0.4 \quad (\text{hydrogen peroxide}) \\ \delta &= 5.15 \pm 0.15 \quad (\text{diamond}) \end{aligned} \quad (3.5.4)$$

which include the values suggested by universality for two- and three-dimensional lattices (see section 1.2). Also from the results of table 3.8, we estimate

$$\begin{aligned} \delta &= 15.4 \pm 0.5 \quad (\text{honeycomb}) \\ \delta &= 5.6 \pm 0.7 \quad (\text{hydrogen peroxide}) \\ \delta &= 5.3 \pm 0.4 \quad (\text{diamond}) \end{aligned} \quad (3.5.5)$$

which are in good agreement with (3.5.4). These estimates for the honeycomb lattice are in good agreement with those given by Yousif (1983) inspite of his shorter series expansions.

The above work suggests that, as expected, δ depends on dimensionality and not on lattice structure. Estimates (3.5.4,5) may be combined to give

$$\begin{aligned}\delta &= 15.3 \pm 0.4 \quad (\text{two dimensions}) \\ \delta &= 5.3 \pm 0.4 \quad (\text{three dimensions}) .\end{aligned}\tag{3.5.6}$$

When one compares these with the results of the above references for the spin-1/2 and spin-1 Ising ferromagnets, one notes the evidence for an extended form of spin independence. This supports the view that our mixed spin model belongs to the same universality class as the standard single spin model.

Table 3.6: Uniform critical isotherm coefficients d_n for two- and three- dimensional lattices.

n	Honeycomb	Hydrogen Peroxide	Diamond
1	0.056848	0.076576	0.103191
2	0.016914	0.029587	0.044949
3	0.013975	0.026155	0.031404
4	0.011267	0.022579	0.025730
5	0.008715	0.018971	0.020062
6	0.006799	0.015876	0.015685
7	0.005677	0.013971	0.013384
8	0.004948	0.012191	0.011456
9	0.004557	0.010687	0.009996
10	0.004137	0.009545	0.008908
11	0.003743	0.008544	0.007987
12	0.003357	0.007694	0.007225
13	0.003053	0.006997	0.006602
14	0.002835	0.006411	0.00607
15	0.002666	0.005921	
16	0.002494		

Table 3.7: Estimates for δ provided by evaluating $[N,D]$ PA's to the series $(1 - \mu) (d/d\mu) M_c(\mu)$, \wedge at $\mu=1$, for two- and three-dimensional lattices.

Honeycomb Lattice

$\begin{matrix} N \\ D \end{matrix}$	5	6	7	8	9	10
6	14.990	15.189	40.739	10.878	14.697	12.781
7	15.145	15.124	15.918	13.576	15.739	
8	15.122	15.154	15.080	15.811		
9	14.795	15.065	15.153			
10	15.252	14.786				
11	15.117					

Hydrogen Peroxide Lattice

$\begin{matrix} N \\ D \end{matrix}$	5	6	7	8	9	10
5	5.5960	5.1126	3.1575	5.7255	4.8595	5.6520
6	6.3000	5.6891	5.6948	5.4358	5.7144	
7	5.7136	4.6116	5.6078	5.6969		
8	5.6516	5.6287	4.4736			
9	5.6588	5.6515				
10	5.6542					

Diamond Lattice

$\begin{matrix} N \\ D \end{matrix}$	5	6	7	8	9
5	5.0702	5.1954	5.9329	6.6249	5.1845
6	5.0792	5.1954	5.2095	5.1364	
7	5.0792	5.0025	5.1953		
8	5.0157	5.0792			
9	5.3121				

Table 3.8 : Estimates for δ calculated from $1/C_n$ (Gaunt's method) for two- and three-dimensional lattices.

n	Honeycomb	Hydrogen Peroxide	Diamond
1	13.19311	9.79419	7.26808
2	19.66621	11.19518	7.20495
3	16.26965	8.49133	6.53770
4	14.85685	7.16698	5.80211
5	14.99858	6.59833	5.64465
6	15.68605	6.35473	5.71338
7	15.93041	6.05064	5.59692
8	15.87993	5.90410	5.55404
9	15.31679	5.83262	5.51785
10	15.08320	5.75242	5.46417
11	15.03817	5.71487	5.43074
12	15.22152	5.69826	5.40375
13	15.34115	5.68029	5.37298
14	15.28649	5.66240	5.34622
15	15.13459	5.63925	
16	15.09621		

3.6 Discussion

Our work clearly supports the views of the universality principle for the uniform spontaneous magnetisation exponent β , in two and three dimensions. It also provides evidence for the equality of β and β^\dagger . The results for γ' , γ'^\dagger and α' are much less accurate and no useful estimates can be made, although tables suggest γ' to be round about 1.3 in three dimensions.

As expected, the critical exponent δ appears to depend upon dimensionality and not on lattice structure, and our range of δ include the values suggested by universality in two and three dimensions.

With respect to the discussion of section 2.1, derived results for critical exponents are appropriate to both ferromagnetism in uniform and staggered fields or to ferrimagnetism in staggered and uniform fields, respectively.

CHAPTER 4

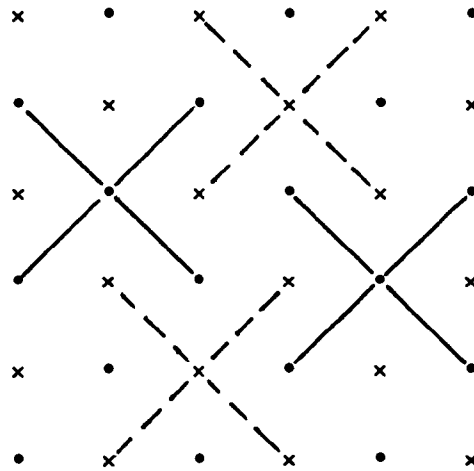
REAL-SPACE RENORMALISATION: PRELIMINARIES

4.1 Introduction

Via the application of RSRG, cluster method (see the next chapter), van Leeuwen (1975) was able to study the details of the flow diagram and the fixed point properties of the spin-1/2 Ising-like model on a square lattice. His Ising-like model was equivalent to the general eight-vertex model (Baxter, 1971;1972), and the five-spin cell choice of his cluster approximation made it possible to obtain antiferro- as well as ferromagnetic fixed points together with a pair of uncoupled sublattice fixed points; whose eigenvalues and corresponding eigenvectors determined the flow along the associated critical surfaces, and indicated the existence of a fixed line of points along which the exponents may depend on the interactions (this corresponds to the zero-field eight-vertex model).

A key point in this choice of cell arrangement is that it ensures the invariance, under renormalisation procedures, of the antiferromagnetic (as well as the ferromagnetic) ground states. This is because, as evident from Fig(4.1), the cell arrangement divides the lattice into sublattices involving either \bullet or \times spin-sites. Thus, an antiferromagnetic fixed point is likely. The existence of two uncoupled sublattice fixed points (corresponding to simultaneous ferro- or antiferromagnetism on two uncoupled sublattices) can also be appreciated in view of the interactions which must be included in order to

close the action of the RG transformation. These turn out to be the nearest, next-nearest and four-spin couplings (van Leeuwen, 1975; see also chapter 5). Note that the blocks now only contain next-nearest couplings.

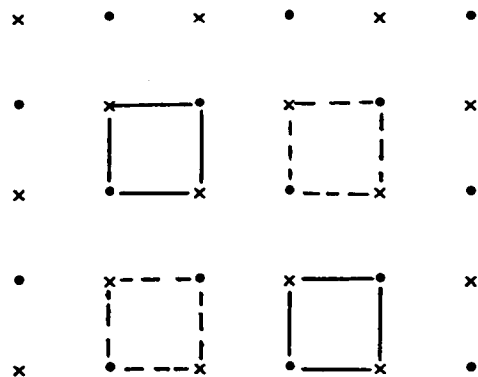


Fig(4.1): Simple-quadratic lattice with dot and cross sublattices. Cells involve either dots or crosses.

By way of contrast, a cell prescription such as shown in Fig(4.2), fails to ensure the invariance of the antiferromagnetic ground state, and also since each cell now involves all the three types of interaction discussed above, the existence of antiferromagnetic as well as 'decoupled' fixed points is not as likely, when calculations are based on such a cell structure (see Nauenberg and Nienhuis, 1974).

Employing the cell structure of Fig(4.1) for a mixed spin square lattice Ising model (involving two sublattices with spin-1/2 and spin-1 objects, respectively, as before); we, in similar fashion, expect to get ferro- and ferrimagnetic fixed points, together with a set of uncoupled sublattice fixed points which would describe the critical behaviour of spin-1/2 and spin-1 Ising models, as well as the shape

of -and flow along- the critical surfaces and any other possibilities which may arise. Obtaining a ferrimagnetic fixed point means that we can study its critical behaviour both in zero and non-zero fields directly, rather than via arguments such as put forward in the beginning of section 2.1 . However, these calculations are generally expected to yield good qualitative (e.g phase diagrams) and poor quantitative results (e.g critical exponents) [see Schick, 1982 and also van Leeuwen, 1975]. We shall also employ the cell structure of Fig(4.2) for our Ising model calculations, where we expect to find at least one fixed point, namely the ferromagnetic. This clustering has been investigated using the cumulant method (see section 4.3) with rather good results by Schofield (1980), where he found a ferromagnetic fixed point; and our cluster approximation calculations here serve mainly as a test for reasons described in chapter 5. We will expand on these in the next chapter, where the details of calculations and analysis of results are presented.



Fig(4.2): Simple-quadratic lattice with a different cell arrangement.

In the following section, the theory of RSRG technique is outlined and in the subsequent one the possibility of tackling our mixed spin model (with the so-called 'sublattice cell choice' of Fig(4.1)) using the

cumulant method is investigated, explaining why it is not fully appropriate. We shall discuss the applications of the cluster theory to our problem in chapter 5.

4.2 Theory of RSRG: An outline

Wilson's first application of RG ideas (Wilson, 1971a;b) to critical phenomena involved systems with continuous spins, where a field theoretical approach made the study of critical behaviour possible. This was called the momentum-space renormalisation group method. Subsequent to this and other related works, development of realisations of the RG specifically designed to treat systems of discrete spins followed. This technique was called real (or position) space renormalisation group and most of its applications have considered spins on a lattice.

In RSRG one deals directly with the microscopic Hamiltonian \mathcal{H} . The method implements an intuitive picture proposed by Kadanoff (1966) [see section 1.4]. In this picture cells of spins in a nearly critical system behave like individual spins in a system somewhat farther from criticality. Fig's(4.1) and (4.2) represent possible assignment of spins into cells. Sites of lattice represent spins which we denote by $\{s\}$ (in this and the following chapter, we show the z-component of spin S^z , simply by s) and the centres of the cells are taken to be the cell spins $\{s'\}$. Now the Gibbsian free energy per spin is, essentially,

$$G = - \lim_{N \rightarrow \infty} N^{-1} \ln Z_N \quad (4.2.1)$$

where N is the number of spins, and the total partition function Z_N for the system is defined by

$$Z_N = \sum_{\{s\}} \exp \mathcal{H}(\{s\}) \quad (4.2.2)$$

in which the summation is taken mean 'sum over all configurations of the N spins', and the factor $\beta=1/\kappa T$ has been incorporated in the definition of the site Hamiltonian $\mathcal{H}(\{s\})$. Adding an arbitrary constant to $\mathcal{H}(\{s\})$ changes the free energy by an additive constant, so we choose the convention $\sum_{\{s\}} \mathcal{H}(\{s\}) = 0$ in order to define $\mathcal{H}(\{s\})$ uniquely.

In RSRG theory, interactions between the cell spins are calculated from those between the site spins. Define a Hamiltonian $C + \mathcal{H}'(\{s'\})$ for the cell spins by

$$\exp[C + \mathcal{H}'(\{s'\})] = \sum_{\{s\}} P(\{s', s\}) \exp \mathcal{H}(\{s\}) \quad (4.2.3)$$

where the condition $\sum_{\{s\}} \mathcal{H}'(\{s'\}) = 0$ is imposed on $\mathcal{H}'(\{s'\})$, so that C (being independent of $\{s'\}$) is uniquely defined. The weight function $P(\{s', s\})$, which couples the cell and site spins, satisfies

$$P(\{s', s\}) \geq 0 \quad , \quad \forall s', s \quad (4.2.4a)$$

$$\sum_{\{s\}} P(\{s', s\}) = 1 \quad . \quad (4.2.4b)$$

The first of these ensures that the right hand side of (4.2.3) is positive and hence C, \mathcal{H}' are real. The second condition guarantees that the partition function of the cell and the site spins are identical. From (4.2.3) one observes that successive applications of the RG will reduce the number of spins and enlarge the lattice constant.

Now expand $\mathcal{H}(\{s\})$ in the form $\mathcal{H}(\{s\}) = \sum_{\alpha} k_{\alpha} \Omega_{\alpha}(\{s\})$, where $\Omega_{\alpha}(\{s\})$ are complete sets of interactions belonging to class α (e.g. nearest neighbours, etc.) generated by repeated applications of (4.2.3) from the initial Hamiltonian of interest, and k_{α} are the cor-

responding coupling constants. In actual calculations, a finite subset of the infinite set $\{\alpha\}$ is considered. $\mathcal{H}(\{s'\})$ can also be expanded in terms of Ω_α with coupling constants k_α' . Then (4.2.3) implies a set of equations

$$\underline{k}' = \underline{k}'(\underline{k}) \quad (4.2.5)$$

relating the coupling constants of the original and renormalised (block) spins. Here \underline{k} and \underline{k}' denote the entire sets of classes k_α and k_α' . There also follows from (4.2.3) together with (4.2.4b), the transformation law for the Gibbsian energy density

$$G(\underline{k}) = g(\underline{k}) + \ell^{-d} G(\underline{k}') \quad (4.2.6)$$

where, of course, $G(\underline{k}')$ is the renormalised free energy density. Here $g=C/N$, $\ell^d = N/N'$ (ℓ being the length re-scaling factor and d is the dimensionality of the system), and the thermodynamic limit is implicitly taken to be $N \rightarrow \infty$. The term $g(\underline{k})$ is associated with spin fluctuations over a range not greater than the block size, and because the Kadanoff transformation leads to the absence of fluctuations over the range stated above (see section 1.4), $g(\underline{k})$ appears as a contribution in (4.2.6). Provided $P(\{s',s\})$ is suitably chosen (see Niemeijer and van Leeuwen, 1976), which is mostly the case in practice, $g(\underline{k})$ is a regular function of \underline{k} (for some relevant domain) and is thus considered unimportant in the determination of the critical behaviour (see also Ravndel, 1976). $G(\underline{k}')$ is, however, associated with large scale fluctuations and is the singular part of the free energy density. Once functions $\underline{k}'(\underline{k})$ and $g(\underline{k})$ are known, $G(\underline{k})$ may be calculated by iterating (4.2.5,6). However, for a study of the singular behaviour of the free energy density, $g(\underline{k})$ becomes irrelevant.

In the RG approach one can calculate critical exponents separately from the free energy. The critical surface (for proper definition see later) of continuous (second order) transitions belonging to a particular universality class is assumed to map onto a fixed point \underline{k}^* of (4.2.5) [of course, there may be more than one fixed point, but not every one of them, in general, will have physical significance]. One of the basic suppositions of the RG theory is that \underline{k}' is a regular function of \underline{k} near non-trivial fixed points (again this is ensured by a suitable choice of $P(\{s',s\})$, see the reference cited above), so that one can deal with the linearised form of the transformation at the fixed point, i.e the matrix

$$T_{\alpha\beta}^* = (\partial k_{\alpha}' / \partial k_{\beta})_{\underline{k}^*} . \quad (4.2.7)$$

Following Wilson, the 'critical properties' of the RG equations are studied by looking for the eigenvalues and eigenvectors of its linearised form at a fixed point. This corresponds to the system at criticality. Let $T_{\alpha\beta}^*$ have eigenvalues λ_i with associated right eigenvectors \underline{v}_i . Then $\{\underline{v}_i\}$ form, in general, a basis for the linear space which is the neighbourhood of the fixed point. Define the scaling fields $u_i(\underline{k})$ (Wegner, 1972) via

$$\delta \underline{k} = \sum_i u_i \underline{v}_i , \quad \delta \underline{k}' = \sum_i u_i' \underline{v}_i \quad (4.2.8)$$

where $\delta \underline{k} = \underline{k} - \underline{k}^*$. It is a simple matter to prove that, under the RG transformation, $u_i' = \lambda_i u_i$, which means that after m applications

$$u_i^{(m)} = \lambda_i^m u_i$$

and also

$$\delta \underline{k}^{(m)} = \sum_i u_i^{(m)} \underline{v}_i$$

as is seen from (4.2.8). ($u_i(k)$ are explicitly given in terms of the left eigenvectors \underline{e}_i , in the form $u_i = \delta \underline{k} \cdot \underline{e}_i$ and $u_i' = \delta \underline{k}' \cdot \underline{e}_i$, where $\underline{e}_i \cdot \underline{v}_j = \delta_{i,j}$. This is useful for certain considerations.) Thus if $|\lambda_i| > 1$ (< 1), $u_i^{(m)}$ increase (decrease) with increasing m , resulting in motion away from (towards) the fixed point along the trajectory specified by \underline{v}_i . In the special case that $\lambda_i = 1$, $u_i^{(m)}$ remains unchanged and no motion takes place. The eigenvalues and corresponding eigenvectors for these cases are referred to as relevant, irrelevant and marginal, respectively. The same terminology has been used for scaling fields too; so that relevant fields increase whereas irrelevant fields decrease and the marginal ones remain unaltered. The fixed point itself, as seen from (4.2.8), corresponds to all $u_i = 0$. The set of points which ultimately end up in the fixed point is termed as the critical surface (or domain of attraction) which is a hypersurface in the parameter space of interactions. It is evident that this surface is locally spanned by a subset of $\{\underline{v}_i\}$ consisting of irrelevant eigenvectors.

Now, we note that each $\mathcal{H}(\{s\})$ is made up of an even part, which is invariant under a flip of all spins, and an odd part, which changes sign under a spin flip (these usually correspond to zero and non-zero applied fields, respectively). If all $P(\{s',s\})$ are chosen such that they are invariant under a simultaneous flip of s' and s spins, then it follows that the subspace of even interactions of $\mathcal{H}(\{s\})$ is invariant under the transformation. Thence it follows that the subspace of the even part of $\mathcal{H}(\{s\})$ is invariant under the transformation, and as a consequence (in most cases, see Niemeijer and van Leeuwen, 1976), fixed points are found in the subspace of even interactions. For such fixed points, the Jacobian matrix (4.2.7) breaks into an even-even and an odd-odd part: for class α even only even class β appears, and

for odd α only odd β will appear, so that $T_{\alpha\beta}^*$ is 'block diagonalised'. Having noted this distinction, one can treat each matrix separately (Niemeijer and van Leeuwen, 1976).

To obtain the critical exponents of interest in terms of the eigenvalues, we first note the 'closure' property of RG transformations: The successive applications of two RG transformations with length re-scaling factors ℓ and $\bar{\ell}$, yields the same results as the application of a single RG transformation with length re-scaling factor $\ell\bar{\ell}$. Using this property, it can be shown (see Ravndel, 1976 for example) that $\lambda_i(\ell)\lambda_i(\bar{\ell}) = \lambda_i(\ell\bar{\ell})$, with the result that $\lambda_i(\ell)$ takes the form

$$\lambda_i(\ell) = \ell^{\gamma_i} \quad (4.2.9)$$

where γ_i are independent of ℓ . To pursue the matters further, one has to see whether a singular behaviour in the powers of the u_i for the free energy density is compatible with (4.2.6), when expressed in terms of u_i :

$$G_{\text{sing}}(u_1, u_2, \dots) = \ell^{-d} G_{\text{sing}}(\lambda_1 u_1, \lambda_2 u_2, \dots) \quad (4.2.10)$$

(The full formula would include $g(u_1, u_2, \dots)$ as well, but since we are interested in the singular behaviour, the regular function g is omitted.) Let us put $u_2 = u_3 = \dots = 0$ and assume power-law singularity of the form $A|u_1|^{a_1}$ for $G(u_1)$. Inserting this into (4.2.10) and using (4.2.9), one finds immediately

$$a_1 = d/\gamma_1 \quad (4.2.11)$$

Therefore, if a power-law singularity is to occur in u_1 , the associated exponent a_1 must be given by (4.2.11). Besides, one also observes that to keep the free energy finite at $u_1=0$ (i.e the fixed point), a_1

must be positive; and in view of equations (4.2.9,11), this implies a relevant eigenvalue (and corresponding scaling field). So only relevant eigenvalues qualify, on physical grounds, for singular behaviour. Next, we look into the dependence on two scaling fields u_1 , u_2 and determine the singular powers $|u_1|^{a_1} |u_2|^{a_2}$ which are allowed by (4.2.9). Comparing exponents left and right, yields the relation

$$a_1 \gamma_1 + a_2 \gamma_2 = d \quad (4.2.12)$$

which is the equivalent of (4.2.11) for this case. Note that for positive a_i at least one of the γ_i has to be positive. Equation (4.2.10) now becomes

$$G_{\text{sing}}(u_1, u_2) = \ell^{-d} G_{\text{sing}}(\ell^{\gamma_1} u_1, \ell^{\gamma_2} u_2) \quad (4.2.13)$$

which shows that G_{sing} behaves as 'generalized homogeneous functions'. This form for the singular part of the free energy density is similar, except for the fact that ℓ is a discrete variable, to Widom's static scaling hypothesis (Widom, 1965a;b).

The connection with the usual scaling theory of critical exponents can now be made. As has already been mentioned, fixed points will lie in the subspace of even interactions (this corresponds to zero magnetic field in our case). A change of temperature is a change of magnitude of all interaction constants k_α (as $1/\kappa T$ was absorbed by definition in \mathcal{H}). Thus a variation of temperature in the fixed points keeps \mathcal{H} in the the even subspace, and the temperature will couple to the even scaling fields. Similarly, a change of the magnetic field couples to odd scaling fields. We, therefore, have two relevant scaling fields (in such appropriate cases), one of which is temperature-like and the other field-like; whose corresponding indices we denote respectively by γ_T and γ_H , defined via (4.2.9). It is a rather trivial

exercise now to obtain from (4.2.13), employing standard thermodynamic formulae, the following expressions for the critical exponents of interest.

$$\begin{aligned}
 \alpha &= \alpha' = 2 - d/\gamma_T \\
 \beta &= (d - \gamma_H)/\gamma_T \\
 \gamma &= \gamma' = (2\gamma_H - d)/\gamma_T \\
 \delta &= \gamma_H/(d - \gamma_H) .
 \end{aligned}
 \tag{4.2.14}$$

From these immediately follow the well known scaling laws

$$\begin{aligned}
 \alpha + 2\beta + \gamma &= 2 \\
 \alpha + \beta(\delta + 1) &= 2 .
 \end{aligned}
 \tag{4.2.15}$$

Furthermore, the 'primed' and 'unprimed' indices relating respectively to the approach to T_C from below and above (see section 1.2) are identical in this theory.

Finally, we briefly mention the possibility of studying first order, rather than a continuous, transition. To be consistent with discontinuities in the first derivatives of the free energy (as occur in first order transitions) equation (4.2.11) must yield $\gamma_1=d$, so that the singular part of the free energy density is now of the form $A|u_1|$ near the transition point. This gives $\lambda_1 = \epsilon^d$ via (4.2.9). Thus, we can see that a fixed point corresponding to a first order transition generally has one (or more) eigenvalue(s) $\lambda_i = \epsilon^d$. Interested readers are referred to Nienhuis and Naunberg (1975) for more details.

The eigenvalues of the linearised transformation determine the values of the critical indices. In order to make these evaluations, one must first 'solve' the transformation (4.2.3) via, of course, ap-

proximate methods. Two of the most common methods, namely the cumulant and the cluster methods, are discussed in this thesis.

4.3 The cumulant method and its application to our mixed system

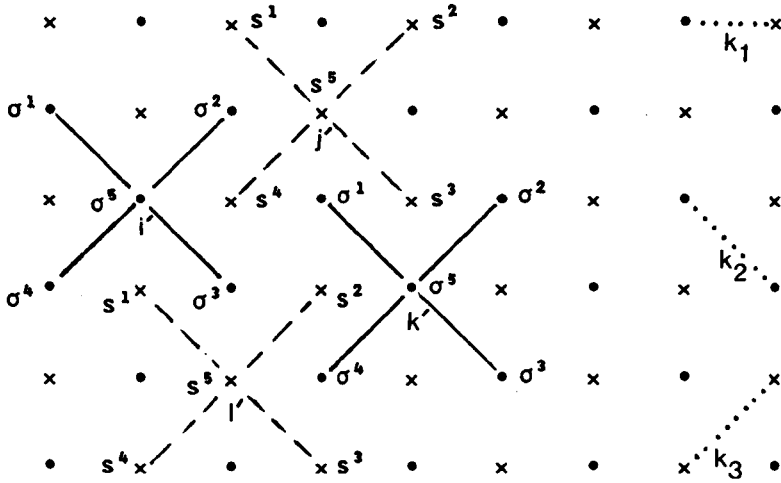
Cumulant method (Niemeijer and van Leeuwen, 1974) is essentially a perturbative one: it is based upon splitting the spin Hamiltonian into a 'manageable' zeroth part \mathcal{H}_0 and a perturbation V , viz.

$$\mathcal{H}(\{s\}) = \mathcal{H}_0(\{s\}) + V(\{s\}) . \quad (4.3.1)$$

Here, \mathcal{H}_0 contains all the intra-block interactions, while V contains inter-block ones. The applicability of the cumulant technique is based on the possibility of finding a 'suitable' separation of \mathcal{H} into \mathcal{H}_0 and V (Niemeijer and van Leeuwen, 1976). As mentioned in section 4.1, this technique has been applied successfully to mixed spin systems such as ours, with cell definition of Fig(4.2) (Schofield, 1980). However, when applied to the same model with block prescription of Fig(4.1); the method 'fails' in that the first and second order perturbation calculations result only in decoupled sublattice fixed points (see later). Although this dramatic effect could not be foreseen, the reason clearly has to do with the choice of cell prescription, which renders the separation (4.3.1) rather 'unsuitable'. To demonstrate this, we present the details of the first order perturbation approximation (in zero field) here. This also serves as a brief illustration of the technique. Second order (and also magnetic field) calculations are not given.

According to the arguments of the previous section, we first look for the fixed points in the subspace of even interactions, i.e when there is no applied external magnetic field. We start with the minimum number of interactions under which the action of the RG transformation

is closed. These turn out to be the nearest neighbour interaction k_1 and the next-nearest neighbour interactions for the spin-1/2 and spin-1 sublattices, denoted by k_2 and k_3 , respectively. Denoting the spin-1/2 and spin-1 variables by σ^i and s^i respectively; the corresponding blocks are shown in Fig(4.3).



Fig(4.3): Dots and crosses denote spin-1/2 and spin-1 objects, respectively. Corresponding cells are represented by full and dashed lines.

Define the cell spins by

$$\begin{aligned} \sigma_i^1 &= \frac{1}{2} \text{sign}(\sigma_i^1 + \sigma_i^2 + \sigma_i^3 + \sigma_i^4 + \sigma_i^5) \\ s_j^1 &= \text{sign}(s_j^1 + s_j^2 + s_j^3 + s_j^4 + s_j^5) \end{aligned} \quad (4.3.2)$$

where subscripts in σ_i^1 , etc. represent the cells, to which σ^1 , etc. belong; and the sign function is defined by

$$\text{sign}(x) = \begin{cases} x/|x| & , \quad x \neq 0 \\ 0 & , \quad x = 0 \end{cases}$$

so that $\sigma_{i'} = \pm 1/2$ and $s_{j'} = \pm 1, 0$. For a given cell prescription, the weight-factor $P(\{s', s\}) [\equiv P(\{s', s ; \sigma', \sigma\})]$ depends only on the site spins inside the cell, so that it factorizes as

$$P(\{s', s ; \sigma', \sigma\}) = \prod_{i'} P^{(1/2)}(\sigma_{i'}, \{\sigma_{i'}\}) \prod_{j'} P^{(1)}(s_{j'}, \{s_{j'}\}) \quad (4.3.3)$$

where i' and j' refer to spin-1/2 and spin-1 blocks respectively, and

$$P^{(1/2)}(\sigma_{i'}, \{\sigma_{i'}\}) = \delta[\sigma_{i'}, \frac{1}{2} \text{sign}(\sigma_{i'}^1 + \sigma_{i'}^2 + \sigma_{i'}^3 + \sigma_{i'}^4 + \sigma_{i'}^5)]$$

$$P^{(1)}(s_{j'}, \{s_{j'}\}) = \delta[s_{j'}, \text{sign}(s_{j'}^1 + s_{j'}^2 + s_{j'}^3 + s_{j'}^4 + s_{j'}^5)]$$

with the kronecker delta defined by

$$\delta[x, y] = \begin{cases} 1 & , \quad x=y \\ 0 & , \quad x \neq y \end{cases}$$

We now have the explicit connection between the cell and site spins, so that (4.2.3) may be re-written as

$$\exp[C + \mathcal{H}'(\{s', \sigma'\})] = \sum_{\{s\}}^{s'} \sum_{\{\sigma\}}^{\sigma'} \exp[\mathcal{H}_0(\{s', s ; \sigma', \sigma\}) + V(\{s', s ; \sigma', \sigma\})]$$

where the sum is over all internal configurations of the spins with fixed configurations of the cell spins (the sums are no longer 'free' as in (4.2.3), therefore constraints are shown as well; this notation will become convenient when we enter into the details of calculations).

The above equation can be re-written

$$\exp(C + \mathcal{H}') = \langle e^V \rangle_0 \sum_{\{s\}}^{s'} \sum_{\{\sigma\}}^{\sigma'} \exp(\mathcal{H}_0)$$

where the averages $\langle A \rangle_0$ are defined by

$$\langle A \rangle_0 = \frac{\sum_{\{s\}}^{s'} \sum_{\{\sigma\}}^{\sigma'} A(\{s', s ; \sigma', \sigma\}) \exp(\mathcal{H}_0)}{\sum_{\{s\}}^{s'} \sum_{\{\sigma\}}^{\sigma'} \exp(\mathcal{H}_0)} . \quad (4.3.4)$$

Making the cumulant expansion for $\langle e^V \rangle_0$,

$$\begin{aligned} \langle e^V \rangle_0 = \exp[& \langle V \rangle_0 + (1/2!) \langle (V - \langle V \rangle_0)^2 \rangle_0 \\ & + (1/3!) \langle (V - \langle V \rangle_0)^3 \rangle_0 + \dots] \end{aligned} \quad (4.3.5)$$

gives, to the first order in this expansion,

$$\exp(C + \mathcal{H}') = \exp(\langle V \rangle_0) \sum_{\{s\}}^{s'} \sum_{\{\sigma\}}^{\sigma'} \exp(\mathcal{H}_0) . \quad (4.3.6)$$

Now with reference to Fig(4.3), our (approximate) zero-field Hamiltonian is

$$\begin{aligned} \mathcal{H}(\{s, \sigma\}) = k_1 \sum_{\langle ij \rangle} \sigma^i s^j + k_2 \sum_{ij}^{\prime} \sigma^i \sigma^j \\ + k_3 \sum_{ij}^{\prime} s^i s^j \end{aligned} \quad (4.3.7)$$

where \sum^{\prime} denotes summation over next-nearest neighbour pairs. Also

$$\begin{aligned} \mathcal{H}_0(\{s', s ; \sigma', \sigma\}) = \\ k_2 \sum_{i'} \sum_{ij}^{\prime} \sigma_{i'}^i \sigma_i^j + k_3 \sum_{j'} \sum_{ij}^{\prime} s_{j'}^i s_j^j \end{aligned} \quad (4.3.8)$$

and

$$\begin{aligned} V(\{s', s ; \sigma', \sigma\}) = \\ k_1 \sum_{\langle i'j' \rangle} \sum_{\langle ij \rangle} \sigma_{i'}^i s_{j'}^j + k_2 \sum_{i'k'}^{\prime} \sum_{ij}^{\prime} \sigma_{i'}^i \sigma_{k'}^j \\ + k_3 \sum_{j'l'}^{\prime} \sum_{ij}^{\prime} s_{j'}^i s_{l'}^j . \end{aligned} \quad (4.3.9)$$

Hence, from (4.3.8),

$$\begin{aligned} \exp(\mathcal{H}_0) &= \exp\left[k_2 \sum_{i'} \sum_{ij} \sigma_{i'}^i \sigma_{i'}^j + k_3 \sum_{j'} \sum_{ij} s_{j'}^i s_{j'}^j\right] = \\ &= \prod_{i'} \exp\left(k_2 \sum_{ij} \sigma_{i'}^i \sigma_{i'}^j\right) \prod_{j'} \exp\left(k_3 \sum_{ij} s_{j'}^i s_{j'}^j\right) \end{aligned}$$

which gives

$$\begin{aligned} \sum_{\{s\}}^{s'} \sum_{\{\sigma\}}^{\sigma'} \exp(\mathcal{H}_0) &= \sum_{\{\sigma\}}^{\sigma'} \prod_{i'} \exp\left(k_2 \sum_{ij} \sigma_{i'}^i \sigma_{i'}^j\right) \\ &= \sum_{\{s\}}^{s'} \prod_{j'} \exp\left(k_3 \sum_{ij} s_{j'}^i s_{j'}^j\right) = \\ &= \{Z^{(1/2)}(k_2)\}^M \{Z_1^{(1)}(k_3)\}^{N_1} \{Z_0^{(1)}(k_3)\}^{N_2} \end{aligned}$$

where M is the number of spin-1/2 cells and N_1 , N_2 are those of spin-1 cells assuming values $\pm 1, 0$; respectively (of course, $N_1 + N_2 = N$ is the total number of spin-1 blocks). Here

$$\begin{aligned} Z^{(1/2)}(k_2) &= \sum_{\{\sigma_{i'}\}}^{\sigma_{i'} = \pm 1/2} \exp\left(k_2 \sum_{ij} \sigma_{i'}^i \sigma_{i'}^j\right) \\ Z_1^{(1)}(k_3) &= \sum_{\{s_{j'}\}}^{s_{j'} = \pm 1} \exp\left(k_3 \sum_{ij} s_{j'}^i s_{j'}^j\right) \\ Z_0^{(1)}(k_3) &= \sum_{\{s_{j'}\}}^{s_{j'} = 0} \exp\left(k_3 \sum_{ij} s_{j'}^i s_{j'}^j\right). \end{aligned} \tag{4.3.10}$$

Note that $Z_{\pm 1}^{(1)}(k_3) = Z_1^{(1)}(k_3)$ because of the up-down symmetry: to get $s_{j'} = -1$ from $s_{j'} = 1$, we just flip all the spins. The same holds for the spin-1/2 blocks, as seen readily from equations (4.3.2). Thus from (4.3.6), up to first order perturbations,

$$\begin{aligned} C + \mathcal{H}' &= \langle V \rangle_0 + M \ln Z^{(1/2)}(k_2) \\ &+ N_1 \ln Z_1^{(1)}(k_3) + N_2 \ln Z_0^{(1)}(k_3). \end{aligned}$$

Following arguments given by Neimeijer and van Leeuwen (1973;1974), the first term in the above equation is related to the free energy of a finite number (five) of spins, and is expected to contain fluctuations occurring inside the spin-1/2 blocks. Similarly, the next two terms are expected to describe fluctuations inside the spin-1 blocks. Hence, these three terms together relate to those fluctuations occurring over a range not greater than the block size, and are therefore associated with the regular part of the free energy in (4.2.6). Thus, the critical behaviour must be contained in V . We, therefore, write for the Hamiltonian \mathcal{H}' of the cell system

$$\mathcal{H}' \sim \langle V \rangle_0. \quad (4.3.11)$$

Higher order perturbation approximations would involve more terms of (4.3.5) in this equation, so that the second order approximation will include $(1/2!) \langle (V - \langle V \rangle_0)^2 \rangle_0$, and so on. Now let us express (4.3.9) as

$$\langle V \rangle_0 = \sum_{\langle ij \rangle} \langle V_{ij} \rangle_0 + \sum_{i'k'} \langle V_{i'k'} \rangle_0 + \sum_{j'l'} \langle V_{j'l'} \rangle_0 \quad (4.3.12)$$

with

$$\begin{aligned} V_{ij} &= k_1 \sum_{\langle ij \rangle} \sigma_i^i s_j^j \\ V_{i'k'} &= k_2 \sum_{ij} \sigma_i^i \sigma_{k'}^j \\ V_{j'l'} &= k_3 \sum_{ij} s_j^i s_{l'}^j. \end{aligned}$$

With reference to Fig(4.3), we can write explicitly for V_{ij} , $V_{i'k'}$, $V_{j'l'}$:

$$\begin{aligned} V_{ij} &= k_1 (\sigma_i^2 s_j^5 + \sigma_i^5 s_j^4 + \sigma_i^2 s_j^1 + \sigma_i^2 s_j^4 + \sigma_i^3 s_j^4) \\ V_{i'k'} &= k_2 (\sigma_i^3 \sigma_{k'}^1 + \sigma_i^3 \sigma_{k'}^4 + \sigma_i^2 \sigma_{k'}^1) \\ V_{j'l'} &= k_3 (s_j^3 s_{l'}^1 + s_j^3 s_{l'}^4 + s_j^2 s_{l'}^1). \end{aligned}$$

In order to compute the averages $\langle \rangle_0$, we first note that since \mathcal{H}_0 does not couple distinct blocks,

$$\langle a_i b_j \rangle_0 = \langle a_i \rangle_0 \langle b_j \rangle_0 .$$

From (4.3.4) and Fig(4.3), one writes explicitly

$$\langle \sigma_i^i \rangle_0 = \frac{\sum_{\{\sigma_i^i\}}^{\sigma_i^i} \sigma_i^i \exp[k_2 \sigma_i^5 (\sigma_i^1 + \sigma_i^2 + \sigma_i^3 + \sigma_i^4)]}{Z^{(1/2)}(k_2)} \quad (4.3.13a)$$

and

$$\langle s_j^i \rangle_0 = \frac{\sum_{\{s_j^i\}}^{s_j^i} s_j^i \exp[k_3 s_j^5 (s_j^1 + s_j^2 + s_j^3 + s_j^4)]}{Z_{0,1}^{(1)}(k_2)} \quad (4.3.13b)$$

where in (4.3.13b), either $Z_1^{(1)}$ or $Z_0^{(1)}$ occurs, depending on the value of the constraint s_j^i . The spin-1/2 partition function is, of course, given by

$$Z^{(1/2)}(k_2) = \sum_{\{\sigma_i^i\}}^{\sigma_i^i = \pm 1/2} \exp[k_2 \sigma_i^5 (\sigma_i^1 + \sigma_i^2 + \sigma_i^3 + \sigma_i^4)]$$

and similarly for $Z_1^{(1)}(k_3)$, $Z_0^{(1)}(k_3)$ [see relations (4.3.10)]. It is obvious, from the form of the cell partition functions, that $\langle \sigma_i^i \rangle_0$ are identical to each other for $i=1$ to 4, and $\langle \sigma_i^5 \rangle_0$ will be different. Clearly, the same can be said about $\langle s_j^i \rangle_0$. Also, from (4.3.13a,b), one can observe that a reversal of the (constraint) cell spin will lead to the same averages, except for a change in sign. Explicit manipulations (using algebraic computing, or else) yield

$$\begin{aligned} \langle \sigma_i^i \rangle_0 &= \psi_1(k_2) \sigma_i^i, \quad i=1 \text{ to } 4 \\ \langle \sigma_i^5 \rangle_0 &= \psi_2(k_2) \sigma_i^i \end{aligned}$$

$$\langle s_{j'}^i \rangle_0 = \phi_1(k_3) s_{j'}^i, \quad i=1 \text{ to } 4$$

$$\langle s_{j'}^s \rangle_0 = \phi_2(k_3) s_{j'}^s$$

where

$$\begin{aligned} \psi_1(k_2) &= 2[\cosh(k_2) + 2 \cosh(\frac{1}{2}k_2)] / Z^{(1/2)}(k_2) \\ \psi_2(k_2) &= 2[\sinh(k_2) + 4 \sinh(\frac{1}{2}k_2) + 3] / Z^{(1/2)}(k_2) \\ \phi_1(k_3) &= 2[\cosh(4k_3) + 3 \cosh(3k_3) \\ &\quad + 5 \cosh(2k_3) + 2 \exp(k_3) + 13/2] / Z_1^{(1)}(k_3) \\ \phi_2(k_3) &= 2[\sinh(4k_3) + 4 \sinh(3k_3) + 10 \sinh(2k_3) \\ &\quad + 8 \exp(k_3) + 19/2] / Z_1^{(1)}(k_3) \end{aligned} \quad (4.3.14a)$$

with the cell partition functions given by

$$\begin{aligned} Z^{(1/2)}(k_2) &= 2[\cosh(k_2) + 4 \cosh(\frac{1}{2}k_2) + 3] \\ Z_1^{(1)}(k_3) &= 2[\cosh(4k_3) + 4 \cosh(3k_3) \\ &\quad + 10 \cosh(2k_3) + 8 \exp(k_3) + 25] \\ Z_0^{(1)}(k_3) &= 32 \exp(-k_3) + 19. \end{aligned} \quad (4.3.14b)$$

$Z_0^{(1)}(k_3)$ does not come into the first order calculations as is seen from (4.3.14a), and is only given for the sake of completeness. Thus, having obtained the relevant first order averages, one finds, using relations (4.3.11,12),

$$\begin{aligned} \Rightarrow \mathcal{H}' &= k_1 [\psi_1(k_2)\phi_2(k_3) + \psi_2(k_2)\phi_1(k_3) \\ &\quad + 3 \psi_1(k_2)\phi_1(k_3)] \sum_{\langle i'j' \rangle} \sigma_{i'}^s s_{j'}^s \\ &\quad + 3k_2 \{\psi_1(k_2)\}^2 \sum_{i'k'} \sigma_{i'}^s \sigma_{k'}^s \\ &\quad + 3k_3 \{\phi_1(k_3)\}^2 \sum_{j'l'} s_{j'}^s s_{l'}^s. \end{aligned}$$

We see that, this equation is of the form (4.3.7) for the original Hamiltonian. So our RG transformation is indeed closed. Writing it in the form

$$\begin{aligned} \Rightarrow \mathcal{H}' = & k_1' \sum_{\langle i'j' \rangle} \sigma_{i'} s_{j'} + k_2' \sum_{i'k'} \sigma_{i'} \sigma_{k'} \\ & + k_3' \sum_{j'l'} s_{j'} s_{l'} . \end{aligned}$$

and comparing coefficients with (4.3.7) yields the following RG equations:

$$\begin{aligned} k_1' &= k_1 (\psi_1 \phi_2 + \psi_2 \phi_1 + 3 \psi_1 \phi_1) \\ k_2' &= 3k_2 \psi_1^2 \\ k_3' &= 3k_3 \phi_1^2 . \end{aligned} \tag{4.3.15}$$

It is easy to work out that, except for the the trivial fixed point $k_\alpha^* = 0$; the above RG equations lead only to fixed points corresponding to uncoupled sublattices, where $k_1^* = 0$. For consistency, one must have $\psi_1^{*2} = \phi_1^{*2} = 1/3$, or that one of the k_2^* , k_3^* is also zero. (In this situation only one of the sublattices is ordered.) Solving

$$\psi_1^2(k_2^*) = \phi_1^2(k_3^*) = 1/3$$

for k_2^* and k_3^* , gives $k_2^* = \pm 2.3725$; $k_3^* = 0.9900, -0.8625$. The 'symmetry' and 'antisymmetry' of these solutions are expected to occur in view of equations (4.3.14a,b). It is seen that $\psi_1(k_2) = \psi_1(-k_2)$, whereas such a relation does not hold for ϕ_i (this is because $\exp(-k_3)$ can not occur in ϕ_i or $Z_1^{(1)}$, as seen from (4.3.13a,b)). The even-even part of the Jacobian matrix is clearly upper-triangular with the implication that its eigenvalues are the diagonal elements, namely $(\partial k_1' / \partial k_1)$, $(\partial k_2' / \partial k_2)$, $(\partial k_3' / \partial k_3)$; given by

$$\begin{aligned}
\partial k_1' / \partial k_1 &= \psi_1 \phi_2 + \psi_2 \phi_1 + 3 \psi_1 \phi_1 \\
\partial k_2' / \partial k_2 &= 3 \psi_1^2 + 6k_2 \psi_1 (\partial \psi_1 / \partial k_2) \\
\partial k_3' / \partial k_3 &= 3 \phi_1^2 + 6k_3 \phi_1 (\partial \phi_1 / \partial k_3) .
\end{aligned} \tag{4.3.16}$$

Evaluating these at the fixed points yields relevant critical exponents via relations (4.2.14). Mathematically, all the eight combinations for the fixed point, namely $(k_1^*, k_2^*, k_3^*) = (0, \pm 2.3725, 0.9900)$, $(0, \pm 2.3725, -0.8625)$, $(0, \pm 2.3725, 0)$, $(0, 0, 0.9900)$ and $(0, 0, -0.8625)$; would be consistent with RG equations (4.3.15). However, one does not expect, in general, the two different sublattices to undergo phase transition at the same temperature. We, therefore, propose to consider the following fixed points which are more likely.

(i) $(0, 2.3725, 0)$: This corresponds to ferromagnetism on the spin-1/2 sublattice and no ordering on the spin-1 sublattice. Equation (4.3.16) yields two relevant eigenvalues, $\lambda_s = 1.1758$ and $\lambda_T = 2.3072$, at this point. From the numerical evaluation of the corresponding right eigenvectors, we see that λ_s (or more precisely, the associated scaling field u_s) is coupled to $\delta k_1 = k_1$ (refer to (4.2.8)) and u_T to $\delta k_2 = k_2 - k_2^*$ (for the latter case, however, there is a relatively small component of the eigenvector in the k_1 -direction; this is considered to be only an artefact of the approximations embodied in the first order perturbation calculations). The existence of λ_s implies a cusp in the k_1, k_2 plane, through relations (4.2.12,13) [see section 5.4 and also van Leeuwen, 1975]. Moreover, one can estimate, via equations (4.2.14) with $\ell = \sqrt{5}$ and $d=2$, that $\alpha = 0.075$; where, of course, λ_T has been used.

(ii) $(0, -2.3725, 0)$: This corresponds to antiferromagnetic ordering on the spin-1/2 and no order on the spin-1 sublattice. Equations

(4.3.16) yield only one relevant eigenvalue $\lambda_T = 2.3072$, with the same α -estimate, of course, as in (i).

(iii) (0,0,0.9900): This corresponds to ferromagnetism on the spin-1 and no ordering on the spin-1/2 sublattice. Here, again we find two relevant eigenvalues, $\lambda_s = 1.1979$ and $\lambda_T = 2.1969$, with u_s coupling to k_1 and u_T to $k_3 - k_3^*$. Similarly, λ_s implies a cusp in the k_1, k_3 plane. Also λ_T yields $\alpha = -0.045$.

(iv) (0,0,-0.8625): This corresponds to antiferromagnetic ordering on the spin-1 and no order on the spin-1/2 sublattice. Only one relevant eigenvalue, $\lambda_T = 2.1131$, is found which gives $\alpha = -0.151$. The fact that this fixed point and that of (iii) are not 'mirror images' of each other (as should be the case, like in (i)-(ii), on physical grounds), is regarded to be also an artefact of the approximations embodied in the first order analysis; it does not contain all the symmetries of the lattice under consideration. Also, this particular cell choice does not exhibit perfect symmetry of the type $k_2 \rightarrow -k_2$, $k_3 \rightarrow -k_3$; as it does for the type $k_1 \rightarrow -k_1$ (see van Leeuwen, 1975)

The failure of the cumulant method to determine 'coupled' fixed points seems to be intrinsic to our particular choice of cells, as other interactions (such as the four-spin coupling which occurs in the four-cell cluster theory, see chapter 5) have also been tentatively included with no success. In particular, the inclusion of self-interactions has no effect on the first order calculations, since they are considered to be a part of the intra-block Hamiltonian \mathcal{H}_0 , rather than V , so that the action of the RG is only closed when this coupling is zero. Second order calculations, in this case, turned out to be unaffected too, as far as coupled fixed points are concerned. This zero-field parameter space imposed by the first order perturbation is,

except for the absence of self-interaction term (believed to be unimportant in determining critical behaviour; see Schofield, 1980), identical to the zero-field parameter subspace of the four-cell cluster approximation (for the cell choice under consideration), when the sublattices are decoupled. We shall refer to the above results, when analysing the outcome of the cluster approximation theory in the next chapter, and will be able to understand them more fully.

CHAPTER 5

RSRG: CALCULATIONS USING CLUSTER APPROXIMATION METHOD

5.1 Introduction

Although the numerical estimates obtained in the previous chapter for α look reasonable in view of the universality hypothesis ($\alpha=0$ for two-dimensional systems), one must employ an alternative technique to achieve the full picture. In this chapter, we apply the method of cluster approximations to our mixed spin system. This seems to be the first such application. Cluster theory has been applied to single spin models (see for example, Niemeijer and van Leeuwen, 1974 ; van Leeuwen, 1975), and the cumulant method to both single and mixed spin systems (see Schofield and the references therein). In view of the discussions of section 4.1, our major aim will be to study the model characterized by the five-spin cells of Fig(4.1). It turns out that, as we shall see later, in the application of cluster theory to models not confined to spin-1/2 objects; the inclusion of self-interactions may be needed in order to have consistency and thus obtain fixed points. Obviously, for our case, the self-couplings will be associated with the spin-1 objects since $\sigma^2=1/4$ is constant. As has been mentioned, such interactions are considered unimportant (in view of the overriding effect of the cooperative phenomena) in determining critical behaviour, and our approach using the cluster approximation technique necessitates the inclusion of such interactions, whose effect on the outcome (as the results will show) can not go unnoticed. We expand further on this in section 5.5 .

After giving a general description of the cluster method (Niemeijer and van Leeuwen, 1974) in the next section, we shall study the four-spin cell arrangement of Fig(4.2) prescribed for our mixed square lattice model, which provides a suitable testing ground for our approach, since the actual numerical calculations are shorter due to fewer number of cell constituents. The two-cell cluster approximation results in a zero-field parameter space which is the same (except for the inclusion of the self-interaction), as the zero-field parameter space of the first order perturbation calculations for the cell choice in question (see Schofield, 1980). The four-cell approximation and the second order cumulant calculations, however, yield very different parameter spaces, which is not surprising. The subsequent section deals with the five-spin block configuration, and in a separate section we present the results and their analysis.

5.2 Cluster approximation theory

One of the main characteristics of this method is that all interactions inside the cluster (i.e a connected set of cells) can be treated to any order, and on equal footing. We assume that $P(\{s',s\})$ is a product over cell weight factors (analogous to 4.3.3), so that we may speak about $P_a(\{s',s\})$ as the weight factor of a cluster 'a'. The RG transformation (4.2.3) for this cluster is

$$\exp[C_a + \sum_{b \subseteq a} k_b^a \Omega_b(\{s'\})] = \sum_{\{s\}} P_a(\{s',s\}) \exp \mathcal{H}_a(\{s'\}) = \sum_{\{s\}} \exp \mathcal{H}_a(\{s',s\}) \quad (5.2.1)$$

where the renormalised energy for cluster a has been decomposed into its constituent contributions $k_b^a \Omega_b(\{s'\})$. The superscript a announces the dependence of k_b^a on cluster a. If a were the whole lattice, the index a would be dropped and the resulting k_b' would

depend only on the class β to which b belongs. Thus for increasing a , k_b^a approaches k_β ; but such a choice is restricted by computational difficulties. In order to see k_β as a sum of increasing cluster contributions we make the Ursell expansion

$$k_b^a = \sum_{b \subseteq p \subseteq a} U_b^p \quad (5.2.2)$$

where U_b^p are to decrease rapidly with increasing p , in order to achieve convergence. Now, to get the inverse of (5.2.2) consider

$$\sum_{b \subseteq a \subseteq c} (-1)^{n(c)-n(a)} k_b^a$$

where $n(x)$ denotes the number of elements in set x (i.e number of cells in cluster x). Substituting (5.2.2) into the above yields

$$\sum_{b \subseteq a \subseteq c} (-1)^{n(c)-n(a)} k_b^a = \sum_{b \subseteq a \subseteq c} \sum_{b \subseteq p \subseteq a} (-1)^{n(c)-n(a)} U_b^p .$$

Defining the zeta and the delta functions on sets by relations

$$\zeta_{a,b} = \begin{cases} 1 & \text{if } a \subseteq b \\ 0 & \text{otherwise} \end{cases}, \quad \delta_{a,b} = \begin{cases} 1 & \text{if } a=b \\ 0 & \text{otherwise} \end{cases}$$

the above equation may be expressed as

$$\begin{aligned} \sum_{b \subseteq a \subseteq c} (-1)^{n(c)-n(a)} k_b^a &= \\ \sum_{b \subseteq p} U_b^p \left\{ \sum_{b \subseteq a \subseteq c} (-1)^{n(c)-n(a)} \zeta_{p,a} \right\} &= \\ \sum_{b \subseteq p} U_b^p \left\{ \sum_{p \subseteq a \subseteq c} (-1)^{n(c)-n(a)} \right\} &= U_b^c \end{aligned} \quad (5.2.3)$$

where we have used the fact that (*)

 (*) Proof of this is as follows. Let there be N cells in c and not in p . Then every $p \subseteq a \subseteq c$ can be characterized by $\{\mu_i\}$ where $i=1, \dots, N$; and $\mu_i=1$ or 0 according to how many of these N elements it contains.

→

$$\sum_{p \subseteq a \subseteq c} (-1)^{n(c)-n(a)} = \delta_{p,c} .$$

For the whole lattice (5.2.2) becomes

$$k_{\beta}' = \sum_{b \subseteq p} U_b^p . \quad (5.2.4)$$

We approximate this by selecting p out of a set which has the full symmetry of the lattice of interest, so that b still depends only on the type β to which it belongs. An efficient choice is to take c out of subsets γ of a basic cluster type δ (Niemeijer and van Leeuwen, 1974). Then our approximation to (5.2.4) will read

$$\begin{aligned} k_{\beta}' &= \sum_{\beta \subseteq \gamma \subseteq \delta} \sum_{b \subseteq p \in \gamma} U_b^p \\ &= \sum_{\beta \subseteq \gamma \subseteq \delta} \left\{ \sum_{b \subseteq p \in \gamma} \sum_{a \subseteq p} (-1)^{n(p)-n(a)} k_b^{\prime a} \right\} \end{aligned} \quad (5.2.5)$$

having used (5.2.3). Once again we use the zeta function to simplify the expression inside the brackets. It equals

$$\begin{aligned} &\sum_{b \subseteq a} k_b^{\prime a} \left\{ \sum_{b \subseteq p \in \gamma} (-1)^{n(p)-n(a)} \zeta_{a,p} \right\} = \\ &\sum_{\beta \subseteq \alpha \subseteq \gamma} \sum_{b \subseteq a \in \alpha} k_b^{\prime a} \left\{ \sum_{a \subseteq p \in \gamma} (-1)^{n(p)-n(a)} \right\} . \end{aligned}$$

Since the class γ of p is fixed in the above, we write $n(p)=n(\gamma)$.

Also writing $n(a)=n(\alpha)$ for $a \in \alpha$, we have

$$\begin{aligned} &\sum_{\beta \subseteq p \in \gamma} \sum_{b \subseteq a \subseteq p} (-1)^{n(p)-n(a)} k_b^{\prime a} = \\ &\sum_{\beta \subseteq \alpha \subseteq \gamma} (-1)^{n(\gamma)-n(\alpha)} k_{\beta}^{\prime \alpha} D_{\gamma}(\alpha) \end{aligned}$$

where

→

Thus $n(c)=n(p)+N$ and $n(a)=n(p)+\sum_{i=1}^N \mu_i$, so that

$$\sum_{p \subseteq a \subseteq c} (-1)^{n(c)-n(a)} = \sum_{\{\mu_i\}} (-1)^{N-\sum_i \mu_i} = (-1)^N \left(\sum_{\mu_i=0}^1 (-1)^{\mu_i} \right)^N = \delta_{p,c} .$$

$$k_{\beta}^{\prime\alpha} = \sum_{b \subseteq a \in \alpha} k_b^{\prime a} , \quad (b \in \beta) \quad (5.2.6a)$$

and

$$D_{\gamma}(\alpha) = \sum_{a \subseteq b \in \gamma} 1 , \quad (a \in \alpha) . \quad (5.2.6b)$$

Inserting this into (5.2.5) gives, in terms of the zeta function,

$$k_{\beta}^{\prime} = \sum_{\beta \subseteq \gamma \subseteq \delta} \left\{ \sum_{\beta \subseteq \alpha} (-1)^{n(\gamma) - n(\alpha)} D_{\gamma}(\alpha) k_{\beta}^{\prime\alpha} \zeta_{\alpha, \gamma} \right\} .$$

Evidently, $\alpha \subseteq \delta$. Hence, we find

$$k_{\beta}^{\prime} = \sum_{\beta \subseteq \alpha \subseteq \delta} k_{\beta}^{\prime\alpha} E_{\delta}(\alpha) \quad (5.2.7)$$

with

$$E_{\delta}(\alpha) = \sum_{\alpha \subseteq \gamma \subseteq \delta} (-1)^{n(\gamma) - n(\alpha)} D_{\gamma}(\alpha) . \quad (5.2.8)$$

In (5.2.6a) $k_{\beta}^{\prime\alpha}$ is the sum over all possible ways that a $k_b^{\prime a}$ can be found with an a of type α covering b of type β . $k_{\beta}^{\prime\alpha}$ may be seen as the interaction coefficient of class β in cluster α (multiplied by the number of times β can be covered by α). The combinatorial factors $E_{\delta}(\alpha)$ in (5.2.7) then determine how the subclusters α of the basic cluster δ have to be combined. The interesting aspect of (5.2.7) is that $E_{\delta}(\alpha)$ do not depend on the class of interaction β one is computing. Moreover, for a symmetric δ , it turns out that most $E_{\delta}(\alpha)$ vanish, which is a pleasant feature of the cluster approximation.

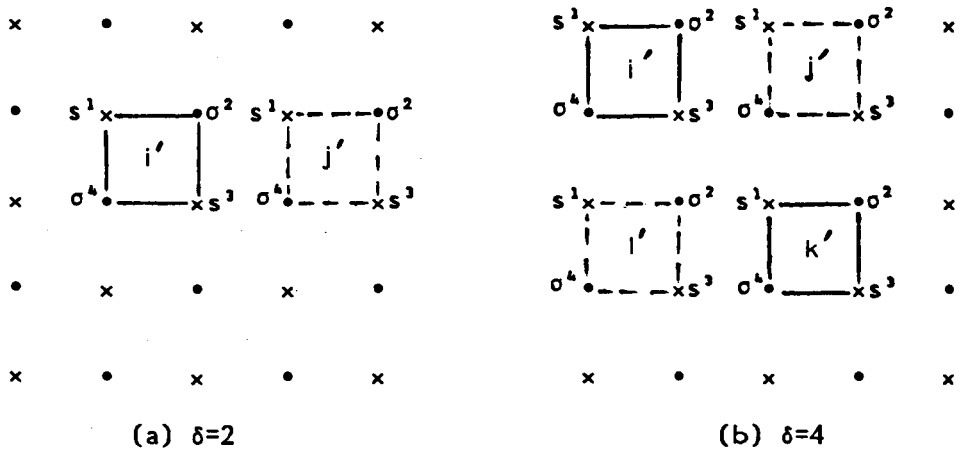
From (5.2.7), one also obtains for the linearized transformation

$$T_{\alpha\beta} = \sum_{\alpha \subseteq \gamma \subseteq \delta} E_{\delta}(\gamma) (\partial k_{\alpha}^{\prime\gamma} / \partial k_{\beta}) . \quad (5.2.9)$$

Having found $D_{\gamma}(\alpha)$ and $E_{\delta}(\alpha)$, equations (5.2.1, 6a, 7) then determine our RG equations.

5.3 Calculations on blocks of four spins

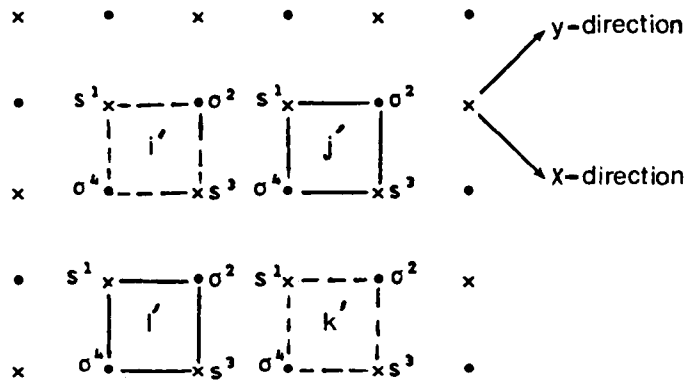
Because our system consists of two different sublattices, the basic cluster δ which preserves the full symmetry of the lattice can be either a cluster of two nearest neighbour blocks or four blocks forming a square, as shown below. (Of course, there can be larger clusters too, but because of high degree of complexity involved in the calculations, they will not be considered.) Notation of Fig(4.3) will be kept throughout this chapter.



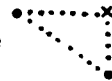
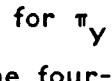

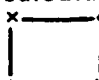
Fig(5.1): (a) Cluster consisting of two cells represented notationally as $\delta=2$. (b) Cluster of four cells, $\delta=4$.

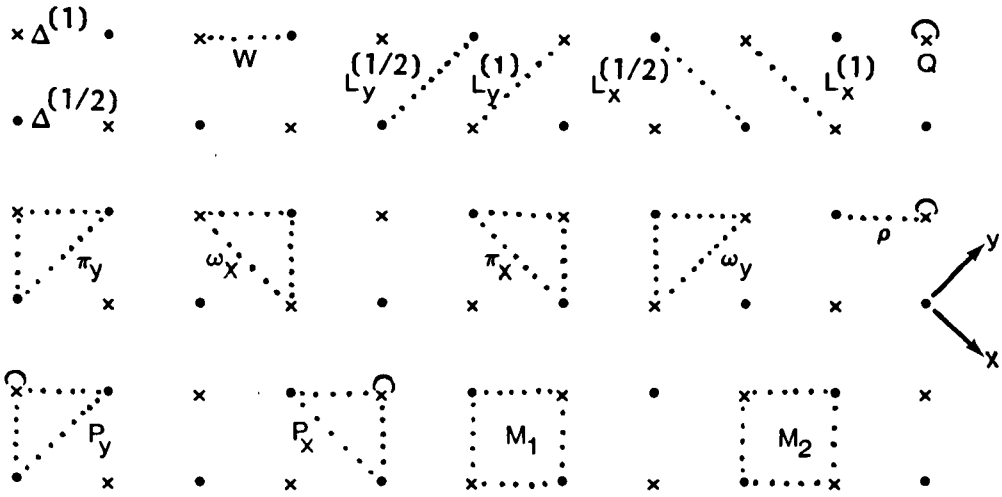
In Fig(5.1b), we chose to call i' and k' spin-1/2 and j', l' spin-1 blocks. But one could reverse the definition as there exists no 'a priori' distinguishing feature amongst these blocks. One would then obtain the following picture for the cluster $\delta=4$ (see Fig(5.2)). The important point one has to note at this stage is the following. Clusters $\delta=4$ of Fig's(5.1b) and (5.2) yield different expressions, for example, for the (renormalised) couplings between next-nearest neighbour blocks (which are of the same kind), when written in terms of site spins. This is easily seen by comparing Fig's(5.1b) and (5.2).

Therefore, directions x and y as shown in Fig(5.2) must be defined in the lattice to remedy this. For cluster $\delta=2$ such a difficulty clearly does not arise (see Fig(5.1a)). This anisotropy is characteristic to our particular four-spin cell choice and it enlarges the parameter space of the interactions by reducing symmetry.



Fig(5.2): An alternative picture for the cluster of four cells, $\delta=4$. Directions x and y must be defined in the lattice.

The four-cell cluster approximation is easily seen to 'generate' the following interaction constants shown in Fig(5.3). These are the interactions that fit into our cluster of cells. When renormalised, some of these couplings (such as ω_y') only occur in Fig(5.1b) and some others (such as ω_x') only in Fig(5.2). In Fig(5.3) loops correspond to terms involving s^2 , and it is apparent that graphs like  and  possess the same coupling constant π_x ; similarly for π_y , ω_x and ω_y . The same, of course, can be said about the four-spin couplings P_x and P_y . Furthermore, interactions W and ρ display no distinction between horizontal and vertical directions. (It is trivial to mention that a calculation employing the block construction  rather than  is identical to the latter, except for an interchange of subscripts x and y .)



Fig(5.3): Odd (distinguished by Greek letters) and even interactions generated by the four-cell cluster approximation.

Now, in order to proceed⁷, we have to be careful about the spin-1/2 cell prescription. The definition of the spin-1 cells via the immediate relation

$$s_{j,i}' = \text{sign} (s_{j,i}^1 + \sigma_{j,i}^2 + s_{j,i}^3 + \sigma_{j,i}^4) \quad (5.3.1)$$

which yields $s_{j,i}' = \pm 1, 0$; clearly presents no problem. However, since (as already mentioned) the block construction of Fig(5.1) does not lead to any natural distinction between s' and σ' blocks, we need to modify the definition of the spin-1/2 cells to render $\sigma' = \pm 1/2$. There are two way of doing this (see Schofield, 1980): There exist a total of 36 internal spin configurations for each cell, 13 of which yield a net spin of 1, and similarly for a net spin of -1 (in the sense of (5.3.1)). The latter are obtained by reversing all the spins in configurations which yielded a net spin of 1. The remaining 10 configurations give a net spin of zero (again, 5 of these can be obtained by reversing the spins of the other 5 configurations). Thus one can proceed (Naunberg and Nienhuis, 1974) by including the 13 configurations with a net spin of 1, plus those (specific) 5 configurations which yield a

zero net spin in the definition of $\sigma'=1/2$; and the spin reversed configurations in the definition of $\sigma'=-1/2$. Another way would be to include in the definition of $\sigma'=1/2$, not only configurations yielding 1 in (5.3.1), but also all those which yield zero. Similarly, we consider for $\sigma'=-1/2$ those configurations leading to -1 in (5.3.1), plus those leading to zero. We, therefore, have to include a factor of 1/2 in the definition of the spin-1/2 cells, so that configurations leading to zero net spin are not counted twice (see shortly). We have preferred the latter choice of spin-1/2 cell prescription which has certain advantages over the former (this is discussed fully by Schofield, 1980).

Since, for a given cell spin, the weight factor $P(\{s',\sigma' ; s,\sigma\})$ depends only on the site spins inside the cell, it can be written as a product over all cell weight factors (in similar fashion to (4.3.3)). For this cell arrangement (5.2.1) reads

$$\exp[C_a + \sum_{b \subseteq a} k_b {}^a \Omega_b(\{s',\sigma'\})] = \sum_{\{s,\sigma\}}^{s'} \sum_{\{s,\sigma\}}^{\sigma'} \exp \mathcal{H}_a(\{s',\sigma' ; s,\sigma\}) \quad (5.3.2)$$

where, from above, we have the exact connection between the cell and the site spins. If i' is a spin-1/2 block, one must write

$$\sum_{\{s_{i'},\sigma_{i'}\}}^{\sigma_{i'}=\pm 1/2} \mathcal{L}_{i'}^{\sigma_{i'}=\pm 1/2} + \frac{1}{2} \sum_{\{s_{i'},\sigma_{i'}\}}^{\sigma_{i'}=0} \quad (5.3.3)$$

with $\mathcal{L}_{i'}$ (associated with spin-1/2 cells) defined by

$$\mathcal{L}_{i'} = \frac{1}{2} \text{sign} (s_{i',1} + \sigma_{i',2} + s_{i',3} + \sigma_{i',4}) . \quad (5.3.4)$$

This is the precise manner in which the factor 1/2 is included in the definition of spin-1/2 blocks. We now proceed to determine the combinatorial factors $E_\delta(\alpha)$ for our case. As seen from equations (5.2.6b,8), $E_\delta(\alpha)$ are sums of

$$(-1)^{n(\gamma)-n(\alpha)} x_{(\text{number of times } \alpha \text{ can be covered by } \gamma, D_\gamma(\alpha))}$$

over subclusters γ of the basic cluster δ , which cover α ($\subseteq \delta$). They are listed in table 5.1, where for convenience, we have numbered the graphs. Note that many of these turn out to be zero for the (symmetric) four-cell cluster $\delta=4$, as asserted in section 5.1 .

$\delta \backslash \alpha$	1	1'	2	2'_x	2'_y	2''_x	2''_y	3_x	3_y	3'_x	3'_y	4_a	4_b
2													
2	-3	-3	1	-	-	-	-	-	-	-	-	-	-
4	1	1	-1	0	0	0	0	0	0	0	0	1	1

Table 5.1: Combinatorial factors $E_\delta(\alpha)$. For convenience spin-1/2 and -1 blocks are indicated by dots and crosses, respectively.

We mention, in passing, that (renormalised) interactions such as Q' (as well as $\Delta^{(1)'}$, of course) [see Fig(5.3)] can take place in subcluster $\alpha=1'$ (among others); and p in $\alpha=2$, etc. . Let us now, by the way of illustration, derive some of the values tabulated above. From (5.2.6b,8), we have for $\delta=2$,

$$E_2(1) = D_1(1) - D_2(1) = 1-4 = -3$$

$$E_2(1') = D_{1'}(1') - D_2(1') = 1-4 = -3$$

$$E_2(2) = D_2(2) = 1$$

because in our square lattice, a spin-1/2 or spin-1 block (which belong to classes $\alpha=1$ and $1'$, respectively), for example, can be covered by two nearest-neighbour cells ($\gamma=2$) in 4 ways, and so on. This can be easily seen by fixing an $\alpha \in \alpha$ on the lattice and collecting various

possibilities in which it may be covered by a 'c' out of δ . Similarly for $\delta=4$, equations (5.2.6b,8) yield

$$\begin{aligned} E_4(1) &= D_1(1) - D_2(1) - D_{2'_x}(1) - D_{2'_y}(1) + D_{3_x}(1) \\ &\quad + D_{3_y}(1) + D_{3'_x}(1) + D_{3'_y}(1) - D_{4_a}(1) - D_{4_b}(1) \\ &= 1-4-2-2+4+4+2+2-2-2 = 1 \end{aligned}$$

$$\begin{aligned} E_4(2) &= D_2(2) - D_{3_x}(2) - D_{3_y}(2) - D_{3'_x}(2) - D_{3'_y}(2) \\ &\quad + D_{4_a}(2) + D_{4_b}(2) = 1-1-1-1-1+1+1 = -1 \end{aligned}$$

$$E_4(2'_x) = D_{2'_x}(2'_x) - D_{3_x}(2'_x) + D_{4_a}(2'_x) = 1-2+1 = 0$$

$$E_4(2''_x) = D_{2''_x}(2''_x) - D_{3_x}(2''_x) + D_{4_b}(2''_x) = 1-2+1 = 0$$

$$E_4(3_x) = D_{3_x}(3_x) - D_{4_a}(3_x) = 1-1 = 0$$

$$E_4(3'_x) = D_{3'_x}(3'_x) - D_{4_b}(3'_x) = 1-1 = 0$$

$$E_4(4_a) = D_{4_a}(4_a) = 1$$

Other $E_4(\alpha)$, such as $E_4(1')$, $E_4(2'_y)$, etc. can be seen, by symmetry, to yield the same values as their symmetric counterparts obtained above. Actual computations prove this.

Having found $E_\delta(\alpha)$, we are now in a position to write down the RG equations explicitly. In what remains of this chapter, we represent the class of interactions Q, ρ, P_x and P_y respectively by $2''', 3'', 4'_x$ and $4'_y$.

(i) $\delta=2$: In zero field, only even interactions appear, yielding in the notation of equation (5.2.7),

$$\begin{aligned} k_2' &= k_2'(2) \\ k_{2'''} &= -3 k_{2'''}(1') + 4 k_{2'''}(2) \end{aligned} \tag{5.3.5}$$

where we have employed (5.2.6a) to write these in terms of $k_b^{i'a}$, which we show by $k_\beta^{i'(\alpha)}$. Of course, $\underline{k} = (k_2, k_2, \dots) \equiv (W, Q)$ in the notation of Fig(5.3). Quantities $k_b^{i'a} (\equiv k_\beta^{i'(\alpha)})$ are to be obtained from (5.3.2) in terms of \underline{k} . Thus, in zero field, (5.3.2) yields for $a \in \alpha = 2$ (with reference to Fig(5.1a)),

$$\begin{aligned} & \exp[C_{(2)} + k_2^{i'(2)} \sigma_{i'} s_{j'} + k_{2,\dots}^{i'(2)} (s_{j'}^2 - 2/3)] = \\ & \sum_{\{s_{j'}, \sigma_{j'}\}}^{s_{j'}} \sum_{\{s_{i'}, \sigma_{i'}\}}^{\sigma_{i'}} \exp[k_2 (\sigma_{i'}^2 s_{j'}^1 + \sigma_{i'}^3 s_{j'}^4 + \sigma_{i'}^1 s_{j'}^2 + \sigma_{i'}^2 s_{j'}^3 \\ & + \sigma_{i'}^3 s_{j'}^4 + \sigma_{i'}^4 s_{j'}^1 + \sigma_{j'}^1 s_{j'}^2 + \sigma_{j'}^2 s_{j'}^3 + \sigma_{j'}^3 s_{j'}^4 + \sigma_{j'}^4 s_{j'}^1) \\ & + k_{2,\dots} \{(s_{i'}^1)^2 + (s_{i'}^3)^2 + (s_{j'}^1)^2 + (s_{j'}^3)^2 - 8/3\}] . \quad (5.3.6a) \end{aligned}$$

The factors 2/3 are included in \mathcal{H} and \mathcal{H}' to comply with the convention $\sum_{\{s\}} \sum_{\{\sigma\}} \mathcal{H}(\{s, \sigma\}) = \sum_{\{s\}} \sum_{\{\sigma\}} \mathcal{H}'(\{s', \sigma'\}) = 0$, as explained in section 4.2 of the previous chapter. These factors will, however, play no part in the actual calculations since they cancel, as we shall see shortly. Also, we have from (5.3.2), when $a \in \alpha = 1'$

$$\begin{aligned} & \exp[C_{(1')} + k_{2,\dots}^{i'(1')} (s_{j'}^2 - 2/3)] = \\ & \sum_{\{s_{j'}, \sigma_{j'}\}}^{s_{j'}} \exp[k_2 (\sigma_{j'}^1 s_{j'}^2 + \sigma_{j'}^2 s_{j'}^3 + \sigma_{j'}^3 s_{j'}^4 + \sigma_{j'}^4 s_{j'}^1) \\ & + k_{2,\dots} \{(s_{j'}^1)^2 + (s_{j'}^3)^2 - 4/3\}] . \quad (5.3.6b) \end{aligned}$$

One can now proceed to solve (5.3.6a,b) for quantities $k_b^{i'a}$. This can be done both 'algebraically' and 'numerically'. The algebraic manipulations based on the relation

$$e^{k\sigma s} = \cosh^2 \left[\frac{1}{2} k \left\{ (1-u^2) + 4u\sigma s + 2u^2 s^2 \right\} \right] , \quad u = \tanh(\frac{1}{2} k)$$

are rather complicated and will not be pursued here. The more straightforward non-algebraic calculations use the following technique.

Taking logarithm of (5.3.2) and multiplying both sides by any of the Ω_b , yields, after summing over all configurations of s', σ' ;

$$k_b'^a \sum_{\{s'\}} \sum_{\{\sigma'\}} [\Omega_b(\{s', \sigma'\})]^2 = \sum_{\{s'\}} \sum_{\{\sigma'\}} \Omega_b \ln \sum_{\{s, \sigma\}}^{s'} \sum_{\{s, \sigma\}}^{\sigma'} \exp \mathcal{H}_a . \quad (5.3.7)$$

As an example, applying (5.3.7) to (5.3.6a) gives

$$k_2'^{(2)} = \frac{1}{2} \ln \sum_{\{s_j, \sigma_j\}}^{s_j'=1 \sigma_j'=1/2} \sum_{\{s_i, \sigma_i\}} \exp[\mathcal{H}] - \frac{1}{2} \ln \sum_{\{s_j, \sigma_j\}}^{s_j'=-1 \sigma_j'=1/2} \sum_{\{s_i, \sigma_i\}} \exp[\mathcal{H}] \\ - \frac{1}{2} \ln \sum_{\{s_j, \sigma_j\}}^{s_j'=1 \sigma_j'=-1/2} \sum_{\{s_i, \sigma_i\}} \exp[\mathcal{H}] + \frac{1}{2} \ln \sum_{\{s_j, \sigma_j\}}^{s_j'=-1 \sigma_j'=-1/2} \sum_{\{s_i, \sigma_i\}} \exp[\mathcal{H}]$$

where \mathcal{H} is the argument of the exponential on the right hand side of (5.3.6a). Note that such relationships involve all the cell-spin configurations for s' and σ' , which is not desirable in view of the computer time involved to generate them. However, symmetries of (5.3.6a) imply

$$k_2'^{(2)} = \ln \left\{ \frac{\sum_{\{s_j, \sigma_j\}}^{s_j'=1 \sigma_j'=1/2} \sum_{\{s_i, \sigma_i\}} \exp[\mathcal{H}]}{\sum_{\{s_j, \sigma_j\}}^{s_j'=1 \sigma_j'=-1/2} \sum_{\{s_i, \sigma_i\}} \exp[\mathcal{H}]} \right\} . \quad (5.3.8)$$

Similarly for $k_{2,\dots}'^{(2)}$, (5.3.6a) yields through (5.3.7)

$$(4/3) k_{2,\dots}'^{(2)} = (1/3) \ln \sum_{\{s_j, \sigma_j\}}^{s_j'=1 \sigma_j'=1/2} \sum_{\{s_i, \sigma_i\}} \exp[\mathcal{H}] + (1/3) \ln \sum_{\{s_j, \sigma_j\}}^{s_j'=1 \sigma_j'=-1/2} \sum_{\{s_i, \sigma_i\}} \exp[\mathcal{H}]$$

$$\begin{aligned}
& + (1/3) \ln \sum_{\{s_j, \sigma_j\}}^{s_j, ' = -1 \quad \sigma_j, ' = 1/2} \exp[\mathcal{H}] + (1/3) \ln \sum_{\{s_j, \sigma_j\}}^{s_j, ' = -1 \quad \sigma_j, ' = -1/2} \exp[\mathcal{H}] \\
& - (2/3) \ln \sum_{\{s_j, \sigma_j\}}^{s_j, ' = 0 \quad \sigma_j, ' = 1/2} \exp[\mathcal{H}] - (2/3) \ln \sum_{\{s_j, \sigma_j\}}^{s_j, ' = 0 \quad \sigma_j, ' = -1/2} \exp[\mathcal{H}].
\end{aligned}$$

Again symmetries of (5.3.6a) imply

$$2 k_{2, \dots, '}(2) = \ln \left\{ \frac{\sum_{\{s_j, \sigma_j\}}^{s_j, ' = 1 \quad \sigma_j, ' = 1/2} \exp[\mathcal{H}] \sum_{\{s_j, \sigma_j\}}^{s_j, ' = 1 \quad \sigma_j, ' = -1/2} \exp[\mathcal{H}]}{\left\{ \sum_{\{s_j, \sigma_j\}}^{s_j, ' = 0 \quad \sigma_j, ' = 1/2} \exp[\mathcal{H}] \right\}^2} \right\} \quad (5.3.9)$$

Therefore, in view of such symmetries, one can obtain simpler relations for k_b^a than those obtained with applications of (5.3.7) alone. This will save on computer time taken to generate the various configurations needed by simply 'throwing away' all those which are not required. But relations (5.3.8,9) could have been immediately written down by appropriately choosing $\sigma_j, ' , s_j, ' in (5.3.6a) and dividing afterwards. We will actually use this equivalent method to save a lot of effort. So, to find $k_{2, \dots, '}(1')$ from (5.3.6b), we put $s_j, ' = 1, 0$ and divide the resulting equations to get$

$$k_{2, \dots, '}(1') = \ln \left\{ \frac{\sum_{\{s_j, \sigma_j\}}^{s_j, ' = 1} \exp[\dots]}{\sum_{\{s_j, \sigma_j\}}^{s_j, ' = 0} \exp[\dots]} \right\}. \quad (5.3.10)$$

Of course, one finds the same equation if one uses (5.3.7). As asserted earlier, factors 2/3 included to comply with convention

$\sum_{\{s\}} \sum_{\{\sigma\}} \mathcal{H}(\{s, \sigma\}) = \sum_{\{s'\}} \sum_{\{\sigma'\}} \mathcal{H}'(\{s', \sigma'\}) = 0$, generally cancel out. Inserting equations (5.3.8,9,10) into (5.3.5) yields our RG equations as far as the two-cell cluster approximation is concerned. These must be solved numerically by some iterative technique (see section 5.5), through generating all $\{s, \sigma\}$ configurations compatible with cell-spin distributions s', σ' . One then obtains numerical values for fixed points, the (even-even) Jacobian $T_{\alpha\beta}^*$ and its associated eigenvalues and eigenvectors at these fixed points (see section 5.5).

Magnetic perturbations give rise to odd interactions $\Delta^{(1)}, \Delta^{(1/2)}$ and ρ (different fields are applied on each sublattice), and take place in 1, 1' and 2. Again in the language of equation (5.2.7), the odd-odd part of $T_{\alpha\beta}^*$ follows from the differentiation of (see (5.2.9))

$$\begin{aligned}
 k_1' &= -3 k_1'^{(1)} + 4 k_1'^{(2)} \\
 k_{1,1}' &= -3 k_{1,1}'^{(1')} + 4 k_{1,1}'^{(2)} \\
 k_{3,1,1}' &= k_{3,1,1}'^{(2)}
 \end{aligned} \tag{5.3.11}$$

evaluated at the fixed point, where obviously $(k_1, k_{1,1}, k_{3,1,1}) \equiv (\Delta^{(1/2)}, \Delta^{(1)}, \rho)$, and the k_b^{ia} are given by (with reference to Fig(5.1a))

$$\begin{aligned}
 \exp(C_{(1)} + k_1'^{(1)} \sigma_{i,1}') &= \\
 \sum_{\{\sigma_{i,1}, \sigma_{i,1}'\}} &\exp[k_1 (\sigma_{i,1}^2 + \sigma_{i,1}^4) + k_{1,1}' (s_{i,1}^1 + s_{i,1}^3) \\
 &+ k_{3,1,1}' \{(s_{i,1}^1)^2 \sigma_{i,1}^2 + \sigma_{i,1}^2 (s_{i,1}^3)^2 + (s_{i,1}^3)^2 \sigma_{i,1}^4 + \sigma_{i,1}^4 (s_{i,1}^1)^2\} \\
 &+ k_2 (s_{i,1}^1 \sigma_{i,1}^2 + \sigma_{i,1}^2 s_{i,1}^3 + s_{i,1}^3 \sigma_{i,1}^4 + \sigma_{i,1}^4 s_{i,1}^1) \\
 &+ k_{2,1,1}' \{(s_{i,1}^1)^2 + (s_{i,1}^3)^2 - 4/3\}]
 \end{aligned} \tag{5.3.12a}$$

and

$$\begin{aligned}
& \exp[C_{(1')} + k_{1'}^{(1')} s_{j'} + k_{2''}^{(1')} (s_{j'}^2 - 2/3)] = \\
& \sum_{\{s_{j'}, \sigma_{j'}\}}^{s_{j'}} \exp[k_1 (\sigma_{j'}^2 + \sigma_{j'}^4) + k_{1'} (s_{j'}^1 + s_{j'}^3) \\
& + k_{3''} \{(s_{j'}^1)^2 \sigma_{j'}^2 + \sigma_{j'}^2 (s_{j'}^3)^2 + (s_{j'}^3)^2 \sigma_{j'}^4 + \sigma_{j'}^4 (s_{j'}^1)^2\} \\
& + k_2 (s_{j'}^1 \sigma_{j'}^2 + \sigma_{j'}^2 s_{j'}^3 + s_{j'}^3 \sigma_{j'}^4 + \sigma_{j'}^4 s_{j'}^1) \\
& + k_{2''} \{(s_{j'}^1)^2 + (s_{j'}^3)^2 - 4/3\}] \quad (5.3.12b)
\end{aligned}$$

and

$$\begin{aligned}
& \exp[C_{(2)} + k_1^{(2)} \sigma_{i'} + k_{1'}^{(2)} s_{j'} + k_{3''}^{(2)} s_{j'}^2 \sigma_{i'} \\
& + k_2^{(2)} s_{j'} \sigma_{i'} + k_{2''}^{(2)} (s_{j'}^2 - 2/3)] = \\
& \sum_{\{s_{j'}, \sigma_{j'}\}}^{s_{j'}} \sum_{\{\sigma_{i'}, \sigma_{i'}\}}^{\sigma_{i'}} \exp[k_1 (\sigma_{i'}^2 + \sigma_{i'}^4 + \sigma_{j'}^2 + \sigma_{j'}^4) \\
& + k_{1'} (s_{j'}^1 + s_{j'}^3 + s_{j'}^1 + s_{j'}^3) + k_{3''} \{(s_{j'}^1)^2 \sigma_{i'}^2 + \sigma_{i'}^2 (s_{j'}^3)^2 \\
& + (s_{j'}^3)^2 \sigma_{i'}^4 + \sigma_{i'}^4 (s_{j'}^1)^2 + (s_{j'}^1)^2 \sigma_{j'}^2 + \sigma_{j'}^2 (s_{j'}^3)^2 \\
& + (s_{j'}^3)^2 \sigma_{j'}^4 + \sigma_{j'}^4 (s_{j'}^1)^2 + \sigma_{j'}^4 (s_{j'}^3)^2 + \sigma_{i'}^2 (s_{j'}^1)^2\} \\
& + k_2 (s_{j'}^1 \sigma_{i'}^2 + \sigma_{i'}^2 s_{j'}^3 + s_{j'}^3 \sigma_{i'}^4 + \sigma_{i'}^4 s_{j'}^1 \\
& + s_{j'}^1 \sigma_{j'}^2 + \sigma_{j'}^2 s_{j'}^3 + s_{j'}^3 \sigma_{j'}^4 + \sigma_{j'}^4 s_{j'}^1 + \sigma_{i'}^4 s_{i'}^3 + \sigma_{i'}^2 s_{j'}^1) \\
& + k_{2''} \{(s_{j'}^1)^2 + (s_{j'}^3)^2 + (s_{j'}^1)^2 + (s_{j'}^3)^2 - 8/3\}] \quad (5.3.12c)
\end{aligned}$$

As a matter of checking; comparing these with (5.3.6a,b), one observes that at a fixed point \underline{k}^* , the k_b^{*a} of (5.3.11), as appear in (5.3.12a-c), must vanish, so that k_α^* in (5.3.11) [where class α is odd] are identically zero and the fixed point does indeed lie in the even interaction subspace. Moreover, by differentiating (5.3.12a) with respect to say k_1 one gets, at \underline{k}^* ,

$$\begin{aligned}
& (\partial C_{(1)}/\partial k_1)_{\underline{k}^*} + \sigma_{i'} (\partial k_1^{(1)}/\partial k_1)_{\underline{k}^*} = \\
& \sum_{\{s_{j'}, \sigma_{j'}\}}^{\sigma_{i'}} (\sigma_{j'}^2 + \sigma_{j'}^4) \exp[\mathcal{H}^*] / \sum_{\{s_{j'}, \sigma_{j'}\}}^{\sigma_{i'}} \exp[\mathcal{H}^*]
\end{aligned}$$

where \mathcal{H}^* is the expression appearing inside the square brackets in (5.3.12a), evaluated at the fixed point where, of course, only even interactions remain. One can now proceed by taking $\sigma_{j'} = \pm 1/2$ (or alternatively through using (5.3.7)) to eliminate for $(\partial k_1^{(1)}/\partial k_1)_{\underline{k}^*}$. Similarly differentiating with respect to k_1 and k_3 , (remember only odd β appear for α odd in the odd-odd part of $T_{\alpha\beta}^*$, see section 4.2) at \underline{k}^* yields values for $(\partial k_1^{(1)}/\partial k_1)_{\underline{k}^*}$ and $(\partial k_1^{(1)}/\partial k_3)_{\underline{k}^*}$, respectively. Other derivatives $(\partial k_b^{(a)}/\partial k_{\beta'})_{\underline{k}^*}$ may be obtained in exactly the same manner via differentiating (5.3.12b,c). Note that from equation (5.3.5), because in the even-even part of $T_{\alpha\beta}^*$ only even β occur for α even, we have

$$\partial k_2^{(2)} \Big|_{\underline{k}^*} = 0, \quad 3 \partial k_{2,\dots}^{(1')} \Big|_{\underline{k}^*} = 4 \partial k_{2,\dots}^{(2)} \Big|_{\underline{k}^*} \quad (5.3.13)$$

where ∂ is taken to mean differentiation with respect to odd couplings k_{β} . Use of such results facilitates the computational labour involved. Having obtained the odd-odd part of $T_{\alpha\beta}^*$, we can determine the corresponding magnetic eigenvalues and eigenvectors. The discussion of numerical results is deferred until section 5.5.

Finally, here we point out the necessity of including self-couplings, in view of the consistency of equations of the form (5.3.2). Since $s_{j'} = -1$ configurations can be achieved by reversing all spins in those configurations yielding $s_{j'} = 1$; we have that, in zero field, equations like (5.3.6b) would not remain consistent, were self-interactions not present. This can be easily checked by putting $s_{j'} = \pm 1, 0$ and noting that C's are independent of $s_{j'}$ (see section 4.2). Similar situations happen for any choice of the basic cluster δ .

(ii) $\delta=4$: Once again (5.2.7) yields, in zero field, what are essentially the RG equations; namely

$$\begin{aligned}
k_2' &= -k_2'^{(2)} + k_2'^{(4_a)} + k_2'^{(4_b)} \\
k_{2_x}' &= k_{2_x}'^{(4_a)} \\
k_{2_y}' &= k_{2_y}'^{(4_b)} \\
k_{2_x}'' &= k_{2_x}''^{(4_b)} \\
k_{2_y}'' &= k_{2_y}''^{(4_a)} \\
k_{4_x}' &= k_{4_x}'^{(4_a)} \\
k_{4_y}' &= k_{4_y}'^{(4_b)} \\
k_{4_a}' &= k_{4_a}'^{(4_a)} \\
k_{4_b}' &= k_{4_b}'^{(4_b)} \\
k_{2'''} &= k_{2'''}^{(1')} - 4 k_{2'''}^{(2)} + 2 k_{2'''}^{(4_a)} + 2 k_{2'''}^{(4_b)}
\end{aligned} \tag{5.3.14}$$

where the connection between the above even (renormalised) couplings k_α' and interaction constants of Fig(5.3) should be obvious. It is quoted below (in terms of the original coupling constants) for quick reference.

$$\begin{aligned}
&(k_2, k_{2_x}', k_{2_y}', k_{2_x}'', k_{2_y}'', k_{4_x}', k_{4_y}', k_{4_a}', k_{4_b}', k_{2''}') \equiv \\
&(W, L_x^{(1/2)}, L_y^{(1/2)}, L_x^{(1)}, L_y^{(1)}, P_x, P_y, M_1, M_2, Q) .
\end{aligned} \tag{5.3.15}$$

The $k_b'^a$ again are to be obtained from (5.3.2) in terms of the ten parameters k_α appearing in (5.3.15). From (5.3.14) it is clear that one must consider clusters of Fig's(5.1a,b) and (5.2) [which include the cluster 1']. For instance, for cluster a of type $\alpha=2$ (see Fig(5.1a)), equation (5.3.2) becomes

$$\begin{aligned}
& \exp[C_{(2)} + k_2^{(2)} s_{j'} \sigma_{i'} + k_{2,\dots}^{(2)} (s_{j'}^2 - 2/3)] = \\
& \sum_{\{s_{j'}, \sigma_{j'}\}}^{s_{j'}} \sum_{\{s_{i'}, \sigma_{i'}\}}^{\sigma_{i'}} \exp[k_2 (s_{i'}^1 \sigma_{i'}^2 + \sigma_{i'}^2 s_{i'}^3 + s_{i'}^3 \sigma_{i'}^4 + \sigma_{i'}^4 s_{i'}^1 \\
& + s_{j'}^1 \sigma_{j'}^2 + \sigma_{j'}^2 s_{j'}^3 + s_{j'}^3 \sigma_{j'}^4 + \sigma_{j'}^4 s_{j'}^1 + \sigma_{j'}^4 s_{i'}^3 + \sigma_{i'}^2 s_{j'}^1) \\
& + k_{2,x} \sigma_{i'}^2 \sigma_{j'}^4 + k_{2,y} (\sigma_{i'}^2 \sigma_{i'}^4 + \sigma_{j'}^2 \sigma_{j'}^4) \\
& + k_{2,x} (s_{i'}^1 s_{i'}^3 + s_{j'}^1 s_{j'}^3) + k_{2,y} s_{j'}^1 s_{i'}^3 \\
& + k_{4,x} \{\sigma_{i'}^2 (s_{j'}^1)^2 \sigma_{j'}^4 + \sigma_{i'}^2 (s_{i'}^3)^2 \sigma_{j'}^4\} + k_{4,y} \{\sigma_{i'}^2 (s_{i'}^1)^2 \sigma_{i'}^4 \\
& + \sigma_{i'}^2 (s_{i'}^3)^2 \sigma_{i'}^4 + \sigma_{j'}^2 (s_{j'}^1)^2 \sigma_{j'}^4 + \sigma_{j'}^2 (s_{j'}^3)^2 \sigma_{j'}^4\} \\
& + k_{4,a} s_{j'}^1 \sigma_{i'}^2 s_{i'}^3 \sigma_{j'}^4 \\
& + k_{4,b} (s_{i'}^1 \sigma_{i'}^2 s_{i'}^3 \sigma_{i'}^4 + s_{j'}^1 \sigma_{j'}^2 s_{j'}^3 \sigma_{j'}^4) \\
& + k_{2,\dots} \{(s_{i'}^1)^2 + (s_{i'}^3)^2 + (s_{j'}^1)^2 + (s_{j'}^3)^2 - 8/3\}] \quad (5.3.16a)
\end{aligned}$$

where $C_{(2)}$ appearing above is, of course, different from that of (5.3.6a) in the two-cell cluster approximation. Also for a $\alpha=1'$,

$$\begin{aligned}
& \exp[C_{(1')} + k_{2,\dots}^{(1')} (s_{j'}^2 - 2/3)] = \\
& \sum_{\{s_{j'}, \sigma_{j'}\}}^{s_{j'}} \exp[k_2 (s_{j'}^1 \sigma_{j'}^2 + \sigma_{j'}^2 s_{j'}^3 + s_{j'}^3 \sigma_{j'}^4 + \sigma_{j'}^4 s_{j'}^1) \\
& + k_{2,y} \sigma_{j'}^2 \sigma_{j'}^4 + k_{2,x} s_{j'}^1 s_{j'}^3 + k_{4,y} \{\sigma_{j'}^2 (s_{j'}^1)^2 \sigma_{j'}^4 \\
& + \sigma_{j'}^2 (s_{j'}^3)^2 \sigma_{j'}^4\} + k_{4,b} s_{j'}^1 \sigma_{j'}^2 s_{j'}^3 \sigma_{j'}^4 \\
& + k_{2,\dots} \{(s_{j'}^1)^2 + (s_{j'}^3)^2 - 4/3\}] \quad (5.3.16b)
\end{aligned}$$

where again $C_{(1')}$ is not to be confused with that of (5.3.6b). One can now eliminate $k_2^{(2)}$, $k_{2,\dots}^{(2)}$ and $k_{2,\dots}^{(1')}$ in exactly the same fashion discussed in the two-cell cluster approximation. Similarly, we can write analogous expressions connecting $k_b^{(4_a)}$, $k_b^{(4_b)}$ to k_α by simply looking at Fig's(5.1b) and (5.2), respectively. These obviously will have more terms on both the left and right hand sides, so elimination of $k_b^{(4_a)}$ will require slightly more effort. Here again

we suitably fix values for s', σ' on the 'left hand sides' and divide appropriately to determine $k_b^{(4_a)}$ and $k_b^{(4_b)}$. This will, as mentioned before, dramatically reduce the computer time spent on evaluating the 'right hand sides' by not needing to deal with every configuration of cell spins. (The effect is more noticeable here in the four-cell approximation; and even more so if one is dealing with cells which contain more spins, e.g those of the next section.) A computer program was written to perform these manipulations and the resulting $k_b^{(a)}$ combined according to (5.2.14) formed our four-cell cluster RG equations which yielded \underline{k}^* and $T_{\alpha\beta}^*$ together with the eigenvalues and corresponding (right) eigenvectors, when solved.

In the case of non-zero magnetic fields (different on each sublattice), odd interactions arise, appearing in $1, 1', 2, 4_a$ and 4_b as prescribed by (5.2.7):

$$\begin{aligned}
 k_1' &= k_1^{(1)} - 4 k_1^{(2)} + 2 k_1^{(4_a)} + 2 k_1^{(4_b)} \\
 k_{1'}' &= k_{1'}^{(1')} - 4 k_{1'}^{(2)} + 2 k_{1'}^{(4_a)} + 2 k_{1'}^{(4_b)} \\
 k_{3_x}' &= k_{3_x}^{(4_a)} \\
 k_{3_y}' &= k_{3_y}^{(4_b)} \\
 k_{3_x'}' &= k_{3_x'}^{(4_b)} \\
 k_{3_y'}' &= k_{3_y'}^{(4_a)} \\
 k_{3''}' &= -k_{3''}^{(2)} + k_{3''}^{(4_a)} + k_{3''}^{(4_b)}
 \end{aligned} \tag{5.3.17}$$

where

$$\begin{aligned}
 (k_1, k_{1'}, k_{3_x}, k_{3_y}, k_{3_x'}, k_{3_y'}, k_{3''}) &\equiv \\
 (\Delta^{(1/2)}, \Delta^{(1)}, \pi_x, \pi_y, \omega_x, \omega_y, \rho) &.
 \end{aligned}$$

We are interested in the odd-odd part of the Jacobian matrix $T_{\alpha\beta}^*$ evaluated at the fixed points (which are in the even subspace). This follows from $\partial|_{\underline{k}^*}$ -differentiation (i.e differentiation with respect to odd couplings at \underline{k}^* , in the notation of (5.3.13)) of (5.3.17). Derivatives $\partial k_b^{(a)}|_{\underline{k}^*}$ are obtained as discussed previously, for instance,

$$\begin{aligned} & (\partial C_{(1')}/\partial k_1)|_{\underline{k}^*} + s_{j'} (\partial k_{1'}^{(1')}/\partial k_1)|_{\underline{k}^*} \\ & + (s_{j'}^2 - 2/3) (\partial k_{2,\dots}^{(1')}/\partial k_1)|_{\underline{k}^*} = \\ & \sum_{\{s_{j'}, \sigma_{j'}\}}^{s_{j'}} (\sigma_{j'}^2 + \sigma_{j'}^4) \exp[\mathcal{H}^*] / \sum_{\{s_{j'}, \sigma_{j'}\}}^{s_{j'}} \exp[\mathcal{H}^*] \end{aligned} \quad (5.3.18)$$

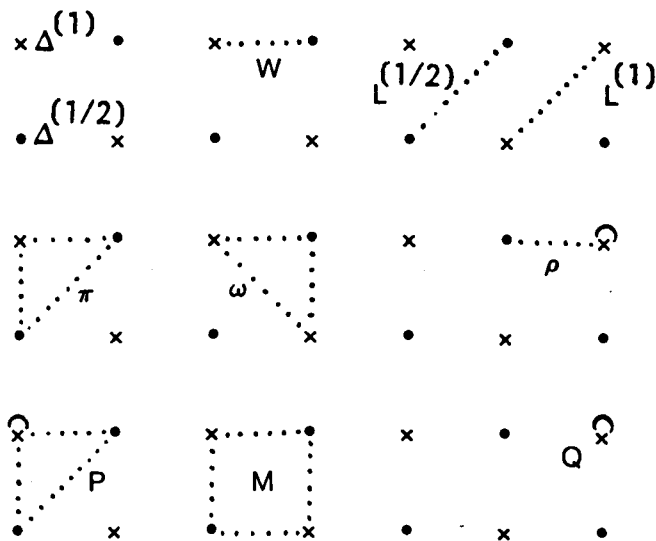
yields $\partial k_b^{(1')}|_{\underline{k}^*}$; \mathcal{H}^* being the expression inside the right hand side (square) brackets of (5.3.16b) evaluated at the fixed point \underline{k}^* . We have avoided writing every such formula for conciseness (although they are very easily obtained), as they have more to do with the numerical calculation side of the work.

5.4 Calculations on blocks of five spins

The procedure here is much the same as that of the previous section. Symmetry preserving basic clusters $\delta=2$ and $\delta=4$ will be considered. The picture of Fig(4.3) corresponds to $\delta=4$ and has the cluster $\delta=2$ as a subfigure. It is apparent, after a little consideration, that the arguments put forward at the beginning of section 5.3 no longer apply for this 'more symmetrical' cell prescription, resulting in the elimination of the anisotropy in directions x and y. This is because there exists a natural distinction between s' and σ' blocks as defined by (4.3.2).

As is obvious by now, the basic limitation of cluster approximation technique is the fact that all interaction types are omitted which

do not fit in the figure chosen. As a result, in the $\delta=2$ analysis, next-nearest neighbour couplings must be omitted. But this implies that there are no intra-block interactions. (In the four-spin cell configuration of the last section, we could still have nearest neighbour couplings among cell constituents.) A little consideration via preliminary (algebraic) calculations thus shows that the two-cell approximation is trivial for this clustering. We therefore proceed to the four-cell cluster analysis which clearly generates the following (isotropic) coupling constants in the lattice.



Fig(5.4): Odd (distinguished by Greek letters) and even interactions generated by the four-cell cluster approximation.

In view of (4.3.3), equation (5.2.1) reads for this cell arrangement:

$$\exp[C_a + \sum_{b \subseteq a} k_b {}^a \Omega_b(\{s', \sigma'\})] = \sum_{[s']} \sum_{[\sigma']} \exp \mathcal{H}_a(\{s', s; \sigma', \sigma\}) . \quad (5.4.1)$$

Table 5.2 lists the relevant combinatorial factors $E_4(\alpha)$ where the notation of table 5.1 is kept.

$$\begin{aligned} & \exp[C_{(2)} + k_2^{(2)} s_{j'} \sigma_{i'} + k_{2''}^{(2)} (s_{j'}^2 - 2/3)] = \\ & \sum_{\{s_{j'}\}} \sum_{\{\sigma_{i'}\}} \exp[k_2 (s_{j'}^5 \sigma_{i'}^2 + \sigma_{i'}^5 s_{j'}^4 + s_{j'}^1 \sigma_{i'}^2 + \sigma_{i'}^2 s_{j'}^4 \\ & + s_{j'}^4 \sigma_{i'}^3) + k_{2'} (\sigma_{i'}^1 + \sigma_{i'}^2 + \sigma_{i'}^3 + \sigma_{i'}^4) \sigma_{i'}^5 \\ & + k_{2''} (s_{j'}^1 + s_{j'}^2 + s_{j'}^3 + s_{j'}^4) s_{j'}^5 \\ & + k_4 \{ \sigma_{i'}^2 (s_{j'}^4)^2 \sigma_{i'}^5 + \sigma_{i'}^3 (s_{j'}^4)^2 \sigma_{i'}^5 \} \\ & + k_{2'''} \{ (s_{j'}^1)^2 + (s_{j'}^2)^2 + (s_{j'}^3)^2 + (s_{j'}^4)^2 + (s_{j'}^5)^2 - 10/3 \}] . \end{aligned}$$

Similarly, $k_{\beta}^{(4)}$ may be evaluated in analogous fashion. These make up all the information needed to determine the zero-field critical behaviour.

Magnetic field (again taking different values on each sublattice) perturbations yield the odd-odd part of $T_{\alpha\beta}^*$, which is obtained by $\partial|_{\underline{k}}^*$ -differentiation of

$$\begin{aligned} k_1' &= k_1^{(1)} - 4 k_1^{(2)} + 4 k_1^{(4)} \\ k_{1'} &= k_{1'}^{(1')} - 4 k_{1'}^{(2)} + 4 k_{1'}^{(4)} \\ k_3' &= k_3^{(4)} \\ k_{3'} &= k_{3'}^{(4)} \\ k_{3''} &= -k_{3''}^{(2)} + 2 k_{3''}^{(4)} \end{aligned} \tag{5.4.4}$$

where, of course,

$$(k_1, k_{1'}, k_3, k_{3'}, k_{3''}) \equiv (\Delta^{(1/2)}, \Delta^{(1)}, \pi, \omega, \rho) . \tag{5.4.5}$$

The necessary derivatives $\partial k_b^a |_{\underline{k}}^*$ would be obtained through relations like (5.3.18).

5.5 Numerical analysis of results

We treat our RG equations as a system of non-linear simultaneous equations to be solved for k_α^* . The solution of these equations is accomplished through the application of NAG library subroutine C05NCF which guarantees a fast rate of convergence. It also provides the Jacobian matrix at the solution (fixed) point. NAG routine F02AGF can then be used to yield the corresponding eigenvalues and (right) eigenvectors. The latter routine is also employed to determine the magnetic eigenvalues and eigenvectors of the odd-odd part of $T_{\alpha\beta}^*$ found numerically. The success of the iterative method embodied in C05NCF is dependent upon a trial solution. One can study various fixed points by introducing appropriate trial solutions. Since in cluster theory (as well as the cumulant technique) we use the fact that short range interactions are most important; one expects the nearest neighbour coupling to dominate over others. This can be used as a criterion for a rough estimate of the starting points. Below, we give the results obtained together with their analysis.

(i) Blocks of four spins: Here $\ell=2$ and $d=2$, of course.

(a) $\delta=2$ - Equation (5.3.5) yields two fixed point values for \underline{k}' , namely an unstable ferromagnetic fixed point $(k_2^*, k_{2,\dots}^*) = (1.1084, 1.0283)$ with a single relevant eigenvalue $\lambda_T = 1.8316$, and a stable (i.e no relevant eigenvalues) one at $(0, 0.3119)$. λ_T yields, through (4.2.14), the estimate $\alpha = 0.291$.

Contrary to our expectation, in the ferromagnetic fixed point, k_2^* and $k_{2,\dots}^*$ are of the same order of magnitude and hence the nearest neighbour coupling does not really play a dominating role. Now, in any spin system, one expects to find the 'origin' $k_\alpha = 0$ as a physically insignificant (trivial) fixed point corresponding to the in-

finite temperature limit of that system (see Niemeijer and van Leeuwen, 1976). However, equations (5.3.6a,b) imply that the origin is not a fixed point. This is easily seen by a preliminary direct iteration starting with $k_2 = k_{2,\dots} = 0$ in (5.3.6a,b). After the first iteration, one observes that $k_2^{(2)} = 0$ but that

$$k_{2,\dots}^{(2)} = k_{2,\dots}^{(1')} = \ln \left\{ \frac{\sum_{\{s_{j,\dots}^{(1)}\}}^{s_{j,\dots}^{(1)}=1} 1}{\sum_{\{s_{j,\dots}^{(1)}\}}^{s_{j,\dots}^{(1)}=0} 1} \right\} \quad (5.5.1)$$

so that (5.3.5) yields $k_2 = 0$, $k_{2,\dots} (= k_{2,\dots}^{(1')}) \neq 0$. As a result, the (stable) origin is shifted by the adverse presence of self-interactions (remember that the inclusion of $k_{2,\dots}^{(1')}$ was compulsory for the consistency of (5.3.6b), see section 5.3) to the stable point (0,0.3199). [It occurred to us late in the pursuit of the work that this may have been remedied by ascribing the same number of states to each block-spin variable so that in (5.5.1) $k_{2,\dots}^{(2)}$ and $k_{2,\dots}^{(1')}$ vanish.] We refer to this point as the 'shifted origin' and believe it has no physical significance. A non-zero value of the self-interaction constant means physically a preference for s spins to be either ± 1 . For finite (positive) values of this coupling, values $s = \pm 1$ minimize the energy of the system as can be seen from the Hamiltonian.

The magnetic eigenvalue at the 'physical' (ferromagnetic) fixed point is found to be $\lambda_H = 3.7749$ yielding, again through (4.2.14), the estimate $\delta = 22.934$ for the critical exponent δ (which should be around 15 for two-dimensional lattices).

Numerical estimates obtained by Schofield (1980) through the application of perturbation theory (whose first order analysis generated a zero-field parameter space consisting of only k_2 , as mentioned in section 5.1) yielded more satisfactory results. When including self-interactions (in the second order calculations, of course), he

found estimates for critical exponents which were further removed from those suggested by universality (although in such analysis the self-coupling does play rather a passive role, as judged by its comparatively small value at the fixed point, see Schofield (1980)). Here, too, we hold the (more active) role of the self-couplings responsible for our poor estimates. We shall not bother with estimates of β and γ as no useful values will be obtained.

(b) $\delta=4$ – In larger cluster approximations one usually expects to get better numerical results (this is not always true, see some of the results given by Niemeijer and van Leeuwen, 1974). Let us initially consider the limit fixed point $k_\alpha=0$, which as explained in (a) is trivial and of no physical significance. Similar approach via direct iterations show that the origin under RG equations (5.3.14) is mapped into a point on the self-coupling axis. This is realised (with slightly more effort) through equations like (5.3.16a,b) which determine k_b^{ia} , after only the first iteration, yielding

$$2 k_{2,\dots}^{(2)} = k_{2,\dots}^{(4a)} + k_{2,\dots}^{(4b)}$$

$$k_{2,\dots}^{(1')} = \ln \left\{ \sum_{\substack{s_j=1 \\ \{s_j, \sigma_j\}}} 1 / \sum_{\substack{s_j=0 \\ \{s_j, \sigma_j\}}} 1 \right\} \quad (5.5.2)$$

and other k_b^{ia} equal to zero. So again the term $k_{2,\dots}^{*(1')}$ makes $k_{2,\dots}^*$ non-vanishing (see also (a)); a by-effect of the presence of self-interactions. Numerical calculations find this shifted origin to be

$$\underline{k}^* = (0,0,0,0,0,0,0,0,0,0,0.3199)$$

with \underline{k}^* given by (5.3.15), of course. This is the stable fixed point of our RG equations which is not surprisingly the same, except for

the fact that the parameter space is ten-dimensional here, as the shifted origin of the two-cell cluster analysis in (a).

The other (physical) fixed point found corresponds to ferromagnetism on the lattice and is at

$$(0.7412, 0.4575, -0.1633, 0.1409, 0.0326, \\ -0.0071, 0.0857, -0.1072, -0.2364, 1.0641)$$

with a relevant eigenvalue $\lambda_T = 1.7546$. This value for λ_T yields an estimate for α which, compared with that obtained in (a), is further removed from the conjecture of the universality principle. This could well be due to the more determining role played by self-couplings in the equations, as judged from the dominance of $k_{2,\dots}^*$ over all other interaction constants at the fixed point. Note that here, the next-most dominating coupling constant is that of the nearest neighbours.

We mention, in passing, that our RG equations did not, of course, yield any fixed points when self-interactions were omitted. Apart from the consistency problem (discussed in section 5.3), above numerical results for the fixed points indicate through comparatively large value for $k_{2,\dots}^*$, the importance of the role of $k_{2,\dots}$. We feel that this is in no contradiction with the fact that self-interactions are physically irrelevant in determining critical behaviour; for the outcome may be viewed as a shortcoming of the approach which mathematically approximates the physical reality.

Magnetic perturbations give rise to only one relevant eigenvalue $\lambda_H = 2.8188$, which again gives no useful estimate for critical exponents. Also we find that the applied fields couple to sublattices differently (but unidirectionally) [a trivial examination of the components of relevant eigenvectors verifies this also for the case (a)]. This is

obvious and means that the analysis contained here and in (a) correspond to ferromagnetism in a uniformly oriented field which may be extended via arguments such as given in section 1.3 to ferrimagnetism in a staggeredly oriented field. But since no useful estimates were obtained, we shall not elaborate on this.

(ii) Blocks of five spins: Here $\ell=\sqrt{5}$, $d=2$ as given in section 4.3; and $\delta=4$. As mentioned in section 4.1, there is little doubt that calculations employing a sublattice cell choice such as the present one provide poor quantitative results in terms of critical exponents (Schick, 1982). The presence of self-interactions would make matters worse, especially if they are to take a vital part in determining fixed points. Our aim, therefore, is to study this case qualitatively in terms of the shape of the critical surfaces and the flow patterns along them (see later).

Let us begin with by examining the possibility of the origin and any decoupled sublattice fixed points which may arise under recurrence relations (5.4.2). Again (5.4.2) yields after only one (direct) iteration, with $k_\alpha=0$ as the starting point,

$$k_{2,\dots}^{(2)} = k_{2,\dots}^{(4)}$$

$$k_{2,\dots}^{(1')} = \ln \left\{ \sum_{\{s_j\}}^{s_j=1} 1 / \sum_{\{s_j\}}^{s_j=0} 1 \right\}$$

and other $k_b^{(a)}$ equal to zero. This should be compared with (5.5.2) where the related comments made in (i) also apply here. Numerically, one finds that the origin is transformed, under the RG equations (5.4.2), to the point

$$\underline{k}^* = (0,0,0,0,0,0.9132)$$

in the six-dimensional (zero-field) parameter space where \underline{k}^* is given by (5.4.3). This point is stable and likewise considered of no physical significance. Another possibility is that of the (unstable) decoupled sublattice fixed points, where according to discussions of section 4.3, we generally expect order on only one of the two decoupled sublattices at a given appropriate temperature. Thus starting with all the parameters zero except for k_2 , (corresponding to order on the spin-1/2 sublattice), via direct iterations (which will not generally yield solutions when unstable fixed points are concerned; it nevertheless is used to give insight, as before) one finds that such a fixed point can not have $k_{2,\dots}^*$ equal to zero (again because of the term $k_{2,\dots}^{*(1')}$). The fixed points corresponding to this situation are found numerically to be

$$(0, \pm 2.6870, 0, 0, 0, 0.9132)$$

for the spin-1/2 sublattice ferro- (SF) and antiferromagnetic (SAF) orderings, respectively. Note that $k_{2,\dots}^*$ here is the same as that appearing in the shifted origin fixed point above. This can be appreciated via arguments employing direct iterations. The above solutions should be compared with the corresponding fixed points found via first order perturbation theory, whose connection with the present case was discussed at the end of section 4.3 .

Now considering the case of spin-1 sublattice ordering, one similarly finds, through direct iterations, that a fixed point of the form $(0, 0, \pm u, 0, 0, v)$ is possible for some appropriate u, v ; corresponding to ferro- and antiferromagnetism, respectively. However, no such solutions were obtained in actual numerical calculations. We believe that this has no physical implications and consider it to be another artefact of the inclusion of self-couplings which, after all,

are defined for spin-1 objects. This likewise should be compared with the corresponding result of the first order cumulant method in which self-interactions were absent.

The 'coupled' fixed points corresponding to ferro- (FO) and ferrimagnetism (FI) on the whole lattice are found to be at

$$(0.5705, -0.0241, 0.0528, 0.0842, 0.0136, 1.8291)$$

and

$$(-0.6815, -0.0379, 0.0287, 0.1016, -0.0259, 2.4016)$$

respectively. One expects, on physical grounds, that the point FO to be the same as FI, but only with k_2^* reversed in sign. The reason for this apparent discrepancy is that the approximation embodied in our four-cell cluster analysis does not exhibit all the symmetries of the lattice. (Regarding this, the difference in sign of k_4^* in the two fixed points is due to its small value: a slight variation in a small quantity can change its sign too.) Note that here also the self-coupling dominates over all other interactions; the next-most important one being the nearest neighbour coupling.

Let us now engage in the study of the eigenvalues and associated eigenvectors. The ferro- and ferrimagnetic fixed points both yield (within numerical approximations, as the points are not quite 'mirror images' of one another) the relevant eigenvalue $\lambda_T = 1.5626$; which, as one expects, implies the same α -estimate for both cases. The corresponding normalised right eigenvectors

$$(\pm 0.4431, -0.0092, 0.0431, 0.0859, 0.0236, 0.8900)$$

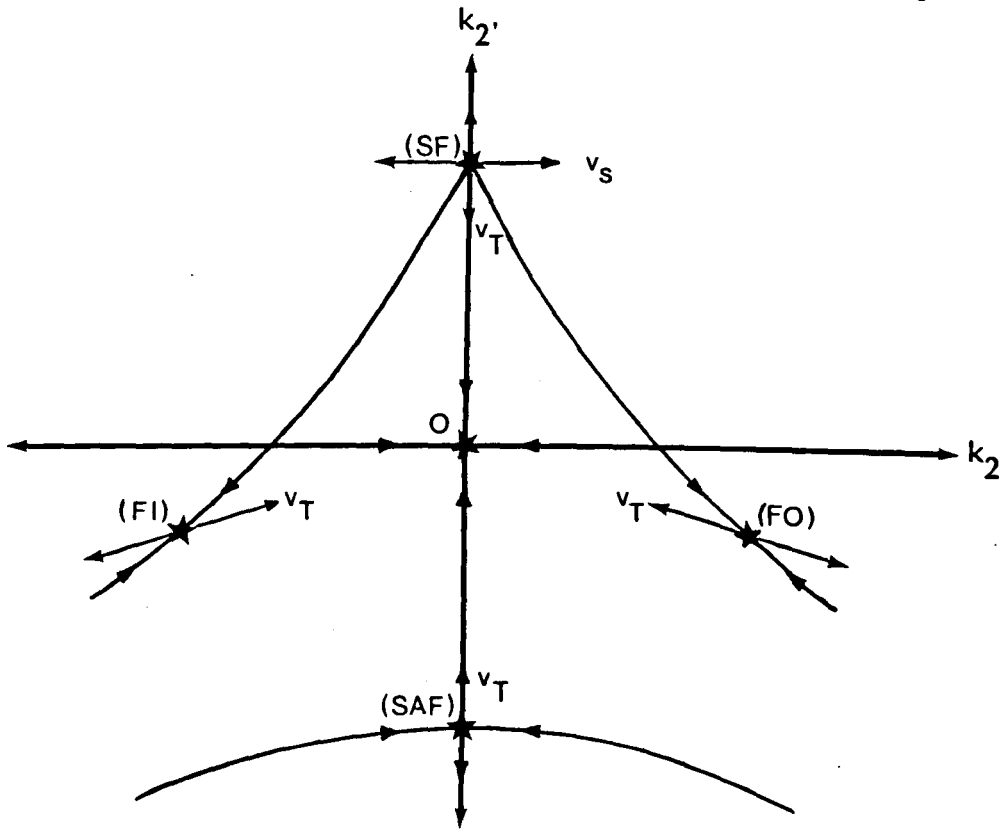
were also obtained respectively for FO and FI. These are, of course, vectors in the k-space of (even) parameters. By comparing the magnitudes of the components of these eigenvectors, one observes that the scaling field u_T couples more strongly (in increasing order) to k_2 and k_2^* , than others, which is understandable in view of the dominance of these couplings at the fixed point. Turning to decoupled sublattice fixed points, we find two relevant eigenvalues for SF (on the spin-1/2 sublattice, of course) namely $\lambda_T = 1.7516$, $\lambda_s = 1.8365$ and only one at SAF which is $\lambda_T = 1.7516$. These expectedly yield the same estimate for α . This estimate is better than that found at the coupled fixed points above, and can be considered to be a result of the fact that in the former situation, the role of the self-interaction is less noticeable as judged by looking at the fixed points. Now the existence of λ_s implies though using relations (4.2.12,13) that the transformation moves a point near SF away along a surface

$$u_s = A u_T^{y_s/y_T} . \quad (5.5.3)$$

Also, the critical surface in the neighbourhood of this fixed point (compared with other fixed points) is reduced in dimensionality by one, because of the presence of one more relevant eigenvector (see section 4.2). Thus if the FO and FI lie on critical hypersurfaces, the point in question lies on their intersection. These critical hypersurfaces are obtained for that value of A in (5.5.3) for which SF reaches FO or FI. As u_T couples to $k_2, -k_2^*$ and u_s to k_2 (see Fig(5.5) below), the intercept of the critical surface cusps in the k_2, k_2^* plane as

$$k_2 = A_C (k_2^* - k_2) y_s/y_T .$$

Again, this should be compared with the corresponding results of the first order cumulant technique. The outcome is schematically summarized in Fig(5.5) [see also the diagram of van Leeuwen, 1975].



Fig(5.5): Schematic location of fixed points, even eigenvectors v_i and critical curves in k_2, k_2' projection.

We ought to mention that v_s as worked out from our numerical manipulations does turn out to have a component along the k_2' -direction (see also section 4.3(i)). This is likewise due to the fact that our approximations do not take account of all the symmetries of the lattice, as this extra component tilts the 'wings' of the cusp to distort the symmetry of the picture in terms of the locations of FO and FI (which were not found to be exactly mirror images, after all). Fig(5.5) therefore indicates the physical picture rather than our approximate findings through cluster theory. The point O may thus be viewed as the origin fixed point, ignoring the 'unphysical' effects of self-

interactions. The diagram would then correspond (partially) to the results of section 4.3 as well. Unfortunately, nothing can be said about the k_2, k_2'' projection of critical surface, as we have no information on the ordered spin-1 (decoupled) sublattice. Although perturbation theory of section 4.3 would suggest a similar situation as embodied in our figure; the possibility of first order phase transitions which may occur in spin-1 systems (when self-couplings are present, see Blume, 1966 and Capel, 1966) complicates matters and renders any such speculations unsafe.

Finally, we discuss the magnetic eigenvalues and eigenvectors. Fixed points FO and FI both yield (within numerical approximations) the relevant eigenvalue $\lambda_H = 2.7249$ in presence of magnetic fields, with corresponding normalised (right) eigenvectors

$$(0.9592, \pm 0.2721, \mp 0.0040, 0.0066, 0.0736)$$

respectively, in the k -space of odd interaction parameters specified by (5.4.5). These obviously indicate that at FO, magnetic fields orient uniformly while at FI the orientation is staggered. λ_H and λ_T therefore yield identical estimates for critical indices in both cases, supporting the fact that ferromagnets in a uniformly (staggeredly) oriented field have the same critical behaviour as ferrimagnets in a staggeredly (uniformly) oriented field. For the 'decoupled' fixed points, one only gets a relevant eigenvalue for the case of ferromagnetic ordering SF, of course. Its value is $\lambda_H = 5.3191$ with the associated normalised eigenvector $(1, 0, 0, 0, 0)$; i.e the field only couples to spin-1/2 sublattice which is again obvious.

5.6 Discussion

The case of cell choice employing four-spins per block was mainly of quantitative relevance. Unfortunately, the effects of self-interactions produced numerical estimates for critical indices which were rather poor.

With the sublattice cell choice of five spins, the cumulant method yields no fixed points corresponding to coupled sublattices. However good quantitative results for the case of decoupled sublattices were obtained. The cluster theory on the other hand provides a useful qualitative picture, especially when the coupled sublattices are concerned. The study of decoupled fixed points, as it turned out, was seriously affected by the crucial role of self-couplings in the RG equations. This was also partially responsible for the very poor estimates obtained for this cell arrangement. Nevertheless, through intuitive arguments and using the results of the two approaches, the flow diagram of Fig(5.5) for the k_2, k_2' projection of the critical surface was obtained.

CHAPTER 6

ISING MODEL WITH REAL SPIN

6.1 Introduction

In this final chapter we aim at generalizing the Ising model to include any arbitrary (real) value for the spin variable. To lie within the context of the thesis, we shall have to consider the case of mixed spin systems. However, since the formalism has not even been addressed to single spin models, we ought to initially proceed with this more immediate case in mind. It is then trivial, as we shall show, to extend the formalism to include mixed spin situations.

The standard spin S (where S is one of the usual integral or odd half-integral values) Ising model has, in the usual notation, the partition function

$$Z_N = \text{tr}_1 \dots \text{tr}_N \exp(k \sum_{\langle ij \rangle} S_i^z S_j^z + L \sum_{i=1}^N S_i^z) \quad (6.1.1)$$

where $k = \beta J / S^2$, $L = \beta m H / S$ and $\text{Tr} = \text{tr}_1 \dots \text{tr}_N$ stands for the 'total trace' or sum over all configurations within the lattice of N sites. The 'partial trace' tr_i in (6.1.1) is defined by the condition that

$$\text{tr}_i F(S_i^z) = (2S+1)^{-1} \sum_{S_i^z \in \mathcal{A}} F(S_i^z) \quad (6.1.2)$$

in which the observable F is any suitable function of S_i^z , and \mathcal{A} is the set

$$\mathcal{A} = \{-S, -S+1, \dots, S-1, S\} . \quad (6.1.3)$$

The factor $(2S+1)^{-1}$ is introduced in (6.1.2) so that $\text{tr}_i 1 = 1$ which is a convenient normalising condition. The connection with thermodynamics is provided via the Gibbsian free energy G_N ,

$$-\beta G_N = \ln Z_N . \quad (6.1.4)$$

Equations (6.1.1-4) allow various properties of the Ising model to be calculated as explicit functions of S . As a first example of this, we note that the leading coefficients in certain exact high-temperature series expansions (in powers of k , of course, see also section 6.3(a)) have been obtained explicitly as functions of S . Table 6.1 makes this clear by quoting some results of Domb and Sykes (1957) ; Yousif and Bowers (1984) for the reduced zero-field susceptibility coefficients on the face centred cubic (FCC) and body centred cubic (BCC) lattices (the results of the latter are, in fact, for a mixed spin Ising model). As a second example of explicit results involving S , we turn to the mean field approximation. Here the complete thermodynamics may be shown to follow (see Smart, 1966) from the partition function

$$Z_N = Z^N , \quad Z = (2S+1)^{-1} \frac{\sinh [(S+\frac{1}{2})H_e]}{\sinh (\frac{1}{2}H_e)} \quad (6.1.5)$$

where H_e is an effective field (see also section 6.3(b)). Similar results apply in other approximation schemes. As a third example of our theme, we refer to the Kac-Hubbard-Stratonovich (KHS) transformation (Berlin and Kac, 1952 ; Stratonovich, 1957 and Hubbard, 1959) used by Hubbard (1972). This allows (6.1.1) to be re-expanded in the (Zero-field) form (see section 6.3(c))

$$Z_N = \{(\pi/2)^N \det(k)\}^{-\frac{1}{2}} \int_{-\infty}^{\infty} \dots \int_{-\infty}^{\infty} \exp[-\frac{1}{2} \sum_{i,j} (k^{-1})_{ij} x_i x_j] \prod_{i=1}^N \Omega_S(x_i) dx_i . \quad (6.1.6)$$

Here $L=0$ and k is now a matrix; the couplings k_{ij} between spins i and j generalizing the previous couplings k . The explicit spin dependence is given by the formula

$$\Omega_S(x_i) = (2S+1)^{-1} \frac{\sinh [(S+\frac{1}{2})x_i]}{\sinh (\frac{1}{2}x_i)} . \quad (6.1.7)$$

The importance of (6.1.6,7) is that for any spin $S=1/2, 1, 3/2, \dots$; they cast the Ising model in a form suitable for the application of Wilson's (1971a;b) field theoretical techniques (see Hubbard, 1972).

The first and third examples (and to a lesser extent the second) indicate methods by which studies have been made of the variation with spin of critical point parameters of the Ising model. Such studies have provided strong evidence in favour of that aspect of the universality referred to as spin-independence of critical exponents. An intriguing point follows from the fact that the above underlying results involve explicit algebraic functions of S . This means that, in an ad-hoc manner at least, the study of spin dependence need not be restricted to $S=1/2, 1, 3/2, \dots$; any real value of S may be considered (for simplicity we leave aside the possibility of complex values here). To give an example, if we put $S = -3.1, \sqrt{2}, \pi$ (say) respectively in the series for susceptibility $\chi_0(k)$ of BCC lattice as given by table 6.1, and then form Pade' approximants to $(d/dk) \ln \chi_0(k)$ (refer to section 3.2), we find the estimates of table 6.2 for the critical exponent γ ($\chi_0(k)$ of FCC yield very short Pade' tables and are therefore not included). These suggest a value of γ near to 1.25 just as for

the usual 'quantum' spin values (for estimates using such values see Yousif and Bowers, 1984). Another example follows if we put the same 'unphysical' values in (6.1.6,7). The argument of Hubbard based on applying Wilson's ideas to (6.1.6,7) suggests that the fixed point is unchanged in going even to these values of the spin. This supports the idea that the spin independence of critical indices may be extended to real S .

The above is, as previously observed, ad hoc: it uses formalism (6.1.1-3) which is only valid when $S=1/2, 1, 3/2, \dots$ and then quite arbitrarily treats resulting formulae as if they apply when $S=\pi$ or any other real number. The purpose of this chapter is to legitimize this. The idea is to generalize (6.1.2,3) in such a way that the resulting model applies for any real S and gives the same results, at least in our examples, for explicit spin dependence as the previous ad hoc procedure (of course (6.1.2,3) must be recovered for $S=1/2, 1, 3/2, \dots$). In this way we define an Ising model for any real spin S and so extend the domain in which such questions as universality can be considered.

In the following sections, after the definition of the model, we discuss the equivalent formalism for the mixed spin systems and subsequently some consequences will be explored.

Table 6.1 : Reduced zero-field susceptibility coefficients of the single spin FCC and the mixed spin (of magnitudes 1/2 and S) BCC lattices. Here $x = S(S + 1)$.

(FCC)

$$\begin{aligned}
 a_0 &= 1 \\
 a_1 &= 2x \\
 a_2 &= x/30 (114 x^2 + 114 x - 3) \\
 a_3 &= x/300 (2124 x^4 + 4248 x^3 + 1988 x^2 - 136 x + 1) \\
 a_4 &= x/453600 (5909832 x^6 + 17729496 x^5 + 17092548 x^4 + \\
 &\quad + 4635936 x^3 - 616050 x^2 + 20898 x - 135)
 \end{aligned}$$

(BCC)

$$\begin{aligned}
 b_0 &= 1/11 (4 x + 3) \\
 b_1 &= 16 x/11 \\
 b_2 &= 2 x/165 (148 x + 99) \\
 b_3 &= 2 x/165 (516 x - 22) \\
 b_4 &= x/6930 (52148 x^2 + 31159 x - 1305) \\
 b_5 &= x/1155 (29018 x^2 - 2775 x + 92) \\
 b_6 &= x/415800 (12482576 x^3 + 6589456 x^2 - 645199 x + 19971) \\
 b_7 &= x/207900 (20370104 x^3 - 3075616 x^2 + 202329 x - 5871)
 \end{aligned}$$

Table 6.2: Estimates for γ provided by forming $[N,A]$ PA's to the series $(d/dk) \ln \chi_0(k)$, on the mixed spin (of magnitudes $1/2$ and S) BCC lattice. S takes the values $-3.1, \sqrt{2}, \pi$.

($S = -3.1$)

$\begin{array}{c} N \\ \backslash \\ D \end{array}$	1	2	3	4	5
2	1.5100	1.0071	1.3254	-	-
3	1.1263	1.2251	1.2611	1.4434	
4	1.2843	1.2695	1.2243		
5	1.2684	1.2842			
6	-				

($S = \sqrt{2}$)

$\begin{array}{c} N \\ \backslash \\ D \end{array}$	1	2	3	4	5
2	1.3901	1.0425	1.3154	-	-
3	1.1134	1.2184	1.2502	1.4377	
4	1.3282	1.2545	1.2175		
5	1.2305	1.3245			
6	-				

($S = \pi$)

$\begin{array}{c} N \\ \backslash \\ D \end{array}$	1	2	3	4	5
2	1.5895	1.0403	1.2892	-	-
3	1.1686	1.2350	1.2781	1.3755	
4	1.2547	1.3069	1.2342		
5	1.2892	1.2542			
6	-				

6.2 Definition of the model

With partial traces normalised as is in (6.1.2), the moments (or mean values) of powers of the spin component S_i^z are simply $\text{tr}_i (S_i^z)^r$, $r=0,1,2,\dots$; in the standard Ising model. These are given, on using (6.1.2,3) and (6.2.8a;b), by

$$\text{tr}_i (S_i^z)^r = \begin{cases} (2S+1)^{-1} \{2/(2n+1)\} B_{2n+1}(S+1) & , \quad r=2n \\ 0 & , \quad r=2n+1 \end{cases} \quad (6.2.1)$$

where $B_r(x)$ denotes the Bernoulli polynomial of degree r defined via

$$y e^{xy}/(e^y-1) = \sum_{r=0}^{\infty} B_r(x) y^r/r! \quad , \quad |y| < 2\pi$$

so that $B_0(x)=1$, $B_1(x)=x-1/2$, $B_2(x)=x^2-x+1/6$, etc.

As is known from the theory of probability distributions, a knowledge of full set of such moments is completely equivalent to the distribution function of spin components. With respect to discussions of section 6.1, it is therefore sufficient to generalize equations (6.1.2,3) such that (6.2.1) is formally valid for any $S \in \mathbb{R}$. This will then determine the spin distribution function uniquely; defining the generalized model via (6.1.1).

Before proceeding, we make the following point. Because the high-temperature series can be expanded in terms of $X=S(S+1)$ (see table 6.1), the series and all informations derived from them are invariant under the transformation $S \rightarrow -S-1$. Using the identity

$$(-1)^r B_r(x) = B_r(1-x) \quad (6.2.2)$$

one also observes that the same invariance applies to the partial trace given by (6.2.1) [this is expected as $\text{tr}_i (S_i^z)^r$ naturally arise from

high-temperature expansions, see section 6.3(a)]. The transformation implies that spins $S \geq 0$ are 'mapped' to $S \leq -1$, and $-1 < S < 0$ to spins within the same range. This is of course ad hoc because the formalism, as yet, does not hold for arbitrary spin value. In our generalization, this invariance must obviously be borne out in the definitions. We shall start by defining the new trace tr_i' and subsequently examine whether the requirements mentioned at the end of section 6.1 for a successful candidate are met. We write

$$|2S+1| \text{tr}_i' F(S_i^z) = \sum_{S_i^z \in \mathcal{A}'} F(S_i^z) + \int_{-i\infty}^{i\infty} W_{|S-[S]|}(u) F(u) du \quad (6.2.3)$$

where $[S]$ is the greatest integer $\leq |S|$, and the integral sign means formally $\lim_{\alpha \rightarrow \infty} \int_{-i\alpha}^{i\alpha}$, with the weight function $W_{|S-[S]|}(u)$ being given in terms of the quantity $0 \leq |S-[S]| < 1$ by

$$W_{|S-[S]|}(u) = \begin{cases} \frac{i \sin 2\pi(|S-[S]|)}{\cos 2\pi u - \cos 2\pi(|S-[S]|)}, & 0 < |S-[S]| < 1 \\ 0, & |S-[S]| = 0. \end{cases} \quad (6.2.4)$$

Here \mathcal{A}' is a union \bigcup of points:

$$\mathcal{A}' = \begin{cases} \left\{ \bigcup p_i: p_i \in -S, -S+1, \dots, -S+[S], S-[S], \dots, S-1, S \right\} \\ \emptyset \\ \left\{ \bigcup p_i: p_i \in S+1, \dots, -|S-[S]|, |S-[S]|, \dots, -S-1 \right\} \end{cases} \quad (6.2.5)$$

for $S \geq 0$, $-1 < S < 0$ and $S \leq -1$ respectively. Note that the implications of the transformation $S \rightarrow S-1$ are fulfilled via this definition (for an alternative, slightly different, definition of \mathcal{A}' and $W_{|S-[S]|}(u)$ see the appendix). In particular \mathcal{A}' reduces to the empty set \emptyset in the

range $-1 < S < 0$, so that the summation of (6.2.3) vanishes, leaving only the integral. Thus $-1 < S < 0$ can not be mapped to any other spin range. The (generalized) moments $\text{tr}_i' (S_i^Z)^r$ are thus obtained from

$$|2S+1| \text{tr}_i' (S_i^Z)^r = \sum_{S_i^Z \in \mathcal{d}'} (S_i^Z)^r + \int_{-i\infty}^{i\infty} W_{|S-[S]|}(u) u^r du. \quad (6.2.6)$$

We must now prove that (6.2.6) indeed yields the same explicit spin dependence as in (6.2.1), for arbitrary real S . First consider the situation for non-integer spins where $0 < |S-[S]| < 1$. We have (Erde'lyi et al, 1953); for $r=2n = 0, 2, 4, \dots$;

$$\int_{-i\infty}^{i\infty} W_{|S-[S]|}(u) u^{2n} du = \int_{-\infty}^{\infty} (-1)^{n+1} \frac{\sin 2\pi(|S-[S]|)}{\cosh 2\pi t - \cos 2\pi(|S-[S]|)} t^{2n} dt = \{2/(2n+1)\} B_{2n+1}(|S-[S]|) \quad (6.2.7)$$

which holds for $0 < |S-[S]| < 1$. The summation in (6.2.6) may be evaluated via relations (Erde'lyi et al, 1953)

$$\int_x^{x+1} B_r(t) dt = x^r \quad (6.2.8a)$$

and

$$\int_x^y B_r(t) dt = \{B_{r+1}(y) - B_{r+1}(x)\} / (r+1) \quad (6.2.8b)$$

with $r=0, 1, 2, \dots$. Whence, for $0 < S-[S] < 1$, i.e positive ^{non-}integers,

$$\sum_{S_i^Z \in \mathcal{d}'} (S_i^Z)^{2n} = \frac{2 \{B_{2n+1}(S+1) - B_{2n+1}(S-[S])\}}{(2n+1)} \quad (6.2.9)$$

and for negative non-integers ≤ -1 ,

$$\begin{aligned} \sum_{S_i^z \in \mathcal{A}'} (S_i^z)^{2n} &= \\ 2 \{B_{2n+1}(-S) - B_{2n+1}(|S-[S]|)\} / (2n+1) &= \\ -2 \{B_{2n+1}(S+1) + B_{2n+1}(|S-[S]|)\} / (2n+1) & \quad (6.2.10) \end{aligned}$$

having used (6.2.2). Thus (6.2.9,10) together with (6.2.6,7) yield

$$\text{tr}_i' (S_i^z)^{2n} = (2S+1)^{-1} \{2/(2n+1)\} B_{2n+1}(S+1) \quad (6.2.11)$$

which holds for every non-integer spin excluding the range $-1 < S < 0$. For this particular range we have $[S]=0$ by definition, and thus one obtains through equations (6.2.2) and (6.2.5-7),

$$\begin{aligned} \text{tr}_i' (S_i^z)^{2n} &= |2S+1|^{-1} \{2/(2n+1)\} B_{2n+1}(|S|) \\ &= (2S+1)^{-1} \{2/(2n+1)\} B_{2n+1}(S+1) \end{aligned}$$

which, as expected, is identical to (6.2.11). So (6.2.11) in fact holds for any non-integer real S and checks with (6.2.1), if in it S is literally taken to belong to (non-integer) \mathbb{R} . When $r=2n+1$ is odd, the integral and the summation of (6.2.6) are easily seen to vanish for any $S \in \mathbb{R}$, implying zero moment for odd powers of S_i^z , consistent with (6.2.1). We remark the interesting case of 'physical' spins $S=1/2, 1, 3/2, \dots$ (where $S-[S]=1/2$; a particular case of $0 < S-[S] < 1$) for which the integral in (6.2.3) vanishes and \mathcal{A}' coincides with \mathcal{A} , so that $\text{tr}_i' \equiv \text{tr}_i$ and thus (6.1.2,3) are recovered for $S=1/2, 3/2, \dots$ etc. .

Next, we consider the case of integer spins where $S-[S]=0$. Here, by definition of the weight function, the integral contribution to moments vanishes. The set \mathcal{A}' is a union of points, thus including any common value (namely 0, occurring only for integers) only once. Having noted this, for any integer value of S equations (6.2.5,6), (6.2.8a,b) and (6.2.2) similarly yield

$$\text{tr}'_i (S_i^z)^r = \begin{cases} (2S+1)^{-1} \{2/(2n+1)\} B_{2n+1}(S+1) & , \quad r=2n \\ 0 & , \quad r=2n+1 \end{cases} \quad (6.2.12)$$

also valid now for integer S . This is to be compared with (6.2.1). A particular case of this is that of physical spins $S=1,2,\dots$; for which \mathcal{L}' coincides with \mathcal{L} implying $\text{tr}'_i = \text{tr}_i$, and so relations (6.1.2,3) are once again recovered.

In this manner, we have defined a new model with the partition function

$$Z_N = \text{tr}'_1 \dots \text{tr}'_N \exp(k \sum_{\langle ij \rangle} S_i^z S_j^z + L \sum_{i=1}^N S_i^z) \quad (6.2.13)$$

where tr'_i are given by (6.2.3-5). As set out to achieve, it is a generalization of the standard Ising model which reduces to it when $S=1/2, 1, 3/2, \dots$ and remains consistent for any other real spin value. Everything derived from this partition function is now formally valid for any $S \in \mathbb{R}$.

Let us now extend the formalism to include mixed spin systems. Let our loose-packed lattice consist of two (non-equivalent) sublattices A and B 'containing' spins S_A and S_B . Then the partition function is (see also section 1.3)

$$Z_N = \text{Tr} \exp(k \sum_{\langle ij \rangle} S_{i,A}^z S_{j,B}^z + L_A \sum_{i \in A} S_{i,A}^z + L_B \sum_{j \in B} S_{j,B}^z) \quad (6.2.14)$$

where $k = \beta J / S_A S_B$, $L_A = \beta m_A H_A / S_A$ and $L_B = \beta m_B H_B / S_B$. Here the total trace is

$$\text{Tr} \equiv (\text{tr}_{1,A} \dots \text{tr}_{N_A,A}) (\text{tr}_{1,B} \dots \text{tr}_{N_B,B})$$

where N_A and N_B are the number of sites on A and B sublattices respectively, and

$$\begin{aligned} \text{tr}_{i,A} F(S_{i,A}^z) &= (2S_A+1)^{-1} \bigwedge_{S_{i,A}^z \in \mathcal{S}_A} F(S_{i,A}^z) \\ \text{tr}_{i,B} F(S_{j,B}^z) &= (2S_B+1)^{-1} \bigwedge_{S_{j,B}^z \in \mathcal{S}_B} F(S_{j,B}^z) \end{aligned}$$

in which

$$\mathcal{S}_A = \{-S_A, -S_A+1, \dots, S_A-1, S_A\}$$

$$\mathcal{S}_B = \{-S_B, -S_B+1, \dots, S_B-1, S_B\} .$$

Equation (6.2.1) clearly holds:

$$\text{tr}_{i,A} (S_{i,A}^z)^r = \begin{cases} (2S_A+1)^{-1} \{2/(2n+1)\} B_{2n+1}(S_A+1) & (6.2.15a) \\ 0 \end{cases}$$

for $r=2n$, $r=2n+1$ respectively and

$$\text{tr}_{j,B} (S_{j,B}^z)^r = \begin{cases} (2S_B+1)^{-1} \{2/(2n+1)\} B_{2n+1}(S_B+1) & (6.2.15b) \\ 0 \end{cases}$$

again for even and odd r , respectively. We can thus proceed in exactly the same manner as before by writing down (6.2.3) for $\text{tr}_{i,A} F(S_{i,A}^z)$ and $\text{tr}_{j,B} F(S_{j,B}^z)$ with (6.2.4,5) defined in terms of S_A and S_B , respectively. Clearly the mathematics is identical to the single spin case and we end up with the result that (6.2.15a,b) become formally valid for any $S_A, S_B \in \mathbb{R}$. So the partition function (6.2.14) with Tr replaced by Tr' defines the required generalization for mixed spin Ising models.

6.3 Some consequences

Here, we discuss some consequences of the new model with respect to assertions of section 6.1. Considering the examples of high-temperature expansions, MFT and the KHS transformation (as used by Hubbard), we show that our generalized Ising model does indeed yield the same results for the explicit spin dependence. Again the case of single spin rather than the mixed spin Ising model is considered, the extension to the latter being trivial but unnecessarily complicated.

(a) High-temperature expansions: Writing the partition function (6.1.1) in the form

$$Z_N = \text{Tr} \left\{ \prod_{\langle ij \rangle} \exp(k S_i^z S_j^z) \prod_{i=1}^N \exp(L S_i^z) \right\} \quad (6.3.1)$$

enables one to employ the method of Brout (1959;1960) for obtaining high-temperature series expansions in the following manner. Expand the above exponentials in powers of k and L ,

$$\begin{aligned} \exp(k S_i^z S_j^z) &= 1 + k S_i^z S_j^z + (k^2/2!) (S_i^z S_j^z)^2 + \dots \\ &\quad + (k^r/r!) (S_i^z S_j^z)^r + \dots \\ \exp(L S_i^z) &= 1 + L S_i^z + (L^2/2!) (S_i^z)^2 + \dots \\ &\quad + (L^r/r!) (S_i^z)^r + \dots \end{aligned}$$

and substitute back into (6.3.1). When the first term of (6.3.1) is multiplied out, the coefficient of k^ℓ gives a contribution from every possible multiply-bonded graph of ℓ lines; every such graph is associated with an appropriate product of $S_i^z, S_j^z, \dots, S_k^z$; there being $S_i^z S_j^z$ for each bond. These must now be multiplied by the expansion of the second term, whose typical coefficient is again an appropriate product of $S_i^z, S_j^z, \dots, S_k^z$. Finally take the trace to get factors like

$\text{tr}_i (S_i^Z)^r$, $r=0,1,2,\dots$; which must be calculated at vertex i . These then determine the coefficients of k^r in the final (exact up to a given r) expansion. In our generalized model we clearly end up with factors $\text{tr}_i (S_i^Z)^r$ which, as proved in the last section, yield the same explicit spin dependence. As a consequence the high-temperature series expansions obtained from the new model are identical to those of the standard Ising system, with the advantage that they are formally valid for all $S \in \mathbb{R}$. The smoothness of estimates of table 6.2 now looks plausible in view of an extended form for the spin-independence of critical exponents.

(b) MFT: The standard spin S Ising Hamiltonian

$$\mathcal{H} = -(J/S^2) \sum_{\langle ij \rangle} S_i^Z S_j^Z - (mH/S) \sum_{i=1}^N S_i^Z$$

can be written as a sum of the site spin Hamiltonian \mathcal{H}_i in the following manner:

$$\mathcal{H} = \sum_{i=1}^N \mathcal{H}_i \quad (6.3.2a)$$

where

$$\mathcal{H}_i = \{-mH/S - (J/S^2) \sum_{j=1}^q S_j^Z\} S_i^Z \quad (6.3.2b)$$

q being the coordination number of the lattice. The basic assumption of the MFT is that the spin-spin interactions are approximately equivalent to the effect of an applied magnetic field proportional to their mean value $\langle S_i^Z \rangle$. We thus let

$$\sum_{i=1}^q S_i^Z = q \langle S^Z \rangle$$

with $\langle S_i^Z \rangle = \langle S^Z \rangle$ for all i . Hence (6.3.2b) yields

$$Z_i = \text{tr}_i \exp(-\beta \mathcal{H}_i) = \text{tr}_i \exp(H_e S_i^Z) \quad , \quad \forall i \quad (6.3.3)$$

for the partition function of site spin i , where the effective field H_e is given by

$$H_e = L + kq \langle S^z \rangle .$$

The total partition function is obviously $Z_N = Z_i^N$ as is seen from (6.3.2,3). Equation (6.3.3) leads directly to the result (6.1.5) via (6.1.2,3).

For our generalized model (6.3.3) becomes

$$Z_i = \text{tr}_i' \exp(H_e S_i^z) \quad (6.3.4)$$

with $Z = Z_i^N$, of course. That is

$$\begin{aligned} |2S+1| Z_i = \\ \sum_{S_i^z \in \mathcal{D}'} \exp(H_e S_i^z) + \int_{-i\infty}^{i\infty} W_{|S-[S]|}(u) \exp(H_e u) du . \end{aligned} \quad (6.3.5)$$

In the case of integer spins ($S-[S]=0$), (6.3.5) yields through (6.2.4,5) the same result, of course, as in (6.1.5) for positive integers, since $\mathcal{D}' \equiv \mathcal{D}$. For negative integers ($S=-|S|$), we have

$$\begin{aligned} Z_i &= \sum_{S_i^z \in \mathcal{D}'} \exp(H_e S_i^z) \\ &= |2S+1|^{-1} \sinh [(|S|-\frac{1}{2})H_e] / \sinh (\frac{1}{2}H_e) \\ &= (2S+1)^{-1} \sinh [(S+\frac{1}{2})H_e] / \sinh (\frac{1}{2}H_e) \end{aligned}$$

which also coincides with (6.1.5). In the case of non-integers (i.e. $0 < |S-[S]| < 1$), the integral contribution ι becomes

$$\begin{aligned} \iota &= \int_{-i\infty}^{i\infty} W_{|S-[S]|}(u) \exp(H_e u) du \\ &= \int_{-\infty}^{\infty} - \frac{\sin 2\pi(|S-[S]|) \exp(-iH_e t)}{\cosh 2\pi t - \cos 2\pi(|S-[S]|)} dt . \end{aligned}$$

With the Fourier transform $F(t)$ of $f(x)$ and its inverse defined respectively by

$$F(t) = (2\pi)^{-\frac{1}{2}} \int_{-\infty}^{\infty} f(x) e^{itx} dx$$

$$f(x) = (2\pi)^{-\frac{1}{2}} \int_{-\infty}^{\infty} F(t) e^{-itx} dt ,$$

we note that τ is just the inverse Fourier transform of

$$\frac{-\sqrt{2\pi} \sin 2\pi(IS-[S]I)}{\cos 2\pi t - \cos 2\pi(IS-[S]I)}$$

which is found from tables (see for instance Gradshteyn and Ryzhik, 1980) to be

$$\tau = \frac{\sinh [(IS-[S]I-\frac{1}{2})H_e]}{\sinh (\frac{1}{2}H_e)} \quad (6.3.6)$$

for $0 < IS-[S]I < 1$. For spin values $-1 < S < 0$ ($[S]=0$), the sum vanishes and (6.3.4) yields through (6.3.6)

$$z_i = (2S+1)^{-1} \frac{\sinh [(S+\frac{1}{2})H_e]}{\sinh (\frac{1}{2}H_e)}$$

again consistent with (6.1.5). We now obtain the summation of (6.3.5) for non-integer spins in the range $S \geq 0$, $S \leq -1$. Equation (6.2.5) implies for positive non-integers ($0 < S-[S] < 1$) that

$$\sum_{S_i^z \in \mathcal{A}'} \exp(H_e S_i^z) = \frac{\sinh [(S+\frac{1}{2})H_e]}{\sinh (\frac{1}{2}H_e)} - \frac{\sinh [(S-[S]-\frac{1}{2})H_e]}{\sinh (\frac{1}{2}H_e)}$$

and for non-integral spins ≤ -1 ,

$$\frac{\sum_{S_i^z \in \mathcal{A}'} \exp(H_e S_i^z)}{\sinh [(|S| - \frac{1}{2})H_e]} = \frac{\sinh [|(S - [S])| - \frac{1}{2})H_e]}{\sinh (\frac{1}{2}H_e)}$$

which yields the same form as (6.1.5) on using equations (6.3.5,6). Thus the new model gives the equivalent of (6.1.5), which is formally valid for any real spin.

(c) KHS transformation: In zero field equation (6.1.1) reduces to

$$Z_N = \text{Tr} \exp\left(\sum_{i,j} S_i^z k_{ij} S_j^z\right) \quad (6.3.7)$$

where the couplings have been generalized as described in section 6.1. KHS transformation reads, for any symmetric positive definite matrix,

$$\exp\left(\sum_{i,j} S_i^z k_{ij} S_j^z\right) = \{(\pi/2)^N \det(k)\}^{-\frac{1}{2}} \int_{-\infty}^{\infty} \dots \int_{-\infty}^{\infty} \exp\left[-\frac{1}{2} \sum_{i,j} (k^{-1})_{ij} x_i x_j + \sum_{i=1}^N x_i S_i^z\right] d^N x_i \quad (6.3.8)$$

Taking the trace as instructed by (6.3.7) yields equation (6.1.6) with $\Omega_S(x_i) = \text{tr}_i \exp(x_i S_i^z)$. This in turn gives (6.1.7) after simple manipulations. These partial traces involved in Ω_S are similar to those which come in the MFT (see (b) above), justifying the resemblance between (6.1.5) and (6.1.7). In the generalized zero-field Ising model everything remains as before, except that

$$\Omega_S(x_i) = \text{tr}_i \exp(x_i S_i^z) .$$

From arguments given in (b), this equation (whose right hand side is identical to (6.3.4) with H_e replaced by x_i) also yields

$$\Omega_S(x_i) = (2S+1)^{-1} \frac{\sinh [(S+\frac{1}{2})x_i]}{\sinh (\frac{1}{2}x_i)}$$

for any $S \in \mathbb{R}$ and is consistent with (6.1.7). The reasoning of Hubbard (see section 6.1) thus becomes formally valid for any real spin, supporting the idea that the spin independence of critical indices may be extended to real S .

We should, at this stage, make the following remark. Equation (6.3.8) holds only for symmetric positive definite matrices (there exist similar transformations, however, which hold true for any symmetric matrix; see Baker, 1962; so that Hubbard's arguments will not be affected in principle), otherwise the multiple integral in (6.3.8) diverges. Now, Ising models with no self-interactions have diagonal elements of k zero and thus the sum of its eigenvalues vanishes, implying that such models always have negative eigenvalues. Hence in order that matrix k remains positive definite, self-interactions must be present. In similar fashion, one observes that the multiple integrals contained within (6.2.13) diverge if self-couplings are excluded. One way to see this is by writing $u=it$ and comparing the real form obtained with (6.3.8). Therefore, although (6.2.13) yields consistent results through various approaches studied above (as was initially set out to do), it can not be treated 'exactly' to yield Z_N (for example the interesting exact solution of one-dimensional case when $S \rightarrow -1/2$, for which the sums vanish; $S=-1/2$ is a 'fixed point' of the transformation $S \rightarrow -S-1$), unless self-interactions are included; in which case it will no longer be a generalization of the pure (nearest neighbour) Ising model. Self-couplings, as has been mentioned in chapters 4 and 5, fortunately do not affect the critical behaviour, so the arguments leading to the notion of an extended form of spin independence of

critical exponents hold correct. The same, of course, goes for the case of the mixed spin Ising model.

APPENDIX

We could have written (6.2.3) with the following alternative definitions

$$W_{|S-[S]|}(u) = \frac{i \sin 2\pi(|S-[S]|)}{\cos 2\pi u - \cos 2\pi(|S-[S]|)}, \quad 0 \leq |S-[S]| < 1 \quad (1)$$

and

$$\mathcal{L}' = \begin{cases} \{-S, -S+1, \dots, -S+[S], S-[S], \dots, S-1, S\} & , \quad S \geq 0 \\ \emptyset & , \quad -1 < S < 0 \\ \{S+1, \dots, -|S-[S]|, |S-[S]|, \dots, -S-1\} & , \quad S \leq -1 . \end{cases} \quad (2)$$

For the case of non-integer spins (1),(2) are identical to (6.2.4,5) and as a consequence, the arguments of section 6.2 apply when $0 < |S-[S]| < 1$. For the case of integers; $S-[S]=0$ will be included twice in \mathcal{L}' as given by (2). This will obviously effect the summation in (6.2.6) only when $r=0$. Also the weight function $W_0(u)$ is now everywhere zero except at the origin $u=0$. To work out the integral part of the moments in (6.2.6) we expand (informally) in a small neighbourhood ϵ of the origin to get

$$\begin{aligned} \int_{-i\infty}^{i\infty} W_0(u) u^r du &= \lim_{|S-[S]| \rightarrow 0} \int_{-\epsilon}^{\epsilon} -\pi^{-1} \frac{|S-[S]|}{t^2 + (S-[S])^2} (it)^r dt \\ &= \begin{cases} -1 & , \quad r=0 \\ 0 & , \quad r=1,2,3,\dots \end{cases} \end{aligned} \quad (3)$$

This is because $|S-[S]|/\pi(t^2+(S-[S])^2)$ is a delta sequence (see for example Gel'fand and Shilov, 1964), i.e as $|S-[S]| \rightarrow 0$, the sequence approaches the delta function $\delta(t)$ with the famous properties

$$\int_{-\infty}^{\infty} \delta(t) dt = 1 \quad , \quad \int_{-\infty}^{\infty} \delta(t-x) f(t) dt = f(x) .$$

Thus the problem with $\text{tr}_i' 1$ in equation (6.2.6) [i.e when $r=0$] is automatically taken care of by the delta-function behaviour of $W_0(u)$ to yield $\text{tr}_i' 1 = 1$, as before. Equations (3) and (6.2.6) then together yield (6.2.12), which is as a result valid formally for any $S \in \mathbb{R}$. However, since \mathcal{L}' no longer coincides with \mathcal{L} for $S=1,2,\dots$; equations (6.1.2,3) can not be recovered, as they were for $S=1/2, 3/2, \dots$. For this reason we have preferred the definitions (6.2.4,5) so that (6.1.2,3) may be recovered for $S=1,2,\dots$ too; rendering the new model a more direct generalization. The results of section 6.3, needless to say, apply equally well to the model defined via (1) and (2).

REFERENCES

- Baker, G.A (1961): Phys. Rev. 124, 768 .
- Baker, G.A (1962): Phys. Rev. 126, 2071 .
- Barber, M.N (1977): Phys. Rep. 29C, 1 .
- Baxter, R.J (1971): Phys. Rev. Lett. 26, 832 .
- Baxter, R.J (1972): Ann. Phys. (N.Y) 70, 193 .
- Berlin, T.H and Kac, M (1952): Phys. Rev. 86, 821 .
- Betts, D.D and Chan, C.F.S (1974): J. Phys. A7, 650 .
- Betts, D.D ; Elliott, C.J and Sykes, M.F (1974): J. Phys. A7, 1323.
- Blume, M (1966): Phys. Rev. 141, 517 .
- Bowers, R.G (1981): J. Phys. C14, L1013 .
- Bowers, R.G and Woolf, M.E (1969): Phys. Rev. 177, 917 .
- Bowers, R.G and Yousif, B.Y (1984): J. Phys. A17, 895 .
- Brout, R (1959): Phys. Rev. 115, 824 .
- Brout, R (1960): Phys. Rev. 118, 1009 .
- Capel, H.W (1966): Physica 32, 966 .
- Dienes, P (1957): "The Taylor Series", Dover Publications, New York.
- Domb, C (1960): Adv. Phys. 9, 149 .
- Domb, C and Sykes, M.F (1957): Proc. Roy. Soc. A240, 214 .
- Erd'lyi, A ; Magnus, W ; Oberhettinger, F and Tricomi, G.F (1953):
"Higher Transcendental Functions" (Bateman Manuscript
Project, CIT), Vol. 1, MacGrow-Hill Co. .
- Essam, J.W and Fisher, M.E (1963): J. Chem. Phys. 38, 802 .
- Fisher, M.E (1959): Phys. Rev. 113, 969 .
- Fisher, M.E (1966): Phys. Rev. Lett.16, 11 .
- Fisher, M.E (1967): Rep. Prog. Phys. 30, 615 .
- Fisher, M.E (1974): Rev. Mod. Phys. 46, 597 .
- Fox, P.F and Gaunt, D.S (1970): J. Phys. C3, L88 .

- Fox, P.F and Gaunt, D.S (1972): J. Phys. C5, 3085 .
- Fox, P.F and Guttman, A.J (1973): J. Phys. C6, 913 .
- Gaunt, D.S (1967): Proc. ^{Phys.} Roy. Soc. 92, 150 .
- Gaunt, D.S and Guttman, A.J (1974): In "Phase Transitions and Critical Phenomena" (C.Domb and M.S.Green, eds.), Vol. 3, Academic Press .
- Gaunt, D.S and Sykes, M.F (1972): J. Phys. C5, 1429 .
- Gel'fand, I.M and Shilov, G.E (1964): "Generalised Functions", Vol. 1, Academic Press .
- Gradshteyn, I.S and Ryzhik, I.M (1980): "Tables of Integrals, Series and Products" (A.Jeffrey, ed.), Academic Press .
- Griffiths, R.B (1970): Phys. Rev. Lett. 24, 1479 .
- Hahne, F.J.W (1983): "Critical Phenomena" (proceedings), Springer-Verlag .
- Heller, P (1967): Rep. Prog. Phys. 30, 731 .
- Heisenberg, W (1928): Z. Phys. 49, 619 .
- Hubbard, J (1959): Phys. Rev. Lett. 3, 77 .
- Hubbard, J (1972): Phys. Lett. 39A, 365 .
- Ising, E (1925): Z. Phys. 31, 253 .
- Kadanoff, L.P (1966): Physics (N.Y) 2, 263 .
- Nauenberg, M and Nienhuis, B (1974): Phys. Rev. Lett. 33, 944 .
- Ne'el, L (1948): Ann. Phys. (Paris) 3, 137 .
- Niemeijer, Th and van Leeuwen, J.M.J (1973): Phys. Rev. Lett. 31, 1411 .
- Niemeijer, Th and van Leeuwen, J.M.J (1974): Physica 71, 17 .
- Niemeijer, Th and van Leeuwen, J.M.J (1975): Phys. Rev. Lett. 34, 1056 .
- Niemeijer, Th and van Leeuwen, J.M.J (1976): In "Phase Transitions and Critical Phenomena" (C.Domb and M.S.Green, eds.),
- ← Huang, K (1963): "Statistical Physics", Wiley, New York.

Vol. 6, Academic Press .

Nienhuis, B and Nauenberg, M (1975): Phys. Rev. Lett. 35, 477 .

Onsager, L (1944): Phys. Rev. 65, 117 .

Ravndel, F (1976): "Scaling and Renormalisation Groups", Lectures given at the Niels Bohr Institute and NORDITA, Copenhagen.

Schick, M (1982): In "Real-Space Renormalisation" (T.W.Burkhardt and J.M.J.van Leeuwen, eds.), Springer-Verlag .

Schofield, S.L (1980): Ph.D Theseis, University of Liverpool .

Schofield, S.L and Bowers, R.G (1980): J. Phys. A13, 3697 .

Schofield, S.L and Bowers, R.G (1981): J. Phys. A14, 2163 .

Smart, J.S (1966): "Effective Field Theories of Magnetism", Saunders Co., Philadelphia and London .

Strtonovich, R.L (1957): Doklady Akad. Nauk S.S.R 115, 1097 .

Sykes, M.F ; Essam, J.W and Gaunt, D.S (1965): J. Math. Phys. 6, 283 .

Sykes, M.F and Gaunt, D.S (1973): J. Phys. A6, 643 .

Sykes, M.F ; Gaunt, D.S ; Essam, J.W ; Heap, B,R ; Elliott, C.J and Mattingly, S.R (1973): J. Phys. A6, 1498 .

Wannier, G.H (1945): Rev. Mod. Phys. 17, 50 .

Wegner, F.J (1972): Phys. Rev. B5, 4529 .

Widom, B (1965a;b): J. Chem. Phys. 43, 3892;3898 .

Wilson, K.G (1971a;b): Phys. Rev. 34, 3174;3184 .

Yousif, B.Y (1983): Ph.D Theseis, University of Liverpool .

Yousif, B.Y and Bowers, R.G (1983): J. Phys. A16, 3361 .

Yousif, B.Y and Bowers, R.G (1984): J. Phys. A17, 3389 .
